ผลของอุณหภูมิต่อการกำจัดไอโทลูอีนโดยใช้ปฏิกิริยาเติมอิเล็กตรอน

นางสาว นันทมาศ ทัตตะวร

วิทยานิพนธ์นี้เป็นส่วนหนึ่งของการศึกษาตามหลักสูตรปริญญาวิศวกรรมศาสตรมหาบัณฑิต
สาขาวิศวกรรมเคมี ภาควิชาวิศวกรรมเคมี
คณะวิศวกรรมศาสตร์ จุฬาลงกรณ์มหาวิทยาลัย
ปีการศึกษา 2543

ISBN 974-13-0767-5

EFFECT OF TEMPERATURE ON REMOVAL OF TOLUENE VAPOR USING THE ELECTRON ATTACHMENT REACTION

Miss Nantamas Dhattavorn

A Thesis Submitted in Partial Fulfillment of the Requirements
for the Degree of Master of Engineering in Chemical Engineering
Department of Chemical Engineering
Faculty of Engineering
Chulalongkorn University
Academic Year 2000

ISBN 974-13-0767-5

Thesis Title Effect of Temperature on Removal of Toluene Vapor Using the Electron Attachment Reaction
By Miss Nantamas Dhattavorn
Field of Study Chemical Engineering
Thesis Advisor Professor Wiwut Tanthapanichakoon

Accepted by the Faculty of Engineering, Chulalongkorn University in Partial Fulfillment of the Requirements for the Master's Degree.

………………………………………….. Dean of Faculty of Engineering
(Professor Somsak Panyakaew, Dr.Eng)

Thesis Committee

………………………………………………… Chairman
(Associate Professor Chirakarn Muangnapoh, Dr. Ing.)

………………………………………………… Thesis Advisor
(Professor Wiwut Tanthapanichakoon, Ph.D.)

………………………………………………… Thesis Co-Advisor
(Associate Professor Tawatchai Charinpanitkul, Dr. Eng.)

………………………………………………… Member
(Assistant Professor Vichitra Chongvisal, Ph.D.)

นันทมาศ ทัตตะวร : ผลของอุณหภูมิต่อการกำจัดไอโทลูอีนโดยใช้ปฏิกิริยาเติมอิเล็กตรอน
(EFFECT OF TEMPERATURE ON REMOVAL OF TOLUENE VAPOR USING THE ELECTRON ATTACHMENT
REACTION) อ.ที่ปรึกษา : ศ.ดร. วิวัฒน์ ตัณฑะพานิชกุล, อ. ที่ปรึกษาร่วม : รศ.ดร.ธวัชชัย ชรินพาณิชกุล,
124 หน้า. ISBN 974-13-0767-5

จุดประสงค์หลักของงานวิจัยนี้คือ ศึกษาผลของอุณหภูมิที่มีต่อการกำจัดโทลูอีนโดยใช้ปฏิกิริยาเติมอิเล็กตรอน เนื่องจากก๊าซที่ปล่อยออกจากโรงงานอุตสาหกรรมจะมีอุณหภูมิสูง ดังนั้น จึงต้องมีความเข้าใจในเรื่องของผลของอุณหภูมิเพื่อที่จะขยายขนาดของเครื่องปฏิกรณ์แบบปล่อยโคโรนาได้ต่อไป สำหรับตัวแปรอื่น ๆ ที่ทำการศึกษา คือ ขนาดของคาโทด กระแสปล่อยออก ความเข้มข้นขาเข้า เปอร์เซ็นต์ของออกซิเจนและปริมาณของไอน้ำในกระแสก๊าซ

จากการทดลองพบว่า ประสิทธิภาพการกำจัดต่อหน่วยเวลาจะเพิ่มตามอุณหภูมิ และพบว่าคาโทดขนาดใหญ่ กระแสปล่อยออกสูง หรือ เปอร์เซ็นต์ของออกซิเจนมาก จะช่วยเพิ่มประสิทธิภาพการกำจัด ในทางตรงกันข้าม เมื่อเพิ่มความเข้มข้นของโทลูอีนหรือไอน้ำ ประสิทธิภาพการกำจัดจะลดลง และแม้ว่าการวิเคราะห์สิ่งที่เกาะติดบริเวณแก้วส่วนบนของเครื่องปฏิกรณ์โดยใช้เครื่องแก๊สโครมาโทกราฟ แมสสเปกโตรมิเตอร์จะไม่สามารถพิสูจน์ได้แน่ชัดว่าคือสารประกอบใด อย่างไรก็ตาม ผลการวิเคราะห์นี้ก็ช่วยชี้แนะได้อย่างดีว่า อาจเกิดโพลีเมอไรเซชันของโทลูอีนขึ้น นอกจากนี้ ในกรณีของออกซิเจน 30 เปอร์เซ็นต์ จะพบโอโซนเกิดขึ้นและลดลงเมื่ออุณหภูมิเพิ่มขึ้น ในขณะที่ไนโตรเจนออกไซด์จะเพิ่มขึ้นตามอุณหภูมิ

ภาควิชา.........**วิศวกรรมเคมี**................ **ลายมือชื่อ**...
สาขาวิชา.........**วิศวกรรมเคมี**................ **ลายมือชื่ออาจารย์ที่ปรึกษา**..
ปีการศึกษา...........**2543**....................... **ลายมือชื่ออาจารย์ที่ปรึกษาร่วม**..

4070312421 : MAJOR CHEMICAL ENGINEERING
KEW WORD GASEOUS POLLUTANT/GAS PURIFICATION/ ELECTRON ATTACHMENT/ CORONA DISCHARGE

NANTAMAS DHATTAVORN: EFFECT OF TEMPERATURE ON REMOVAL OF TOLUENE VAPOR USING THE ELECTRON ATTACHMENT REACTION. THESIS ADVISOR: PROF. WIWUT TANTHAPANICHAKOON, Ph.D. THESIS CO-ADVISOR: ASSOC. PROF. TAWATCHAI CHARINPANITKUL, Dr.Eng., 124 pp. ISBN 974-13-0767-5

The objective of this research is to investigate the effect of temperature on toluene removal using electron attachment reaction. Because of the high temperature found in the exhaust gas from many industrial sources, temperature effect must be understood in order to scale up of the corona discharge reactor. The other parameters investigated are the cathode diameter, discharge current, inlet concentration, percentage of oxygen and the amount of water vapor in the gas stream.

As seen from the experimental results, the removal efficiency per residence time generally increases with the temperature. It is found that the thicker the cathode diameter, the higher the discharge current, or the higher the percentage of coexisting oxygen, the removal efficiency becomes. On the other hand, the higher the inlet concentration of toluene or water vapor, the lower the removal efficiency becomes. Though the analysis of the deposit sample found the glass section at the top of the reactor has been carried out using a gas chromatograph/mass spectrometer, the identification of the compounds is not completed yet. However, the evidence strongly suggests that polymerization of toluene may occur. Moreover, in the case of 30 percent oxygen, ozone concentration is measured and found to decrease when the temperature increases, while NO_x increases with the temperature.

Department…**Chemical Engineering**…. **Student's signature**………………………………………………
Field of study…**Chemical Engineering**... **Advisor's signature**……………..…………………..…………..
Academic year….……**2000**..………...…. **Co-advisor's signature**……………………………….……………

ACKNOWLEDGEMENT

I am very grateful to my thesis advisor, Prof. Wiwut Tanthapanichakoon for his helpful suggestion. He has given me encouragement to continue during hard times. I am also grateful to Assoc. Prof. Tawatchai Charinpanitkul (my thesis co-advisor), Assoc. Prof. Chirakarn Muangnapoh and Assist. Prof. Vichitra Chongvisal for their stimulative comments and participation as the thesis committee.

I would like to thank Dr. Noriaki Sano for his training, useful guidance, hospitality, and educational suggestions. It has been my great pleasure to share good times with his nice friendship.

I would like to express my gratitude to Dr. Jirdsak Tscheikuna for his kindness to allow me to setup the experimental apparatus in the Hazardous Reaction Laboratory over 1 year and thanks to all members of his laboratory for everything. I have had a nice year during that period.

I would like to acknowledge the TJTTP-JBIC and the Thailand Research Fund (TRF). The present work is part of a joint Thailand-Japan research project. I have also received monthly financial support and material support from TRF given via Prof. Wiwut's TRF Senior Research Scholar Award in Particle Technology.

Sincere thanks are due Mr. Paisarn Khongphasarnkaln for his training and good suggestion and Mr. Somchai Mahitthiroch for his suggestion and information on the analytical instruments. Also I want to thank Mr. Bancha Ounpanich for his help in the setting of the temperature-profile checking.

Thanks to all members of the Particle Technology and Material Processing Laboratory for their warm collaborations.

Last, but far from least, the love, patience and encouragement of my parents were indispensable

CONTENTS

Page

CONTENTS (Cont.)

Page

CONTENTS (Cont.)

Page

LIST OF TABLES

LIST OF FIGURES

Page

Page

NOMENCLATURES

C_{in} = inlet concentration [ppm]

C_{out} = outlet concentration [ppm]

C_{out} = outlet concentration [ppm]

C_{out} = outlet concentration [ppm]

ψ = apparent removal efficiency [%]

ψ' = removal efficiency [%]

ψ'' = removal efficiency per residence time [%/s]

I = discharge current [mA]

P = power consumption [W]

p = pressure [Pa]

SV = space velocity [hr^{-1}]

V = discharge voltage [V]

R = anode radius [m]

R_0 = cathode radius [m]

CHAPTER I

INTRODUCTION

Nowadays, air pollution has become one of the most serious environmental problems. There are many sources of air pollutants such as heavy concentration of vehicles that release a large amount of toxic and obnoxious emissions. In addition, urban and suburban air quality may have deteriorated to an unacceptable level of various gaseous pollutants as well as particulate matter because of emission from a sizable number of industrial plants.

In the chemical industry, organic solvents such as aromatic hydrocarbons, alcohol, ketones and esters are widely found in many applications, including plastic industry, printing ink industry, paint and adhesive industry. Several chemical solvents are not only used as solvent but also used to extract, or as reagent for preparing, other chemicals. Although these chemicals are useful and necessary to meet human needs, they also lead to strong impact on the environment. In short, their properties are often toxic to the life cycle, flammable and sometimes malodorous. If there happens any leakage from a process to the environment, it can cause adverse effect to the environment and human health. It is also known that cancer may result from repeated and/or prolonged exposure to some dilute solvent vapor. The emission standard of solvents from a stack to the atmosphere is often controlled at the level of parts per million (ppm) and the total amount of each chemical released in a specified time duration is also controlled. In any case inadequately treated emission will lead to air contamination problems, not to mention bad smell that becomes public nuisance.

Calm wind also aggravates the air pollution problem. If there is not sufficient wind dilution effect, the pollutant gas will not disperse well to the atmosphere. Then the pollutant gas will drop back to the ground level not far from the plant, thus causing problems to the community around the factory. Several instances have happened around the Mabtaput Industrial Estate, including one widely reported in May 1996. In that incident, teachers and students in Mabtaput Panpittayakarn School, Buddhist monks in Wat Sophonwanaram and several communities numbering about 15,000 persons around the Industrial Estate were affected by malodorous gases that spread from the Estate, and many of them became sick. Their symptoms were respiratory irritation, bronchial asthma, vomit and skin irritation.

Most factories in the chemical process industry utilize many types of solvents or volatile organic compounds (VOCs) in their processes. Generally the regulated emission values are set at the level of ppm. However in some cases, such as dioxins, the current emission standard may be too high for the long-term health of human being. In addition, some conventional gas purification methods are not economically suitable for the effective treatment of low concentration gas. Because of wider public complaints and heightened awareness of the danger associated with polluted air, more attempts at air pollution control have increasingly been made. In this research, electron attachment reaction in a corona discharge reactor will be used for the treatment of low concentration air pollutants.

The VOCs investigated in this research is toluene (methyl benzene), which has an aromatic-hydrocarbon structure. This chemical has the 24th highest production rate in the USA and is widely used in the chemical industry. Toluene is on the “list of hazardous air pollutants” which gives general information on the source of the pollutant and the nature of the known or suspected adverse health effects associated with exposure. Inhalation of toluene may cause irritation of the upper respiratory tract. Symptoms of overexposure may include fatigue, confusion, headache, dizziness and drowsiness. Peculiar skin sensations (e.g. pins and needles) or numbness may be produced. Very high concentrations may cause unconsciousness and death.

The major use of toluene is as a mixture added to gasoline to improve its octane ratings. Toluene is also used to produce benzene and as a solvent in paints, coatings, adhesives, inks, and cleaning agents. Toluene is also used in the production of polymers related to nylon, plastic soda bottles, and polyurethanes and in the production of pharmaceuticals, dyes, cosmetic nail products, and the synthesis of organic chemicals. The vapor may cause headache, nausea, dizziness, drowsiness, confusion and incoordination. Toluene also causes skin and eye irritation. It is an aspiration hazard and swallowing or vomiting of the liquid may result in aspiration into the lungs.

By the way, it has been reported that toluene vapor is the adverse component of the highest concentration in the gas samples taken at the Maptaput Industrial Estate when the above-mentioned incident happened in May 1996.

In this research emphasis will be placed on the effect of the gas temperature because it has not been investigated while the exhaust temperature of most stack gases is always higher than room temperature.

1.1 Objective of research work

1.1.1 Carry out experiments to find out the effect of temperature on the removal efficiency of toluene from an inert gas at atmospheric pressure using the deposition-type reactor.

1.1.2 Investigate the influence of coexisting gas components on the removal efficiency of toluene vapor from nitrogen.

1.2 Scope of research work

1.2.1 The experimented gas in this research is toluene

1.2.2 The influence of coexisting gas components is:

- Oxygen or water vapor

1.2.3 The experimented conditions investigated are as follows:

- 3 discharge currents
- 3 cathode sizes are investigated
- 3 inlet concentrations
- Space velocity gas at room temperature is 55.8 hr^{-1}
- Temperature range is room temperature to 400 °C

CHAPTER II

LITERATURE REVIEW

Gas discharge technology is one promising method of achieving ultrahigh purification. Application of gas discharge processes with high-energy electrons has existed for over a hundred years, dating to the first electrostatic precipitator of Lodge (Oglesby and Nichols, 1978) and ozonizer of Simens (Horvath, 1980). The electrostatic precipitator (ESP) is a device-utilizing corona discharge for removing particulate pollutants in the form of either a solid (dust or fumes) or a liquid (mist) from a gas using the electrostatic force. One may realize that the corona-discharge reactor for the gaseous pollutant remover used in this work has the same working principle as ESP. Most information on ESP however focuses on the removal of particulate matter, whereas the reactor proposed in this work, utilizing low-energy electrons in gas discharge to induce electron attachment reaction, aims at separating gaseous impurities from a gas stream. Application of the electron attachment (a reaction of low-energy electrons and gas molecules to produce negative ions), first proposed by Tamon et al. (1989), is still innovative for gas seperation processes nowadays.

Many publications on electron attachment and other reactions of electron with many kinds of gas molecules have appeared but most of them involve only the reaction kinetics (Moruzzi and Phelps, 1966, Caledonia, 1975 and Massay, 1976). In fact basic information on gas purification using electron attachment and the proposed use of the selectivity of electron to remove the electronegative gaseous molecules are still scarce.

Applications of gas discharge technology conducted to date are reviewed as follows.

Castle, Inculet, and Burgess (1969) discussed briefly about surface oxidation of discharge electrodes used in a wire-tube electrostatic precipitator. The rate of ozone generation in the precipitator with both stainless steel and copper wires was clarified. The reaction rate of ozone depended on the intensity of electron flux through the gas. The concentration of ozone generated was a linear function of current but decreased as the gas temperature increased.

Dorsey and Davidson (1994) reported an assessment of the contribution of contaminated wires and plates to ozone production in electrostatic air cleaners. It was found that runaway ozone generation due to contamination of electrode surfaces was a limiting factor in the long-term (7 weeks) effectiveness of electrostatic air cleaners. The corona discharge degraded to streamers after only two weeks, causing increased ozone levels. Wire contamination alone can increase ozone generation. These findings have serious implications for the safe operation of electrostatic air cleaners.

Chemical Vapor Decomposition (CVD) occurring on a discharge wire of an electrostatic air cleaner causes the corona current to decrease more than 95% at the same voltage (after 180 hrs operation). This phenomenon was shown by Jan H. Davidson et al. (1998). Neither current drop nor deposition occurred when operated with clean or dry air (after 2 days).

Tamaki et al. (1979) reported the use of DC and AC coronas for the removal of NO from a flue gas under several discharge conditions. However, the process was energywise inefficient, and the performance was poor. The poor performance was probably due to the small ionization region of DC coronas (small active treatment volume), and the power efficiency was low because a large amount of energy was expended on ion migration, which did not contribute to the production of radicals.

Several types of DC energized point-electrode reactors have been developed and tested for gas chemistry applications. Although designed with different purposes in mind, the configurations could be put to other uses.

Castle, Kanter, Lee, and Kline (1984) tested a narrow-gap, multipoint-to-plane geometry device in which the gas passed through a corona discharge at high velocity (approximately 100 m/s). The upper multipoint electrode (cathode) was separated from the lower flat electrode (anode) by acrylic spacers that electrically isolated the electrodes and allowed visual observation of the corona. The narrow gap spacing ensured that the inter-electrode space was filled with corona induced plasma. However, the lateral spacing of the pins allowed major fractions of the gas flow to bypass the corona zones. A DC current was applied to the multipoint pins through current limiting resistors.

Another type of a multipoint-to-plane device was constructed by Yamamoto, Lawless, and Sparks (1988, 1989). This device was in the form of a narrow-gap, triangle-shaped, DC corona discharge device. The design was intended to reduce the electrical sneakage (bypassing of the corona induced plasma) which was the major problem for the device with multipoint-to-plane geometry. The volumetric filling factor of the corona induced plasma in this device was much higher than in the typical multipoint device.

An experimental investigation has been conducted by Chang, Jen-Shih et al. (1988) to obtain electrode surface temperature profiles of cylindrical hollow electrodes under corona discharges. The result show that a slight temperature increases (about 5 Kelvin within the 10 W input for discharge power level) occurs near the edge of the cylindrical hollow electrodes. Thus, the corona discharge still can be categorized as a cold discharge region.

The pulsed electron technology has also been shown to be capable of generating ozone and active radicals and decomposing several unwanted gases as well as aerosol particles.

Higashi, Sugaya, and Ueki (1985) and Weiss (1985) conducted the reduction of CO_2 the in exhaust gas from a diesel engine vehicle. It was shown that CO_2 concentration in a N_2-CO_2 or even pure CO_2 gas could be reduced by DC and pulsed corona discharges, respectively. Further experiments for soot elimination and NO_x and SO_x reduction in a diesel-engine exhaust by a combination of discharge plasma and oil dynamics have been investigated by Higashi, Uchida, Suzuki, and Fujii (1991, 1992).

Chang (1989) and Chakrabarti et al. (1995) found that the removal of NO_x, SO_x, and aerosol particles could be achieved when NH_3 or H_2O was introduced into a pulsed streamer corona reactor. The pulsed electrons have been shown to cause reactions between oxidizing radicals such as OH, O, and O_3 on the one hand and NO_x and SO_x on the other hand at the concentrations found in flue gases to form several acidic aerosol particles with NH_3 or H_2O injections.

Recent experimental study done by Helfritch (1993) led to the conclusion that H_2S decomposition to hydrogen and sulfur could be directly achieved electronically. A wire-in-tube pulsed corona reactor was energized by short voltage spikes to decompose small concentrations of H_2S contained in nitrogen. Some parameters including the reactor geometry, H_2S concentration, corona power, and the nature of the products were investigated.

Mizuno, Clements, and Davis (1986) compared the performance of the pulsed streamer corona, DC corona, and electron-beam processes. It was found that a pulsed streamer corona discharge produced the radicals instead of a high-energy electron beam. A positive pulsed streamer corona discharge in a nonuniform electrode geometry showed better energy efficiency and higher removal performance than a DC corona discharge. Based on the delivered power, the pulsed streamer corona process removed more than 90% of SO_2 with at least two times better power efficiency than the energetic electron-beam process.

Masuda, Sato, and Seki (1984) developed a high-efficiency ozonizer using traveling wave pulse voltage. The test results relating to the pulse-induced ozone generation showed a great enhancing effect on the speed of reactions by positive pulse corona producing streamers bridging across the entire electrode gap. It was believed that the ozone generated in a corona discharge was a two step process: generation of oxygen free radicals by ionic processes and generation of ozone by free radical reactions. It was found that the ozone generation processes were substantially reduced by increasing the gas temperature, while the ozone loss processes were significantly enhanced by increasing the gas temperature. It was therefore recommended to operate an ozonizer in lower temperature conditions.

High-voltage pulser was used in a pulse-induced plasma chemical processing unit (PPCP unit). This pulser comprised a synchronous rotary spark gap that produced a very sharp negative pulse voltage. High electron energies could be achieved by both units since higher electric fields were allowed in surface-corona and pulse-corona systems than in direct-current systems because of the breakdown limits of the discharge.

Eliasson, Hirth, and Kogelschatz (1987) applied a dielectric-barrier discharge for ozone generation from oxygen. The resulting efficiency of the generation was reported. A value of 1200 g/kWh was the theoretical ozone generation efficiency calculated by thermochemical theory. He also estimated the maximum ozone generation efficiency of 400 g/kWh for pure oxygen by analyzing a Boltzmann equation. The actual ozone generation efficiency was approximately 200 g/kWh for pure oxygen, which was very low compared to the theoretical values. It was because the discharge energy was consumed not only in producing the ozone but was also dissipated in heating the test gas and the electrodes of the ozonizer. Also some of the ozone produced was destroyed by the heat.

After the work of Eliasson et al., there has been attempt to improve the ozone generation efficiency. Ito, Ehara, Sakai, and Miyata (1990) reported that the efficiency in the silent discharge showed a rise of 3-6% by the radiation of ultra-violet ray from the discharge in nitrogen gas. Later, Hattori, Ito, Ehara, and Miyata (1992) reported the superposition effect of two types of discharge in the same discharge space, silent and surface discharges, on ozone generation. Their ozonizer had two power sources with a variable-phase shifter. A 22-30% increase in the efficiency was observed in their ozonizer.

A packed ferroelectric (high-dielectric ceramic) pellet layer used for an electrostatic precipitator was originally developed by Mizuno (1986). Basic performance of the AC energized ferroelectric packed-bed reactor was studied. The effect of the dielectric constant of the packed ferroelectric pellets on the particle collection efficiency was also investigated. In the operation to collect precharged particles, the particle penetration became minimum at a certain voltage V_{aco} and increased when the applied voltage exceeded V_{aco}. The value of V_{aco} became lower with the increase in the dielectric constant value. V_{aco} was always higher than the initiation voltage of partial discharge for all the pellets tested.

Later in 1988, Mizuno and Ito started to apply a packed bed reactor with ferroelectric $BaTiO_3$ pellets to decompose ammonia from dry air. The reactor employed the AC discharge generated inside a pellet layer held within the tube arrangement by two mesh electrodes. An intense electric field was formed around each dielectric pellet contact point, producing high energy free electrons as well as molecular ions throughout the cross section of the reactor.

Yamamoto et al. (1992) constructed a laboratory-scale plasma reactor with a packed ferroelectric (high-dielectric-ceramic) pellet layer and a nanosecond pulsed corona reactor. This study was the first attempt to develop baseline engineering data on the application of these plasma reactors to the destruction of various volatile organic compounds (VOC's) at ppm levels. The conversion rate of VOC's was found to be dependent on the electron energies in the reactor and may also be related to how strongly halogen species were bonded to the carbon.

Mizuno, Chakrabarti, and Okazaki (1993) was the first group that developed the combination of corona and catalyst technology. They reported a corona/catalyst arrangement, which consisted of a needle and a grounded mesh electrode with 40-mm separation. Immediately after the corona section, the 20-mm thick catalyst layer consisting of Al_2O_3 pellets was held in place by the screen. Gas was exposed to the pulsed corona, immediately followed by the catalyst. This was considered a two-stage process.

Yamamoto et al.(1996) demonstrated a new concept--single-stage, catalysis-assisted packed-bed plasma technology, to decompose CCl_4, one of the ozone-depleting substances. The objective of the concept was twofold: to enhance the decomposition efficiency catalytically, and to selectively reduce the by-products. Either $BaTiO_3$ or $SrTiO_3$ pellets were packed in the ferroelectric packed-bed reactor employing an AC power supply. The configuration employed a unique one-stage catalysis/plasma process in which the $BaTiO_3$ pellets were coated or impregnated by active catalysts such as Co, Cu, Cr, Ni, and V. Enhancement of the CCl_4 destruction and the conversion of by-product CO to CO_2 were demonstrated using Ni catalyst in the one-stage plasma reactor.

The so-called non-thermal plasma including corona discharge has been widely studied

A nonthermal plasma chemical process with an AC powered ferroelectric packed-bed reactor was again tested by Zhang, Yamamoto, and Bundy (1996). In this work, the targeted gases to be decomposed were ammonia and odorous compounds gathered from animal houses. The plasma reactor packed with $BaTiO_3$ pellets produced high energy free electrons and radicals, which in turn, decomposed the targeted compounds. Four important parameters affecting the reactor performance were investigated: gas residence time, power voltage, power frequency and initial ammonia concentration.

Tamon, Sano, and Okazaki (1989) proposed a novel method of gas separation based on electron attachment. Two kinds of separation devices using either photocathode or glow discharge as electron source were constructed. They reported high efficiency for the removal from nitrogen of SF_6 at very low concentrations. Recently, Tamon et al. (1995) used two types of corona-discharge reactors, deposition-type and sweep-out-type reactors, to remove from nitrogen dilute sulfur compounds, dilute iodine and oxygen. They also discussed the purification mechanism and presented simulation models for predicting the removal efficiency. Subsequently, Tamon, Sano, and Okazaki (1996) investigated the influence of coexisting oxygen and water vapor on the removal of six sulfur compounds from nitrogen. They discovered that the presence of oxygen and water vapor increased the removal efficiency.

Sano et al. (1996) used a new type of corona-discharge reactor, the wetted-wall reactor, and the conventional deposition-type reactor to remove iodine and methyl iodide from nitrogen. The removal mechanism of I_2 and CH_3I in the reactor was also discussed.

Kittisak Larpsuriyakul et al. (1996) and Wiwut Tanthapanichakoon et al. (1996) reported experimental results regarding the influence of the structure of the corona-discharge reactor on the removal of dilute gases. The effects of the reactor structure, namely the cathode diameter, the anode shape, and the number of cathodes, were investigated. The results revealed that the thicker the cathode diameter, the higher the removal efficiency. In contrast, the smaller the reactor diameter among three equivolume reactors, the higher the removal efficiency. As for the number of cathodes in a single reactor vessel, the single-cathode reactor always exhibited a higher removal efficiency than the 5-cathode one.

Paisarn Khongphasarnkaln (1997) investigated the application of electron attachment to the removal of dilute gaseous pollutants using a corona-discharge deposition-type reactor. It has been found that the presence of O_2 enhanced the removal efficiency of each impurity gas. The enhancement was experimentally shown to be attributable to the ozone reaction in the removal of $(CH_3)_3N$ from O_2-N_2 mixed gas. Water vapor also enhanced the removal efficiency of $(CH_3)_3N$ and CH_3CHO. Furthermore, The high selectivity of electron attachment to electronegative gas molecules was utilized in the simultaneous removal of dilute $(CH_3)_3N$-CH_3CHO, NH_3-CH_3CHO, SO_2-$(CH_3)_3N$, SO_2-CH_3CHO, NO_2-CH_3CHO and CO_2-CH_3CHO from the air in the single reactor. Compared to single impurity removal, it has been shown that the presence of SO_2 enhanced the removal efficiency but retarded that of CH_3CHO in the single reactor. Some reaction by-products generated could be avoided by using two independently operated reactors in series. In the case of coexisting of NO_2, it was noted that the lower the inlet NO_2 concentration, the lower the discharge current that still yielded beneficial effect. At higher discharge currents, the retarding effect of CO_2 on CH_3CHO removal was obviously significant.

Han S. Uhm (1998) investigated the influence of the chamber temperature on the properties of the corona discharge system. It was found that the critical voltage V_c required for the corona discharge breakdown was inversely proportional to the chamber temperature T. The electrical energy w_c required for corona discharge breakdown was inversely proportional to the square of the chamber temperature T. Thus, the electrical energy consumption for the corona discharge system decreased significantly as the temperature increased. The plasma generation by corona discharge in a hot chamber was much more efficient than that in a cold chamber.

CHAPTER III

FUNDAMENTAL KNOWLEDGE

The self-sustaining discharge in a heterogeneous electric field between a thin wire and a coaxial cylinder is called a corona discharge. This name is descriptive of the glowing light effects found if the voltage is several kilovolts. Corona discharge can be generated at or near atmospheric pressure. The gas pressure need not be high for the discharge to occur, but at low gas pressure the corona is not visible. The luminous part of the discharge is usually restricted to a region close to the wire, which may be positive or negative with respect to the cylinder. One distinguishes between positive and negative coronas, by the voltage of the central electrode.

Coronas are by no means a product of man only. It is the phenomena of the glow or corona surrounding the sun and is only seen during a total eclipse of the sun. Besides, nature produces them between and within electrically charged clouds. A theory on cloud electrification attributes this process to the corona on and around ice particles in the clouds. According to this theory, corona is not only the effect but also the cause of the appearance of charged clouds and therefore of lightning and thunderstorms.

In corona discharge reactor, there are three regions in the space between the anode and cathode.

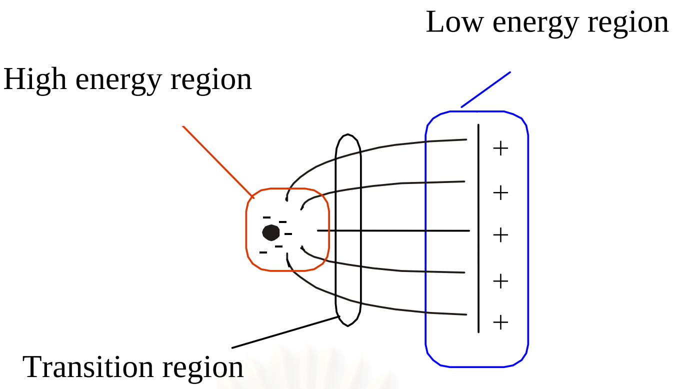

Figure 3.1 Wire to plate electrodes

In the high electron energy region, free electrons are emitted from the cathode and strongly accelerated. Gas molecules will be ionized after collision with high-energy electrons and positive ions are produced. In the transient region, electron energy is just enough to dissociate gas molecules to produce neutral radicals. In the last region of low-energy electrons, electrons are captured after collision with gas molecules. Cluster formation and electron attachment reaction generally take place in this region.

3.1 Electron attachment reaction

When low-energy electrons collide with electronegative gas molecules, some of the electrons are captured by some gas molecules, and negative ions are formed. This phenomenon is called "electron attachment" (Massay, 1976). Electron attachment depends on the electron energy level, the structure of the gas molecule, and its electron affinity. There is a huge difference between the electron attachment probability of the electronegative gas molecules and that of the neutral carrier gas. This high selectivity is reflected in the production of negative ions (Caledonia, 1975 and Massay, 1976, 1979). Therefore, electronegative impurities of very dilute concentration become negative ions by electron attachment, and they can effectively be separated from the neutral gas (for example, N_2) in an electric field.

In the case of an excessively-high-energy electron colliding with the gas molecule, the molecule would not only be negatively ionized but may also be dissociated or positively ionized due to the loss of one electron from the molecule itself. In contrast, if an electron whose energy is too low reaches the molecular orbital, the electron can not be captured by the molecule. It is necessary to take into account the moderate (appropriate) range of electron energy when the attachment probability is to be enhanced. A great deal of effort has been devoted to generate or utilize electrons with a variety of energy range via quite a number of gas-discharge devices. However, the appropriate range of electron energy contributing exclusively to electron attachment generated by such devices has not been clarified because of the limitation of measurement devices and/or techniques.

At the exact moment when an electron is captured by a gas molecule, the molecule would be placed in an excited state. To become stable, the molecule must release the excess energy in quanta, for example, by collision with another electron, by collision with another gas molecule, by being decomposed, or by radiation. Various processes for the electron attachment reaction have been reported (Moruzzi and Phelps, 1966) as illustrated by **Eq. (3.1), (3.2), and (3.3).** A mixture of an electron-attaching gas, AB, and an appropriate gas species, M, is considered in these processes.

Dissociative attachment: $e + \mathrm{AB} \rightarrow \mathrm{A}^- + \mathrm{B}$ (3.1)

Three-body attachment: $e + \mathrm{AB} + \mathrm{M} \rightarrow \mathrm{AB}^- + \mathrm{M}$ (3.2)

Radiative attachment: $e + \mathrm{AB} \rightarrow \mathrm{AB}^- + h\nu$ (3.3)

Since the electron attachment probability of the gas molecule is dependent upon its electron affinity, it is reasonable to expect that a molecule that contains one or more atoms with high electron affinity would have a high probability of electron attachment. For example, in a comparison between SF_6 and N_2, the electron affinities of S, F, and N are 200 kJ/mol, 333 kJ/mol, and –26 kJ/mol, respectively. So it is not surprising that the probability of electron attachment for SF_6 molecule is reportedly 10^{11} times that of N_2 molecule (Hickman and Fox, 1956). This huge difference in the electron attachment probability among various kinds of gas molecules results in high selectivity in the formation of the corresponding negative ions. Therefore, even a specific gas component whose concentration is extremely low can effectively be separated from the main (neutral) gas in an electric field by utilizing the electron attachment reaction. As a consequence, the method based on electron attachment can be expected to be one of the most efficient methods of gas purification.

3.2 Principle of gas purification

Figure 3.2 illustrates the principle of gas purification by the removal of an impurity, AB, from an inert gas in a cylindrical corona-discharge reactor (Tamon et al., 1995). The corona discharge is employed here because it is an efficient

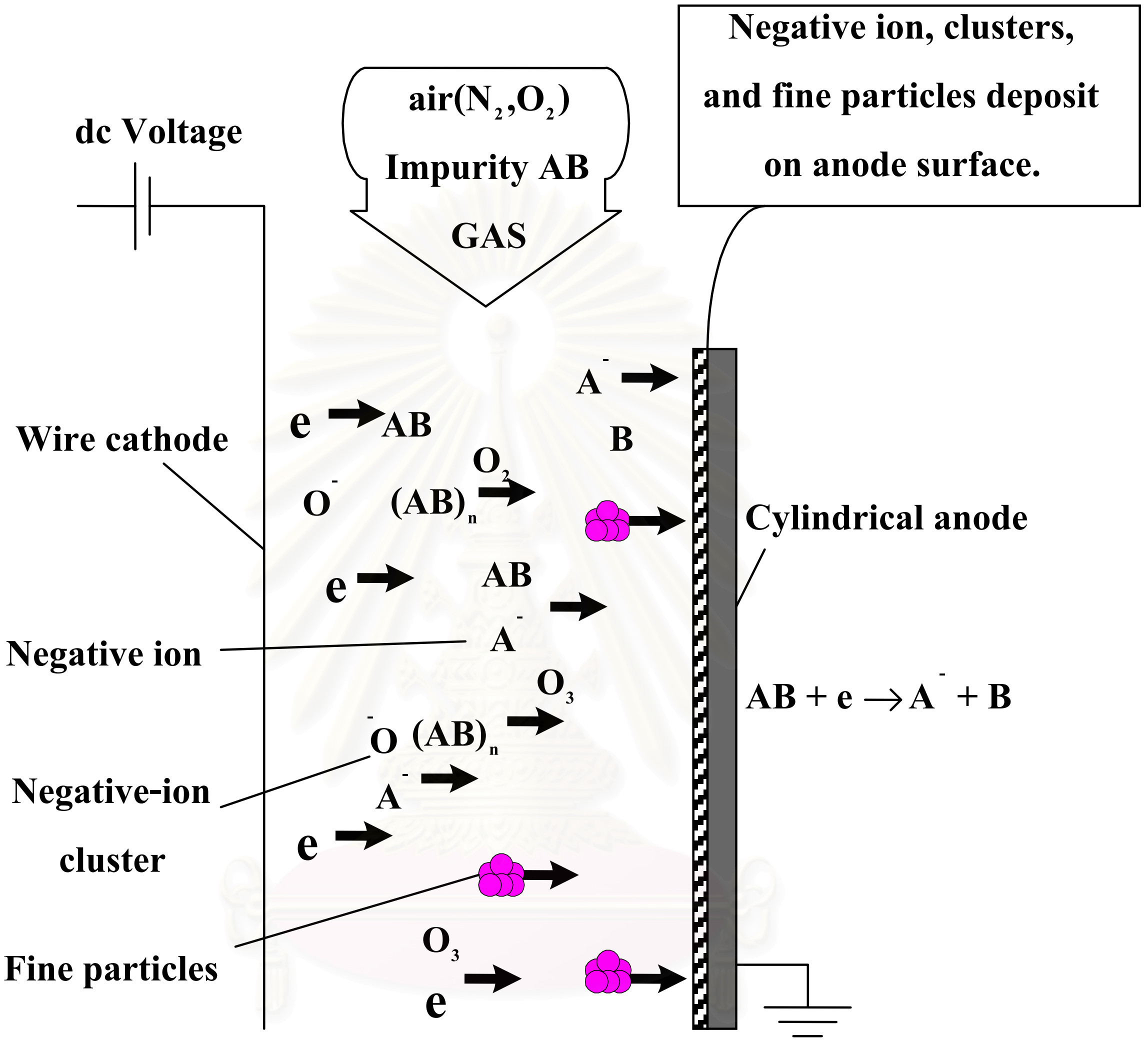

Figure 3.2 Principle of Gas Purification

method to supply a large number of low-energy electrons to the gas stream. A wire stretched along the axis of the reactor acts as cathode and the outer cylinder acts as grounded anode. High DC voltage applied to the cathode induces corona discharge in the reactor. Electrons generated at the cathode drift to the anode along the applied electric field. During their drift, a portion of them collides with the gas molecules. Negative ions, A^-, are thus selectively produced by electron attachment and they likewise drift to the anode as the electrons do.

In an ideal case, the number of electrons generated in the reactor is sufficient for all gaseous impurities to hitch up with the electrons and all negative ions thus generated are able to completely deposit at the anode surface. In other words, the outlet gas is devoid of unwanted impurities and complete removal is achieved.

In reality, upon their arrival at the anode, certain kind of negative ions might discard their charges but do not deposit on its surface. In this case such gaseous impurities can not be separated using the simple deposition-type reactor. It is therefore very desirable to capture most of the negative ions arriving at the anode surface. The idea of how to remove negative ions at the anode will be described later.

Besides the above-mentioned removal mechanism associated with electron attachment reaction in a corona-discharge reactor, it is believed that other removal mechanisms may simultaneously affect the removal efficiency. When negative ions are produced in the reactor, they may possibly interact with other gas molecules via their electrostatic forces and negative-ion clusters may be formed. Each cluster then contains more than one of the gas molecules targeted for removal. When the clusters drift to the anode and deposit there, the removal efficiency is enhanced by the formation of negative-ion clusters.

Another possible mechanism contributing to the removal efficiency is the so-called radical reaction. When dissociative electron attachment also takes place in the reactor, not only negative ions but also reactive radicals are produced. In particular, radicals may readily be produced in the immediate vicinity of the cathode surface where high electric field strength exists. It is logical to assume that the removal efficiency would be enhanced by radical reaction, which often results in the generation of by-products.

The reaction of gas molecules with O_3 is frequently mentioned. Ozone reaction can take place when oxygen coexists in the gas stream. High energy electrons close to the cathode collide with O_2 molecules to dissociatively produce O radicals. O radicals can next react with O_2 molecules to produce O_3, which is reactive with various kinds of gases. Hence, ozone reaction is expected to contribute to the oxidative destruction of a number of gaseous impurities in the gas stream, thus improving the removal efficiency.

3.3 Types of reactor

As mentioned above, in some cases certain kind of negative ions produced by electron attachment would drift towards but do not easily adhere to the anode surface. Thus they end up as uncaptured electronegative impurities at the outlet of the simple deposition-type reactor, and cause a decrease in their removal efficiency. It is therefore essential to find out how to remove such negative ions at the anode. This has motivated Tamon et al. to propose three types of reactor, as shown in **Figure 3.3**.

3.3.1 Deposition-type reactor

Some negative ions readily adhere to the anode surface of the reactor after releasing their negative charges there. Thus they may form solid particles or react with the metallic anode. The solid particles form a deposition layer on the anode surface. In this case, the so-called deposition-type or (simple) reactor is adequate for the removal of negative ions. Periodical cleaning of the anode surface or its replacement is necessary to maintain high removal efficiency.

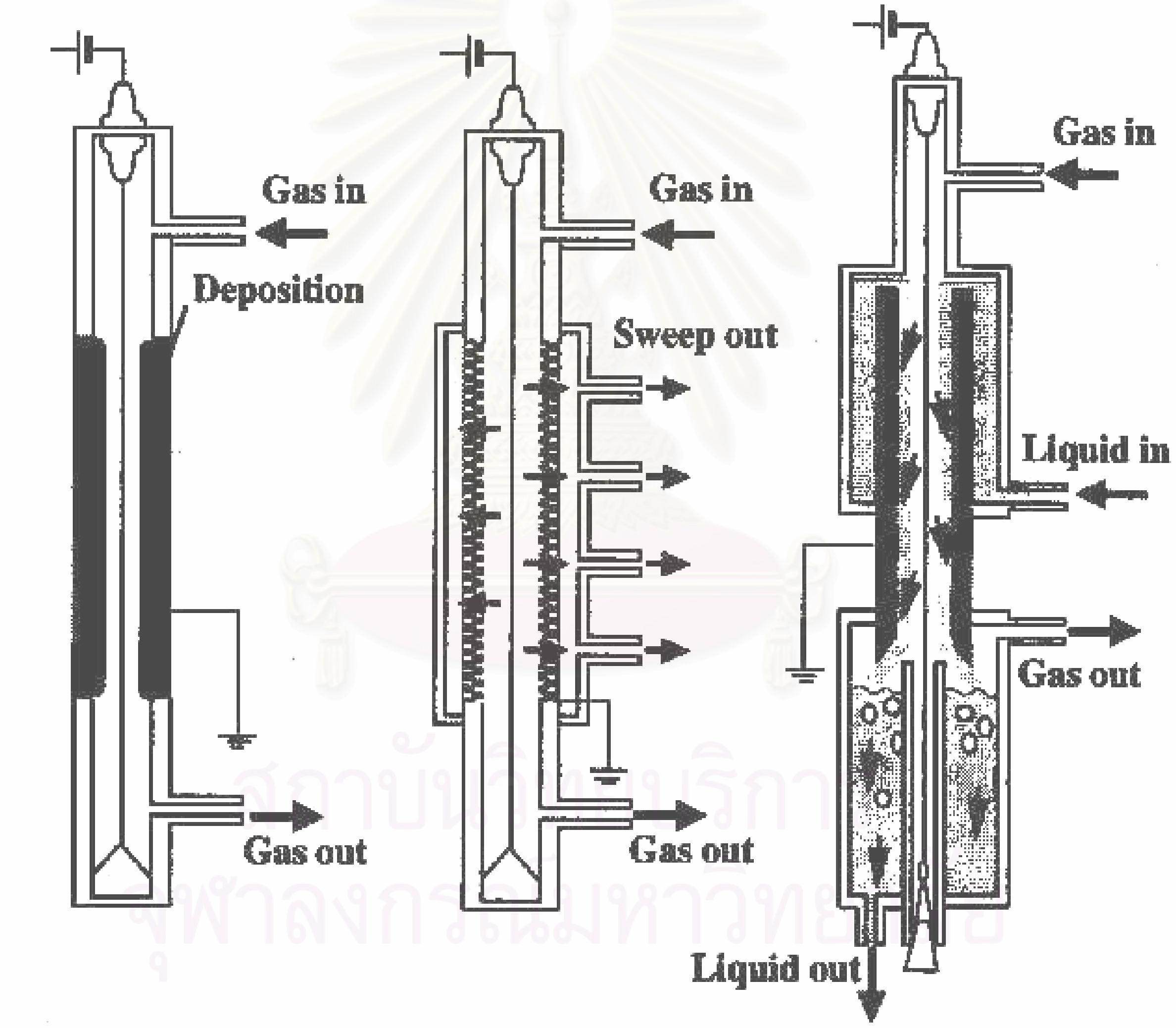

(a) Deposition-type (b) Sweep-out-type (c) Wetted-wall

Fig 3.3 Concepts of corona-discharge reactor

3.3.2 Sweep-out-type reactor

In some cases certain negative ions do not easily deposit on the anode surface but change back to the original molecules after releasing electrons at the anode surface. In such cases, the deposition-type reactor is not suitable because the original molecules of the gas impurities are not removed but diffuse back to the main gas stream. To solve this problem, the sweep-out-type reactor that uses a porous pipe made of sintered metal as anode is recommended. A small amount of the gas around the anode surface is swept out by suction through this pipe to restrict backward diffusion of the enriched electronegative impurities in order that the removal efficiency would be kept high. The swept-out stream with high concentration of the gas impurities can then be treated using a suitable conventional method.

3.3.3 Wetted-wall reactor

Another option to remove negative ions at the anode surface is the wetted-wall reactor. Negative ions reaching the anode of the reactor can be absorbed into a flowing liquid film on the anode surface. This absorption of the ions improves the removal efficiency. The advantage is the self-cleaning of the anode, which makes it suitable even for dirty gas streams containing dust and gaseous pollutants. The major drawback is the need for a liquid (mostly water) treatment and recycle system.

Anyway, the corona-discharge reactor to be investigated in this work is only the deposition-type one because it is easier to construct and operate, and is applicable as a first step of the fundamental study in a laboratory.

3.4 Effect of oxygen (ozone effect)

When O_2 is present in a gas mixture, it could react with discharged electrons. Electron attachment on O_2 has been reported in the literature (Morruzzi and Phelps, 1966; Massay, 1976; Rapp and Briglia, 1976; Chantry and Schulz, 1967).

$$O_2 + e^- \longrightarrow O_2^- \qquad (3.4)$$

$$O_2 + e^- \longrightarrow O + O^- \qquad (3.5)$$

Moruzzi and Phelps (1966) reported that the reaction in **Eq. (3.4)** occurs in the low electron energy range ($E/p < 1.5$ V.m^{-1}.Pa). In contrast, the reaction of **Eq. (3.5)** occurs in the higher electron energy range. Also in the corona-discharge reactor, the closer the electrons are to the cathode wire, the higher their energy level.

When O_2 collides with a high-energy electron near the cathode wire in the corona-discharge reactor, production of O^- is expected as in **Eq. (3.5)**. Then O_3 is produced from the reaction of O^- with O_2 (Loiseau et al., 1994; Hadj-Zaine et al., 1992).

In short, some ozone (O_3) is produced. Since O_3 is very reactive, the ozonation reaction is used in some commercial devices for deodorization and sterilization. The same ozonation reaction is expected to contribute to the removal of gas impurities in the present corona discharge reactor.

3.5 Effect of negative-ion cluster

If a negative ion induces the formation of a cluster with gas molecules, the removal efficiency of the impurities will be improved. This effect is significant because one negative ion and several gas molecules constitute a cluster.

3.6 Effect of temperature

The influence of reactor temperature on the relationship between the voltage and the current has been confirmed Sano et al. (1997): the higher the temperature is, the lower the required voltage becomes. Reportedly, several factors may be considered as the reason for the temperature dependency of the voltage-current relationship. They are (1) the change in the frequency of the thermal electron emission from the cathode surface to initiate the corona discharge; (2) the change in the propagation rate of free electrons in the high electric field region around the wire cathode; (3) the change in the ionization rate of the gas molecules; (4) the change in the mobility of the ions.

Concerning the temperature effect on the dissociative electron attachment of O_2, it was reported that the dissociative electron attachment rate increased when the temperature increased. It can be considered that the formation of cluster is inhibited by temperature elevation because the ion clusters are thought to be less stable at high temperature condition.

CHAPTER IV

EXPERIMENTAL

4.1 Test Materials and Chemicals

Table 4.1 The Specifications of test materials and chemicals

Type	Use	Company	Purities / Grade
Toluene (l)	For preparing toluene vapor(normally 2000 ppm)		
Distilled Water	For preparing water vapor	-	-
Oxygen	Coexisting gas	TIG*	Industrial grade
Nitrogen (g)	Carrier and diluent gas to reactor	TIG	UHP 99.999 % min
Nitrogen (g)	Carrier in GC (FID detector)	TIG	HP 99.99 % min
Hydrogen	For flame ignition	TIG	HP, 99.99%
Air Zero	For flame ignition	TIG	N/A
Helium	Carrier in GC (TCD detector)	TIG	HP, 99.99%

* Thai Industrial Gases Co., Ltd.

4.2 Experimental setup

Figure 4.1 shows the actual arrangement of the experimental apparatus of the gaseous pollutant remover used in the present work. **Figure 4.2** presents its schematic diagram.

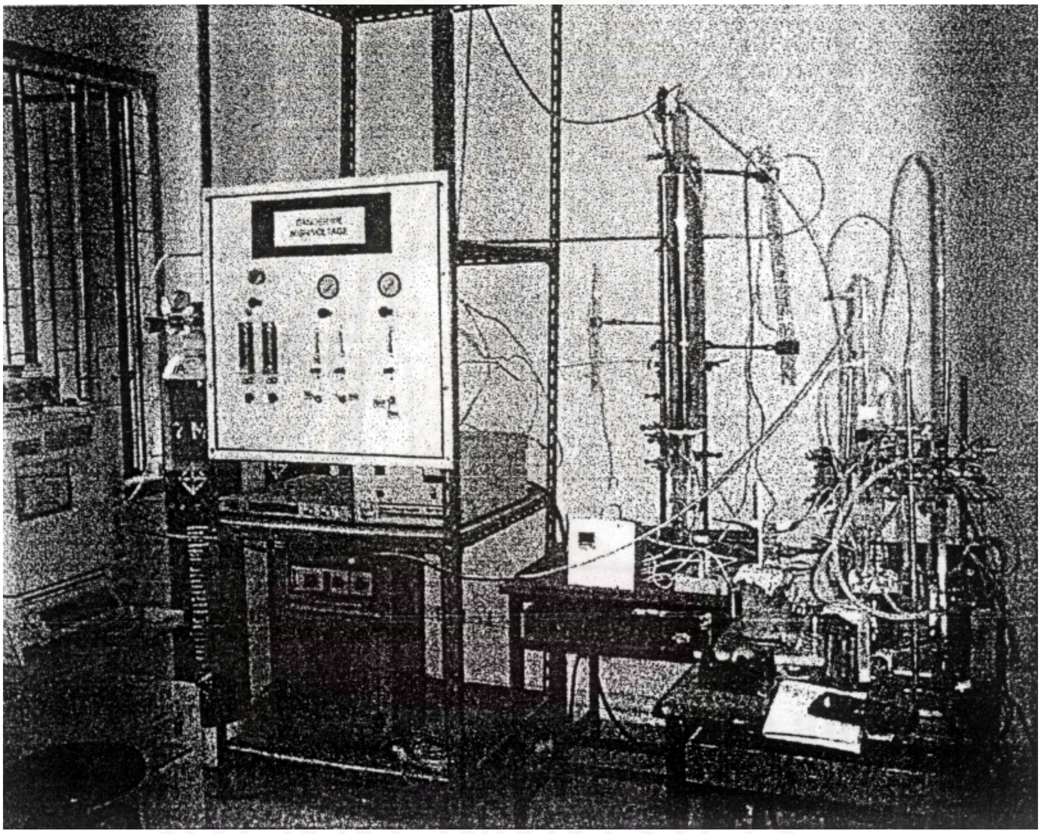

Figure 4.1 Arrangement of present experimental apparatus

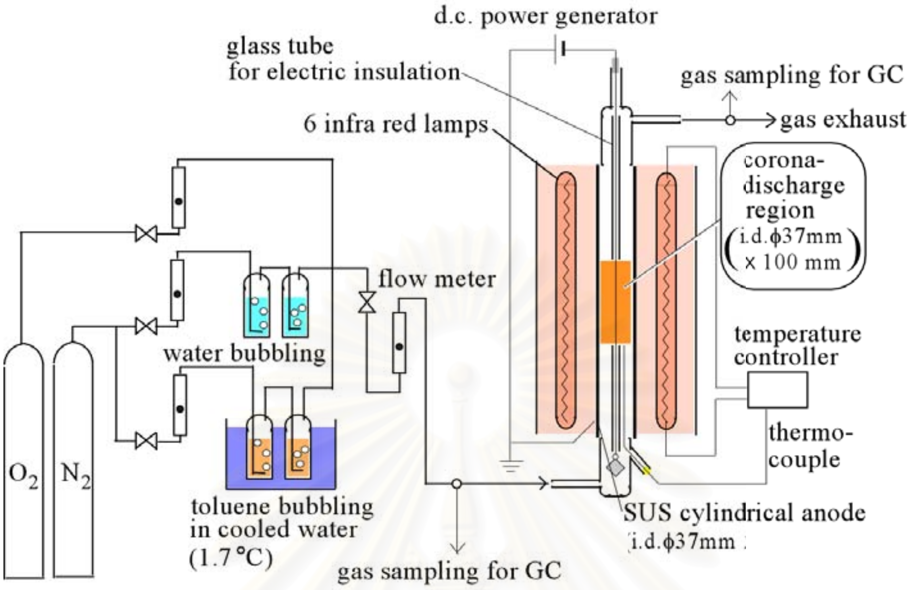

Figure 4.2 Schematic diagram of experimental apparatus

4.2.1 Details of device

Figure 4.1 and **4.2** show the photograph and the schematic diagram of the experimental setup that consists of a deposition-type corona-discharge reactor, a test gas mixing system, a high-voltage DC generator, a cooling water bath, a temperature controller and a soap film flow meter. The present deposition-type corona-discharge reactor consists of a SUS pipe, 3.7 cm. inner diameter and 80 cm. length, as the anode. The cathode is a stainless-steel wire suspended by silicone plug at the top of the reactor and straightened along the axis of the anode by a weight. A high-voltage DC generator (Matsusada, HAR-30N5) is connected to the cathode to supply high voltage DC current. The high-voltage DC generator whose maximum allowable voltage is 50 kV is utilized to supply a steady stream of energetic electrons to the corona-discharge reactor. It has been found that the required maximum voltage to generate discharge current of 0.5 mA is about 17 kV in all experimental conditions.

The effect of the cathode diameter on the removal efficiency is investigated by changing the size of the cathode diameter. A slim pyrex glass tube is used to cover either end of the cathode in order to limit the corona discharge zone in the middle section of the reactor to about 10 cm. The discharge zone is restricted to the mid-section of the reactor to achieve a uniform axial temperature distribution. A type-K thermocouple is inserted into the reactor to measure the temperature in the corona discharge zone. To control the reactor temperature, 6-infrared heating lamps (200V, 700W) are installed around the outside perimeter of the reactor. The temperature control unit consists of a temperature controller (FENWAL, AR-24L) and a thyrister power regulator (Shimaden, PAC15C003081-NO). Gas mixture with the desired concentration of toluene vapor is prepared by feeding nitrogen gas through a series of two toluene bubbling bottles in a cold water bath. To reduce the concentration of toluene vapor in the gas mixture, the cold water bath is necessary to decrease the saturated vapor pressure of toluene in the bubbling bottles. To study the influence of water vapor on the removal efficiency, the desired concentration of water vapor is also achieved by bubbling nitrogen gas through distilled water in a temperature–controlled bath.

Figure 4.3 Deposition-type corona discharge reactor

Figure 4.4 High-Voltage DC generator

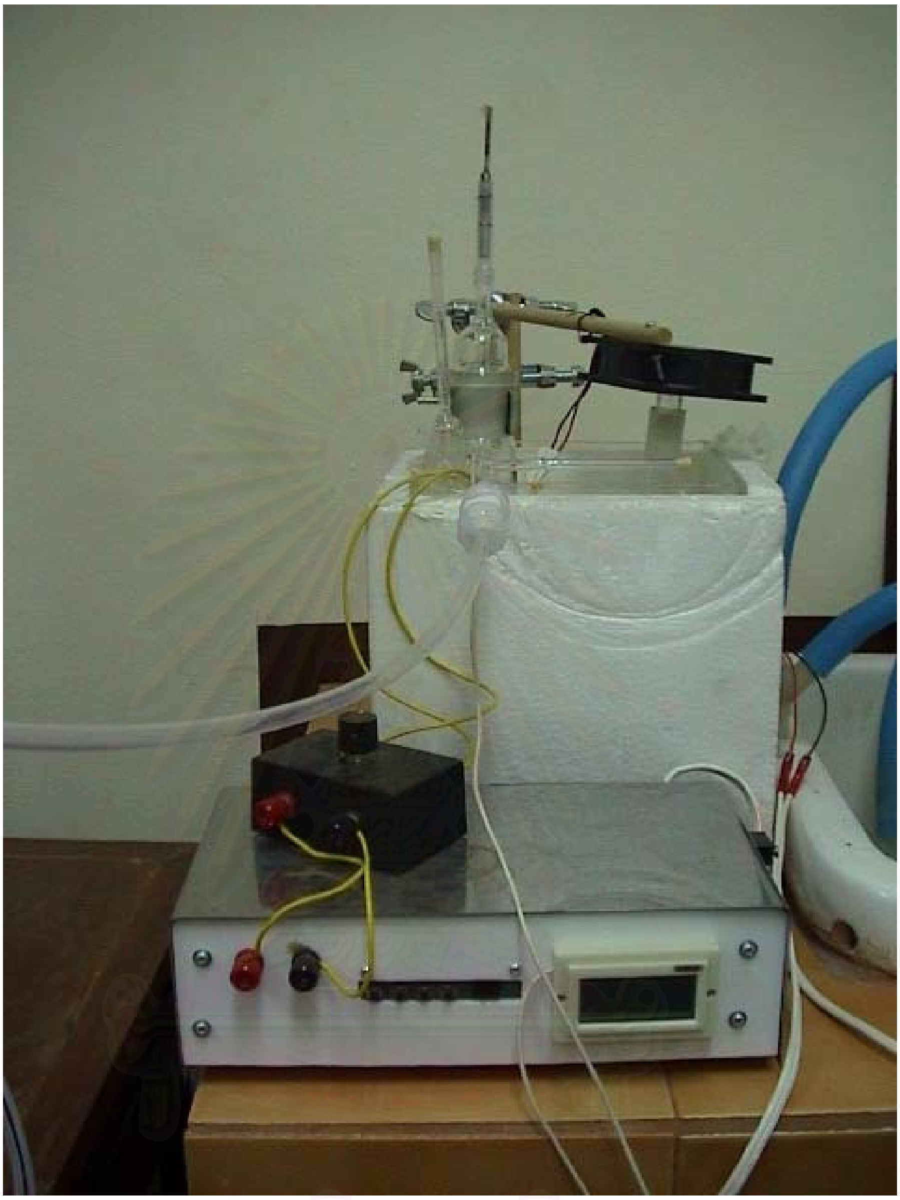

Figure 4.5 Cold water bath

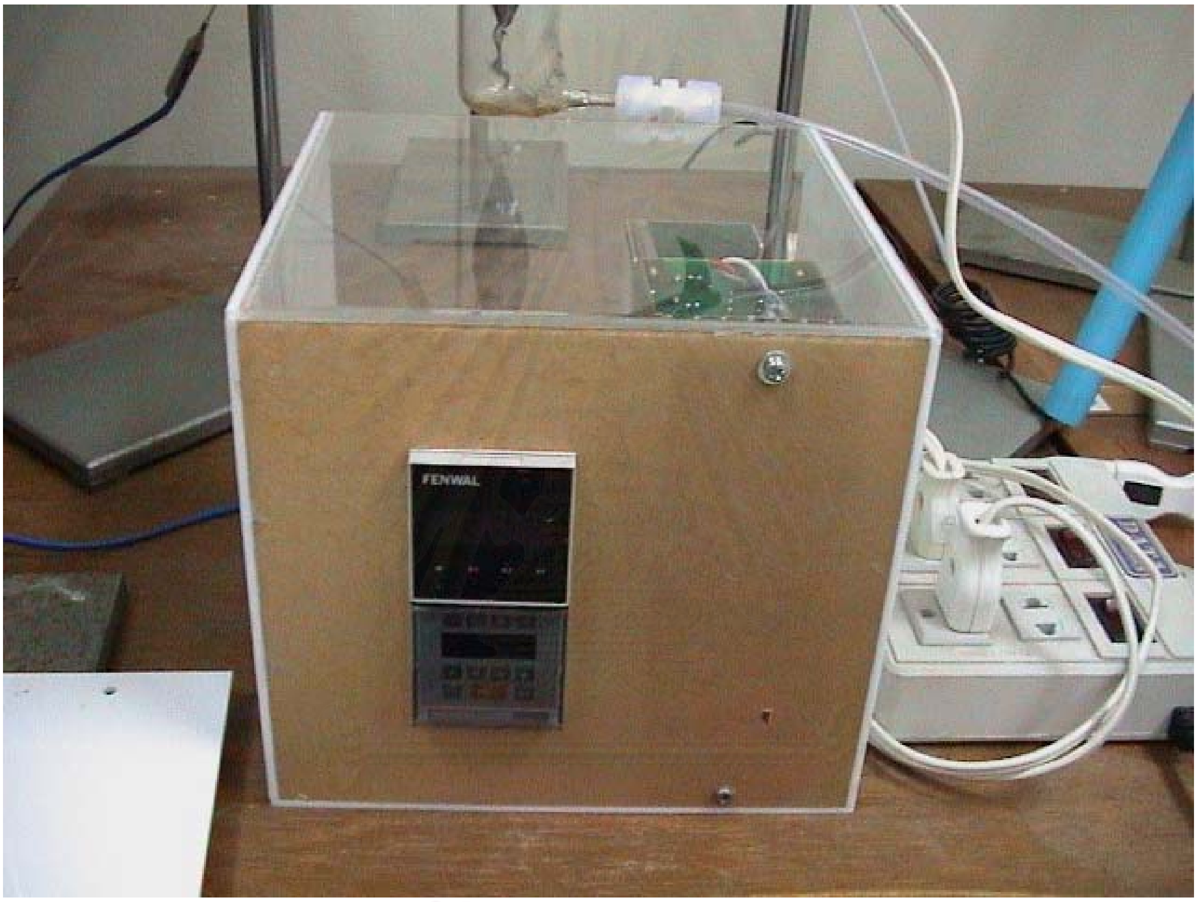

Figure 4.6 Temperature control unit

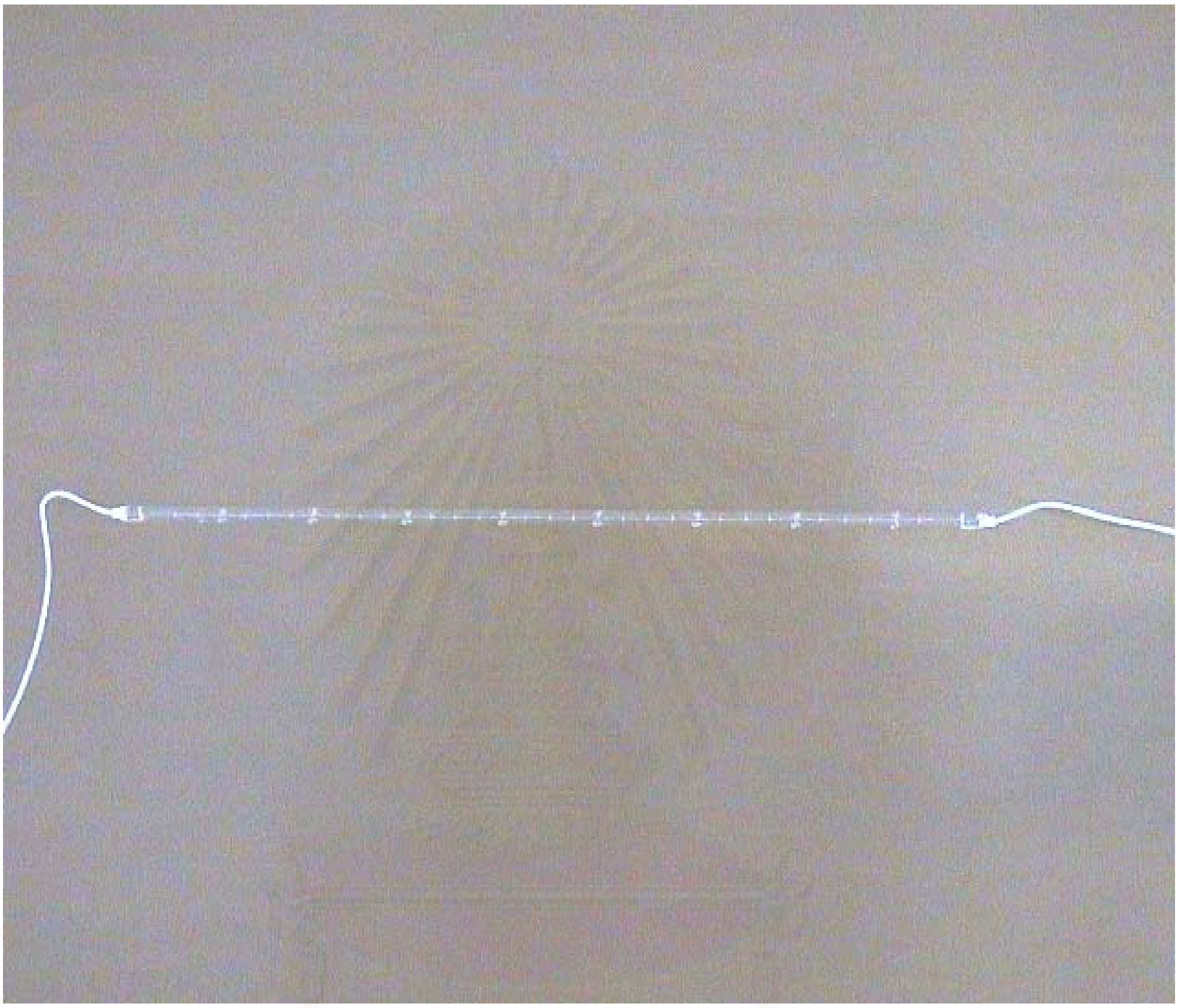

Figure 4.7 Infrared lamp

4.2.2 Analytical Instrument

Inlet and outlet concentrations of toluene vapor are analyzed using a gas chromatograph (Shimadzu Corp., GC 9A) equipped with a flame ionization detector (FID). The packed material in the GC column used for detecting the concentration of toluene is PEG-20M uniport B (GL Science Inc.) with 60/80 mesh size and usable at maximum temperature of 230ºC. A calibration curve between the FID peak area of the GC and the concentration of toluene vapor is obtained as shown in the Appendix.

Figure 4.8 FID-Gas chromatograph

Another gas chromatograph (Shimadzu Corp., GC 14A) with a thermal conductivity detector (TCD) is used to analyze the concentration of carbon dioxide and water vapor. The packed material in the GC column is polydivinylbenzene (Millopore Corp., Porapak Q) with 80/100 mesh size and the usable maximum temperature is 250ºC. A calibration curve between the TCD peak area of the GC and the concentration of either carbon dioxide or water vapor are obtained as shown in the Appendix.

Figure 4.9 TCD-Gas chromatograph

Table 4.2 Operating conditions of both GC units.

Sample Gas	Column Temp. (ºC)	Injection Temp. (ºC)	Detector Temp. (ºC)	Retention time (min)
Toluene	120	125	125	1.547
CO_2	50	100	110	1.075
H_2O	50	100	110	4.108

4.3 Experimental Procedure

To perform the gaseous pollutant removal experiments, the following implementation steps must be carried out carefully because of the great risk of physical injury caused by the high voltage supplied to the reactor.

a. Ensure that the reactor is grounded and each unit of the experimental apparatus is securely connected.
b. Immerse the toluene bubbling bottles in the cold water bath and pass the desired flow rate of nitrogen gas through the bubbling bottles to achieve the saturated concentration of toluene vapor.
c. Mix the aboved stream with another gas stream in the gas mixing device and measure the total flow rate with the soap film flow meter.
d. Feed the gas mixture to the inlet of the reactor and wait until its inlet and outlet concentrations become stable at the reactor temperature of interest.
e. Take gas samples at the reactor inlet and outlet to analyze their concentrations in the blank test (0 mA).
f. Turn on the high-voltage DC generator, adjust the discharge current as desired, and then keep the current stable throughout each experiment.
g. Take gas samples at the inlet and outlet of the reactor and analyze their concentrations. Stop the current after finish in one experiment.

h. To study the effect of reactor temperature, adjust the temperature as desired and wait until it becomes stable. Return to step (e) until all reactor temperatures have been investigated.

i. Wait for the reactor temperature to cool down sufficiently, stop the flow of the gas mixture and turn off the DC generator after the completion of the experiment. Be careful that high voltage does not remain in the reactor.

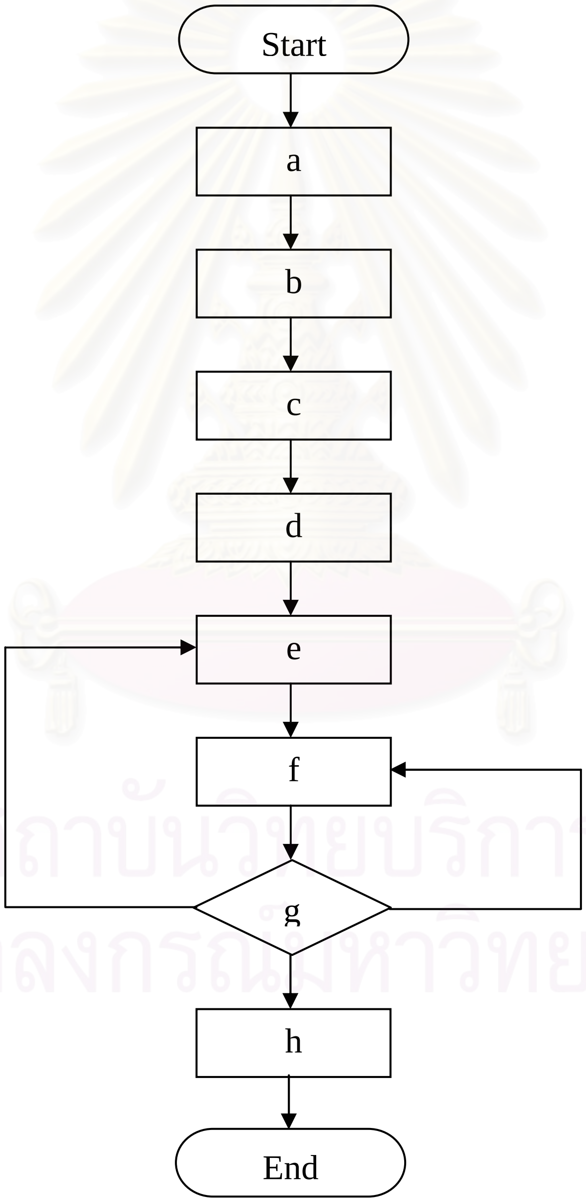

4.4 Experimental Conditions

Table 4.3 Operating conditions for the study of all experiments.

Temp (°C)	I (mA)	Inlet Conc.(ppm)	Cathode Dia. (mm)	Remove from	Flow Rate (cc/min)
1) 28-400	0.1 0.3 0.5	2000	0.5	N_2	100
2) 28-400	0.1 0.3 0.5	2000	0.5	$N_2 – O_2$ (O_2 20 %)	100
3) 28-400	0.5	2000	0.3 0.5 0.9	N_2	100
4) 28-400	0.5	2000	0.3 0.5 0.9	$N_2 – O_2$ (O_2 20 %)	100
5) 28-400	0.5	2000	0.5	$N_2 – O_2$ (O_2 0%, 5%, 20%, 30%)	100
6) 28-400	0.5	500 1000 2000	0.5	N_2	100
7) 28-400	0.5	500 1000 2000	0.5	$N_2 – O_2$ (O_2 20%)	100
8) 28-400	0.5	2000	0.5	N_2 - H_2O (H_2O 1882 ppm 7453 ppm 2000 ppm)	100

CHAPTER V

RESULTS AND DISCUSSION

5.1 Data analysis

This section will describe the various definitions of the removal efficiency.

5.1.1 Apparent removal efficiency

$$\psi = \frac{(C_{in} - C_{out})}{C_{in}} \times 100$$

5.1.2 Removal efficiency (by discharge effect only)

$$\psi' = \frac{(C_{out\ at\ 0\,mA} - C_{out\ at\ any\ mA})}{C_{out\ at\ 0\,mA}} \times 100$$

This removal efficiency excludes the adsorption effect inside the reactor from the above ψ and thus represents the pure corona discharge effect.

5.1.3 Removal efficiency per unit residence time

$$\psi'' = \frac{\psi'}{residence\ \ time}$$

$$= \frac{\dfrac{(C_{out\ at\ 0\,mA} - C_{out\ at\ any\ mA})}{C_{out\ at\ 0\,mA}}}{residence\ \ time}$$

The removal efficiency per unit residence time is defined to evaluate the reaction rate because the actual residence time depends on the gas temperature in the reactor even though the inlet gas flow rate (volume basis) remains constant.

5.2 Blank test for the investigation of the effect of temperature on toluene removal

Figure 5.1 shows the results of the blank test for the investigation of temperature effect on toluene removal. Here the concentration of toluene at the reactor outlet was measured in the absence of the discharge current. There was a significant concentration drop around 200 ppm at 28°C, which is considered to be due to adsorption. The effect of adsorption inside the reactor decreased when the reactor temperature increased until 300°C. At 400°C, the outlet concentration again decreased. The effect of this highest temperature may come from the thermal decomposition of toluene. In contrast, adsorption should not be significant when the temperature was very high.

5.3 Effect of temperature on required voltage to generate corona discharge

The effect of temperature on required voltage to generate corona discharge is investigated by supplying room air through the corona-discharge reactor as shown in **Figure 5.2**. The reason of the lower voltage required at the higher temperature can be considered as follows: 1) At the same current, the required voltage is decreased when increasing the temperature because of reduced gas density; 2) electrons can be emitted more easily from the cathode at high temperature, 3) the rate of the electron propagation process around the cathode $(A + e \rightarrow A^{+} + e + e)$ may increase as the temperature increases, 4) electron detachment from an electronegative molecule becomes significant at high temperature, thus resulting in more free electrons to carry the electric current and causes less resistance, and 5) ion-clusters become unstable, again causing less resistance.Consequently, the electrons can drift to the anode more

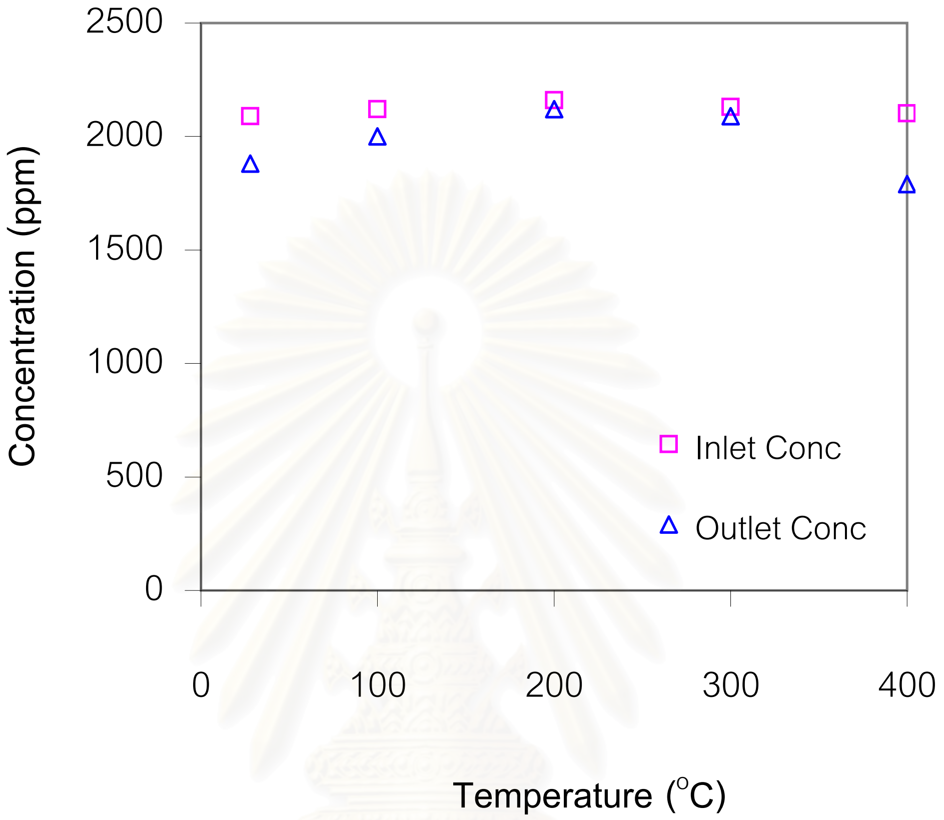

Figure 5.1 Blank test for the investigation of the effect of temperature on toluene; inlet concentration 2000 ppm, 0% O_2.

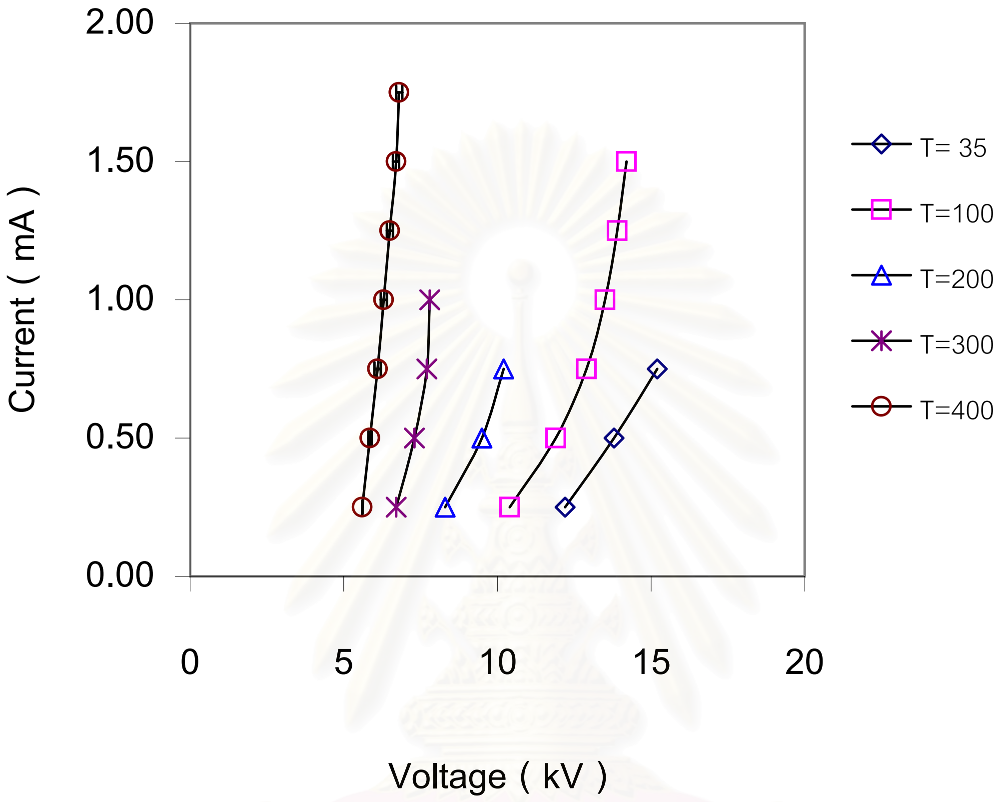

Figure 5.2 Relationship between discharge current and required voltage when the reactor temperature increases

easily and causes less voltage drop. Low applied voltage produces more low energy electrons.

5.4 Effect of cathode diameter

5.4.1 Effect of cathode diameter on electron energy

As mentioned earlier, the probability of electron attachment depends on the electron energy, and type of gas component. Electron energy in the reactor may be represented by the ratio of the local electric field strength, *E*, to the local gas density, *N*, i.e. *E/N*. Electrons are accelerated in *E*, and the probability of collisions between electrons and gas molecules which causes deceleration is proportional to N. Thus, if *E/N* is high, electron energy is also high. The local electric field strength *E* is as given by Eq.(5.1).

$$\mathrm{E} = \mathrm{V}/\{\mathrm{r}\ln(\mathrm{R}/\mathrm{R}_0)\} \tag{5.1}$$

As seen in **Eq. (5.1)**, the electric field strength increases when the corona voltage increases. Larpsuriyakul et al. (1997) reported the relation between the discharge current, *I*, and voltage, *V*, for CH_3I removal from dry air. Generally, a thicker cathode diameter requires a significantly higher *V* to yield the same current. The average electric field strength per gas density is given as follows.

$$< E/N > = \frac{\int_{R_0}^{R}(2\pi r)(E/N)dr}{\pi\left(R^2 - R_0^2\right)} = \frac{2V}{N\left(R + R_0\right)ln\left(R/R_0\right)} \tag{5.2}$$

When the cathode diameter R becomes thicker at the constant *V*, *E* at the cathode becomes small. So, to keep the critical *E* to initiate discharge current, *V* must be increased. Then, when *V* is increased, <*E/N*> become large, so a thicker cathode makes large <*E/N*>. as shown in **Figure 5.3**

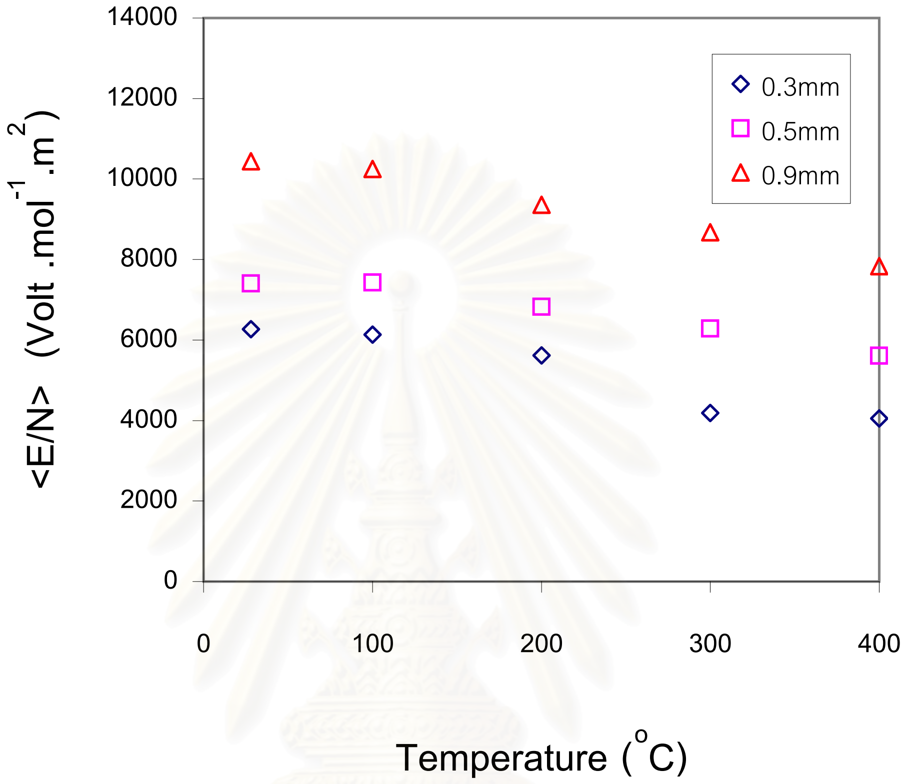

Figure 5.3 Relationship between average electric strength per gas density and temperature at various cathode diameter

5.4.2 Effect of cathode diameter and temperature on removal of toluene from N_2

The removal efficiency of toluene from pure N_2 is shown in **Figure 5.4**. **Figure 5.4(a)** shows the removal efficiency versus temperature. The abscissa is the temperature and the ordinate is the removal efficiency. **Figure 5.4(b)** shows the removal efficiency per residence time versus temperature The abscissa is the temperature and the ordinate is the removal efficiency per unit residence time.

We see that as the temperature increases, the toluene removal efficiency becomes lower from room temperature to 300^oC and then the tendency reverse again at 400^oC in Figure 4(a). Figure 4(b) shows the monotonically increasing tendency of the removal efficiency per residence time, which simply means the actual reaction rate is always increases with the temperature.

Moreover, it can be found that when the cathode diameter increases, the toluene removal is also increased. As mentioned in **section 5.4.1**, a thick cathode will yield a large $<E/N>$, so the average electron energy increases with increasing cathode diameter. This is the reason that a thicker cathode provides a higher ψ. Although a thicker cathode wire provides a higher ψ, the required voltage, V, becomes higher as well, resulting in an undesirable higher power consumption.

5.4.3 Effect of cathode diameter and temperature on toluene removal from N_2-O_2

A set of experiments to remove toluene from N_2-O_2 (20% O_2) mixture has been conducted. **Figure 5.5** shows the removal efficiency of toluene from N_2-O_2. **Figure 5.5(a)** shows the removal efficiency versus temperature. The abscissa is the temperature, and the ordinate is the removal efficiency. We see that as the temperature increases, the toluene removal becomes lower starting from room

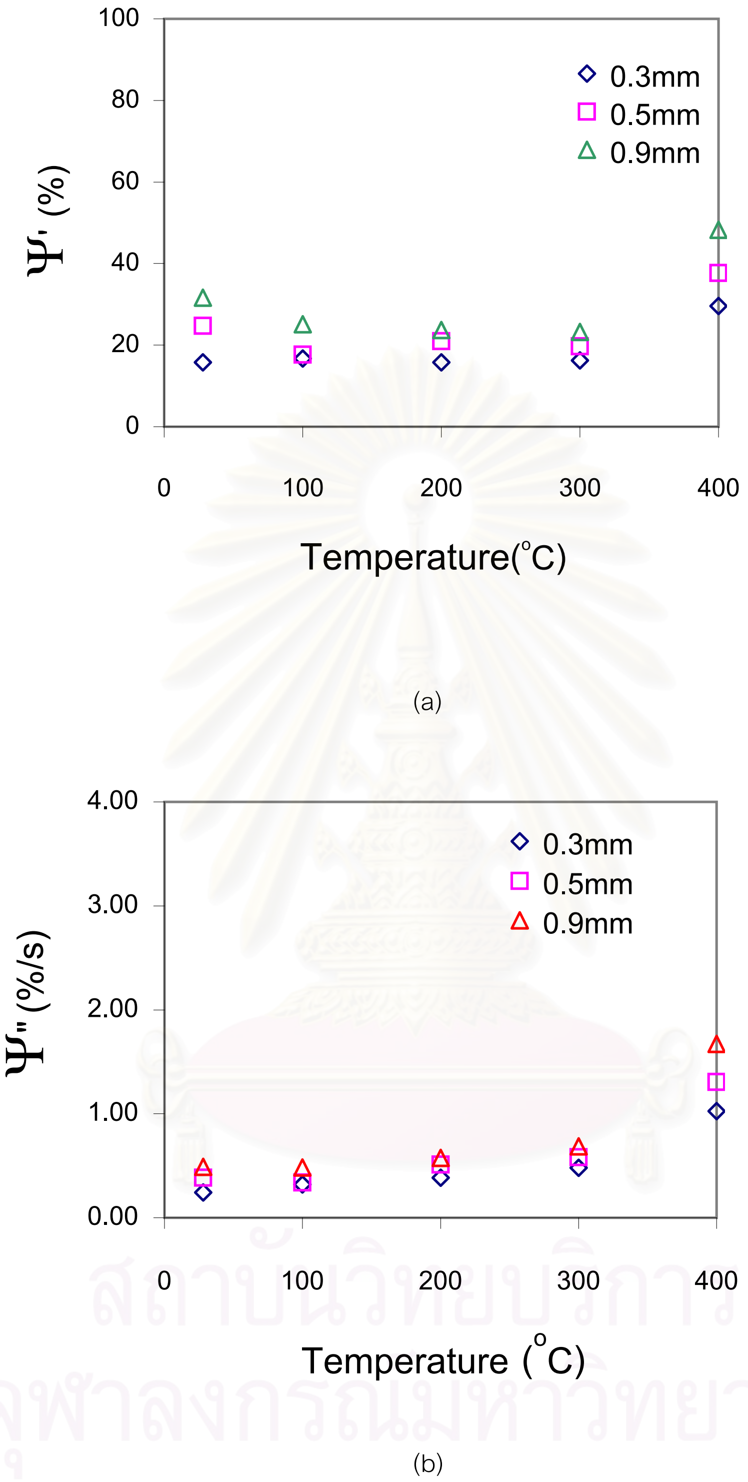

(a)

(b)

Figure 5.4 Effect of cathode diameter on the removal of toluene from N_2 ; C_{in} 2000 ppm
$I = 0.5$ mA, SV = 55.8 hr^{-1} at room temperature

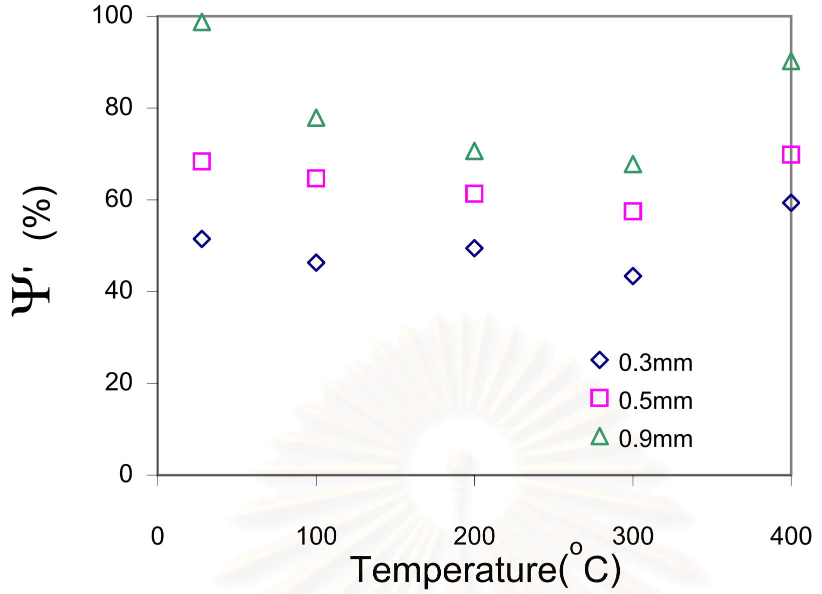

(a)

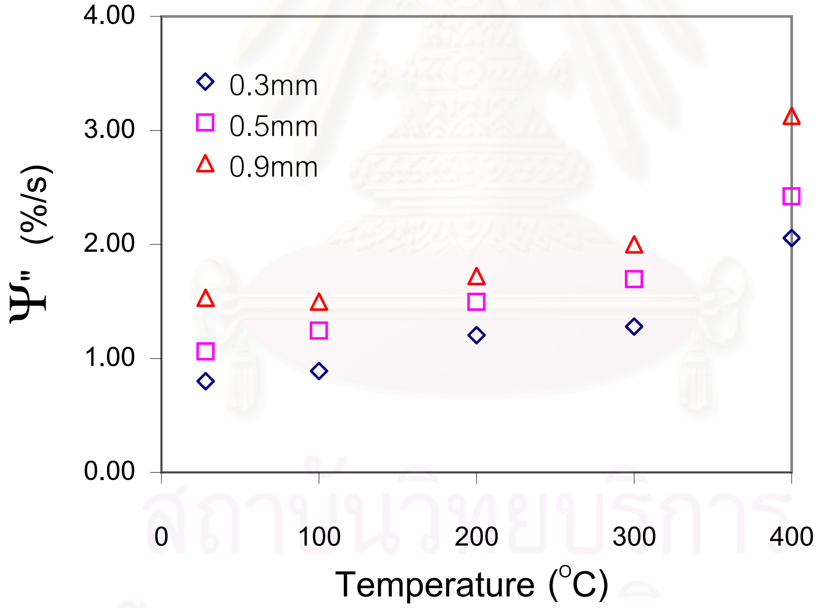

(b)

Figure 5.5 Effect of cathode diameter on the removal of toluene from N_2-O_2 ; C_{in} 2000 ppm, I = 0.5 mA, SV = 55.8 hr^{-1} at room temperature

temperature to 300^{o}C and then the tendency reverses at 400^{o}C. **Figure 5.5(b)** shows the removal efficiency per residence time versus temperature. The abscissa is the temperature, and the ordinate is the removal efficiency per residence time. From this figure we found that the monotonically increasing tendency of the removal efficiency per residence time simply means that the true reaction rate always increases with the temperature.

It can be found that when the cathode diameter increases, the toluene removal is also increased. The tendency of the temperature effect is same as in **section 5.4.2** but the removal efficiency is significantly higher than the removal from N_2. The explanation is that oxygen may contribute to the formation of negative ion-clusters.

In fact, the stability of negative ion-clusters is low in the high temperature condition. Therefore, at high temperature, negative ion cluster is expected to contribute less to the removal. However, at 400^{o}C, the dominant mechanism is the thermal decomposition of toluene enhanced by electron bombardment.

5.5 Effect of discharge current and temperature on toluene removal

5.5.1 Effect of discharge current and temperature on toluene removal from N_2

Figure 5.**6** shows the removal efficiency of toluene from pure N_2**. Figure 5.6(a)** shows the removal efficiency versus temperature. The abscissa is the temperature, and the ordinate is the removal efficiency. We see that as the temperature increases, the toluene removal becomes lower starting from room temperature to 300^{o}C and then the tendency reverse at 400^{o}C. **Figure 5.6(b)** shows the removal efficiency per residence time versus temperature The abscissa is the temperature, and the ordinate is the removal efficiency per residence time. From this figure we found that the monotonically increasing tendency of the

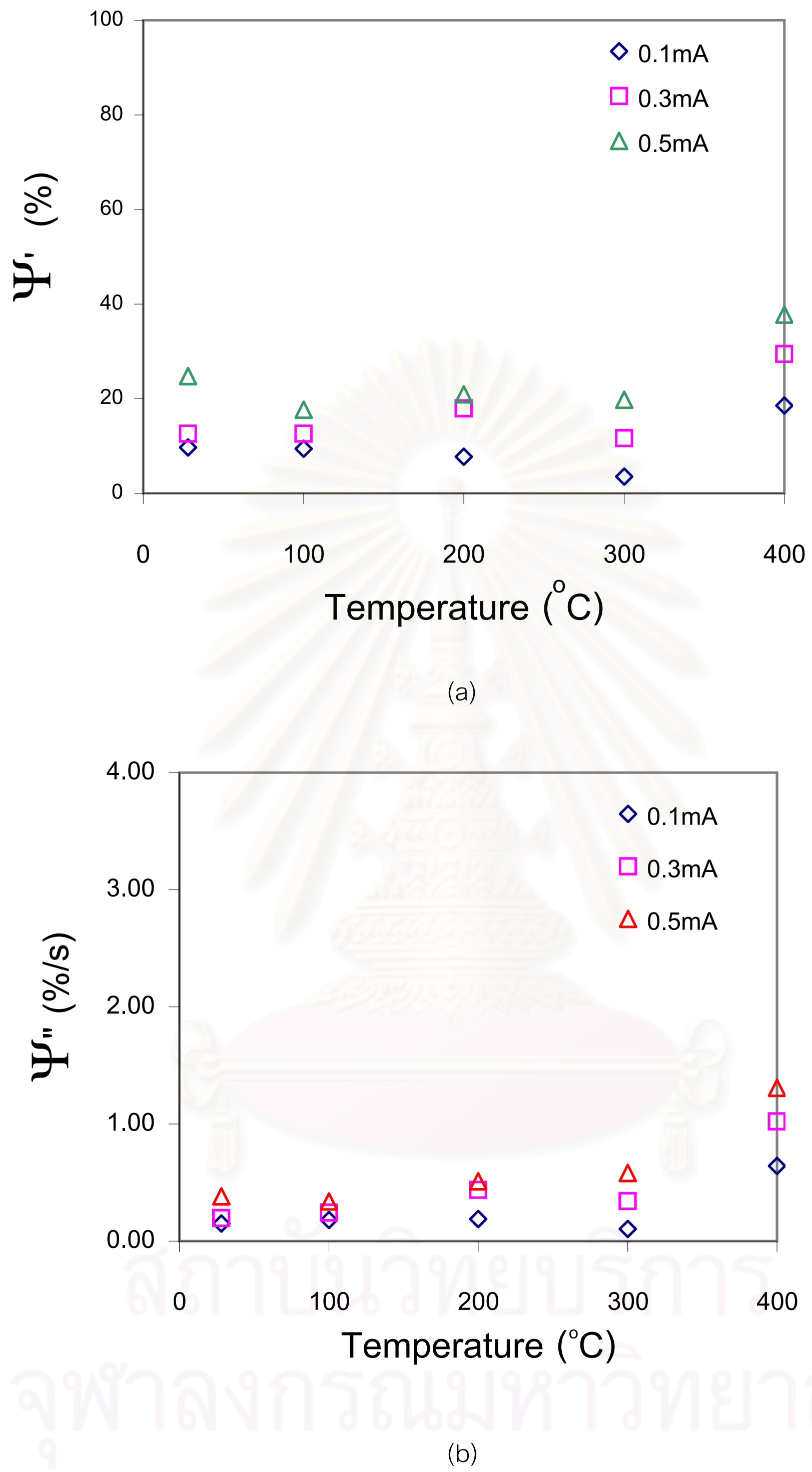

Figure 5.6 Effect of discharge current on the removal of toluene from N_2; C_{in} 2000 ppm

Cathode diameter 0.5mm

SV = 55.8 hr^{-1} at room temperature

removal efficiency per residence time simply means that the actual reaction rate always increases with the temperature.

As reported by Tamon et al. (1995), the higher the discharge current, the higher the removal efficiency. The experimental results in this thesis are consistent with the said report even in the high temperature condition. It can be seen that the toluene removal increases with the discharge current.

The discharge current is proportional to the number of electrons which are emitted in the discharge. If the current is high, the emitted number of electrons become high as shown in **Eq. (5.3)**.

$$n_e = I / c \qquad (5.3)$$

where n_e : number of emitted electron per unit time (electron/s)
I : current (coulomb/s)
and c : electronic charge = 1.602×10^{-19} (coulomb/electron)

As a consequence, the probability of an electron captured by an electronegative gas molecule is enhanced, so that the removal efficiency rises.

5.5.2 Effect of discharge current and temperature on toluene removal from N_2-O_2

Figure 5.7 shows the removal efficiency of toluene from N_2-O_2. **Figure 5.7(a)** shows the removal efficiency versus temperature. The abscissa is the temperature and the ordinate is the removal efficiency. We see that as the temperature increases, the toluene removal efficiency become lower starting from room temperature to 300°C and then the tendency reverses at 400°C. **Figure 5.7(b)** shows the removal efficiency per residence time versus temperature.

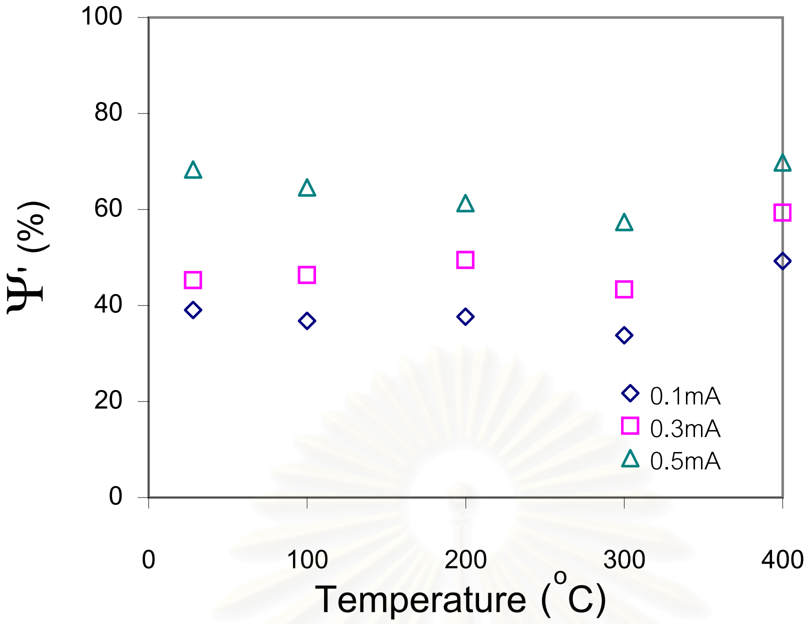

(a)

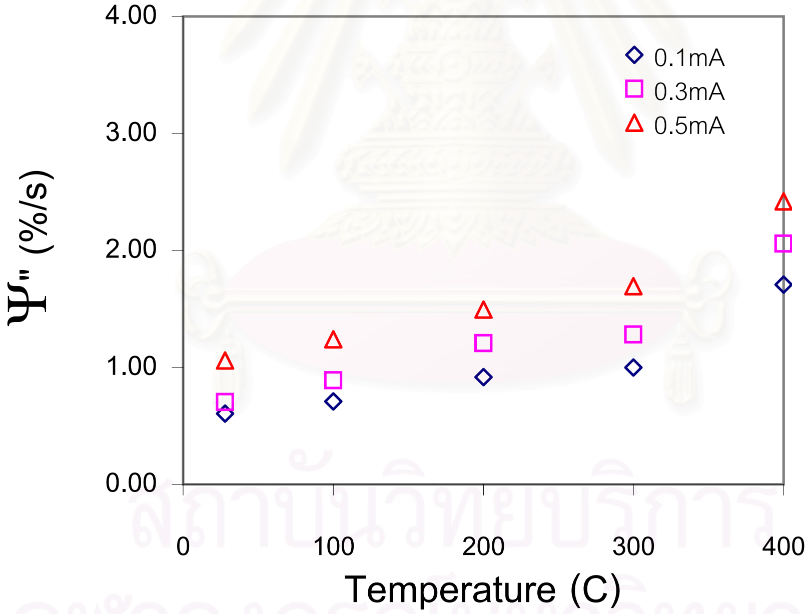

(b)

Figure 5.7 Effect of discharge current on the removal of toluene from N_2-O_2; C_{in} 2000 ppm

Cathode diameter 0.5mm

SV = 55.8 hr^{-1} at room temperature

The abscissa is the temperature and the ordinate is the removal efficiency per residence time. From this figure we found that the monotonically increasing tendency of the removal efficiency per residence time simply means that the actual reaction rate always increases with the temperature.

From the figure, the tendency is same as the removal from N_2. If more electrons exist in the reactor by increasing the current, the probability for the electron attachment becomes larger and the removal efficiency is enhanced. The comparison between the toluene removal from N_2 and from N_2-O_2 indicates that the latter condition has higher efficiency. It can thus be concluded that oxygen can significantly enhance the removal efficiency.

5.6 Effect of oxygen coexisting gas on toluene removal

In actual applications of gas purification, there are many cases of coexisting gases. Therefore it is necessary to study the influence of coexisting gases on the removal efficiency. In the previous sections, coexisting oxygen is a significant parameter that enhances the removal of toluene.

Figure 5.**8** shows the removal efficiency of toluene from N_2-O_2. **Figure 5.8(a)** shows the removal efficiency versus temperature. The abscissa is the temperature and the ordinate is the removal efficiency. We see that as the temperature increases, the toluene removal efficiency becomes lower starting from room temperature to 300^{o}C and then the tendency reverses at 400^{o}C. **Figure 5.8(b)** shows the removal efficiency per residence time versus temperature. The abscissa is the temperature, and the ordinate is the removal efficiency per residence time. From this figure we found that the monotonically increasing tendency of the removal efficiency per residence time means the overall reaction rate increases with the temperature.

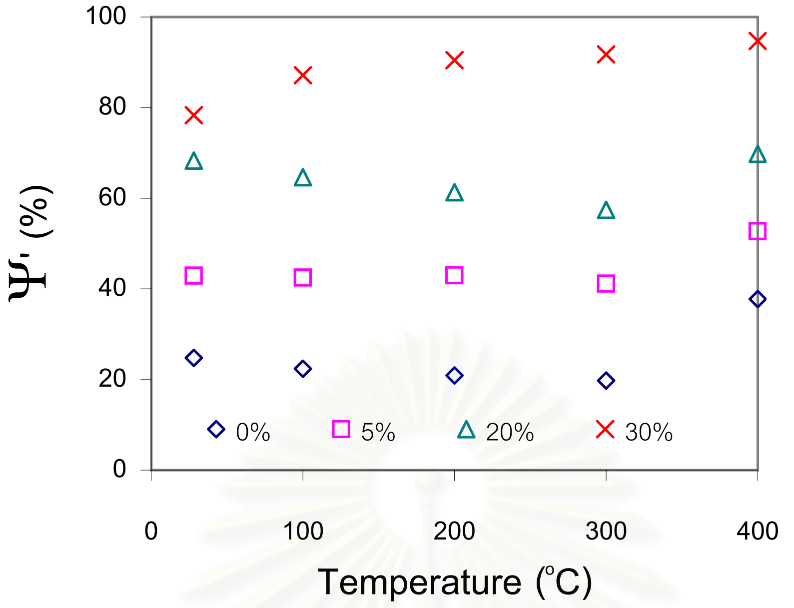

(a)

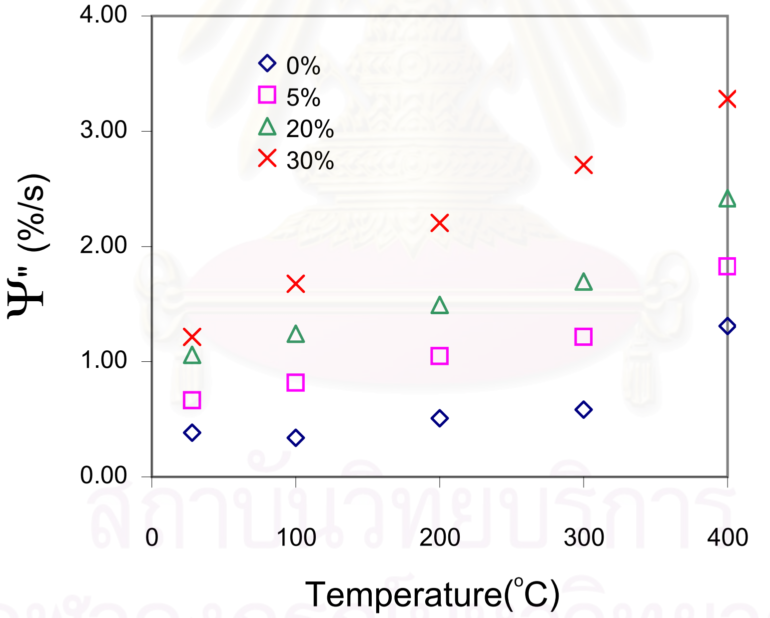

(b)

Figure 5.8 Effect of oxygen coexisting gas on the removal of toluene from N_2-O_2; C_{in} 2000 ppm, cathode diameter 0.5mm. SV = 55.8 hr^{-1} at room temperature

The removal efficiency is found to increase when the concentration of coexisting O_2 is increased. This can be described that the ozonation effect is the important mechanism to enhance the removal efficiency. The most significant effect of coexisting O_2 is found at 30% O_2.

In this experimental investigation, the outlet concentrations of O_3 and NO_x are detected using suitable gas detector tubes. Ozone and NO_x are produced in the reactor, as shown in **Figure 5.9**. From the figure, it can be seen that ozone is tend to decrease when the temperature increases, while NO_x increases with the temperature. This can be explained that when O_2 is present in a gas mixture, it could collide with a high-energy electron near the cathode wire, production of O^- is expected as is **Eq. (3.5)**. Then O_3 is produced from the reaction of O^- with O_2. Nitrogen and excess oxygen can be oxidized by ozone to be NO_x. At high temperature, the ozone concentration decreases because the reaction rate of ozonation effect is very fast. Then ozone is found to decrease when increases the temperature.

5.7 Effect of inlet toluene concentration

5.7.1 Effect of inlet concentration and temperature on the removal of toluene from N_2

Figure 5.10 shows the removal efficiency of toluene from N_2. **Figure 5.10(a)** shows the removal efficiency versus temperature. The abscissa is the temperature, and the ordinate is the removal efficiency. As expected, when the temperature increases, the toluene removal efficiency becomes lower starting from room temperature to 300°C and then the tendency reverses at 400°C. **Figure 5.10(b)** shows the removal efficiency per residence time versus temperature The abscissa is the temperature and the ordinate is the removal efficiency per residence time. From this figure we see that the monotonically increasing tendency of the removal efficiency per residence time simply means that the overall reaction rate increases with the temperature.

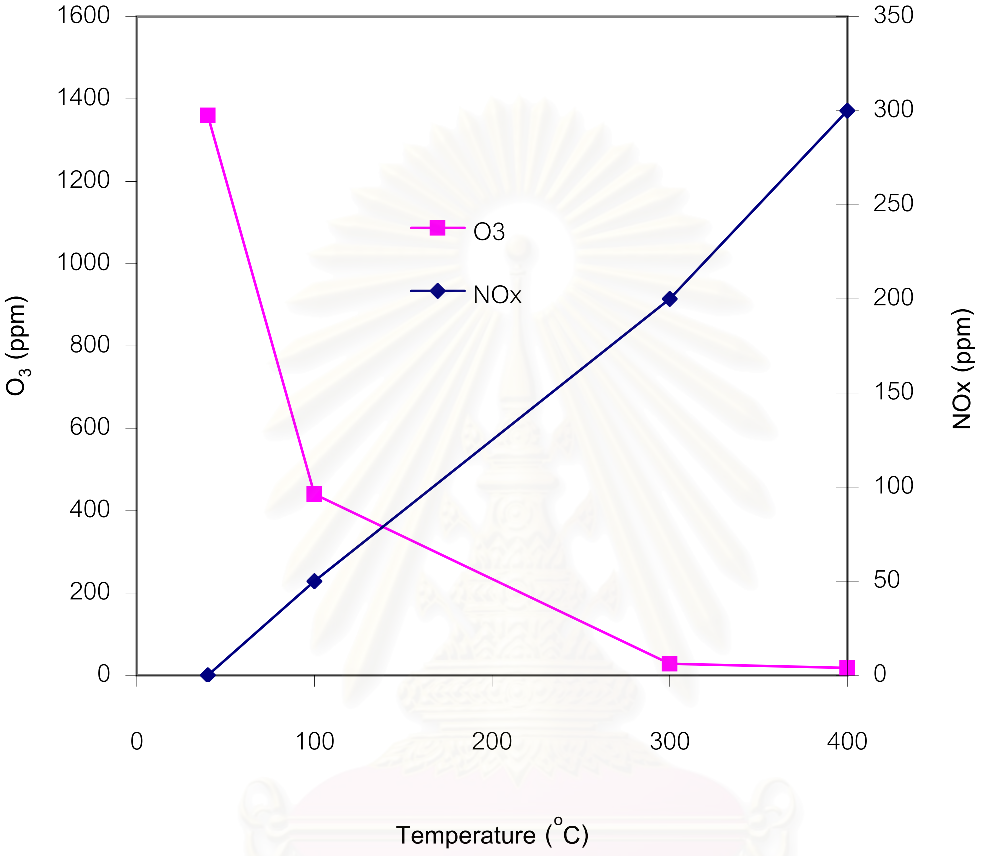

Figure 5.9 Relationship between ozone and NO_x generation at various temperatures for the toluene removal from N_2-O_2 (30% O_2 content)

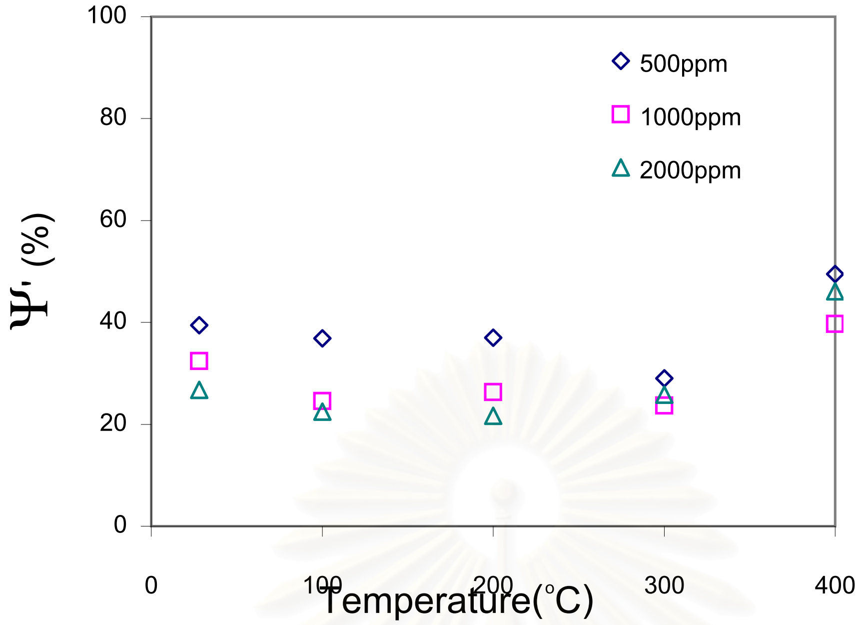

(a)

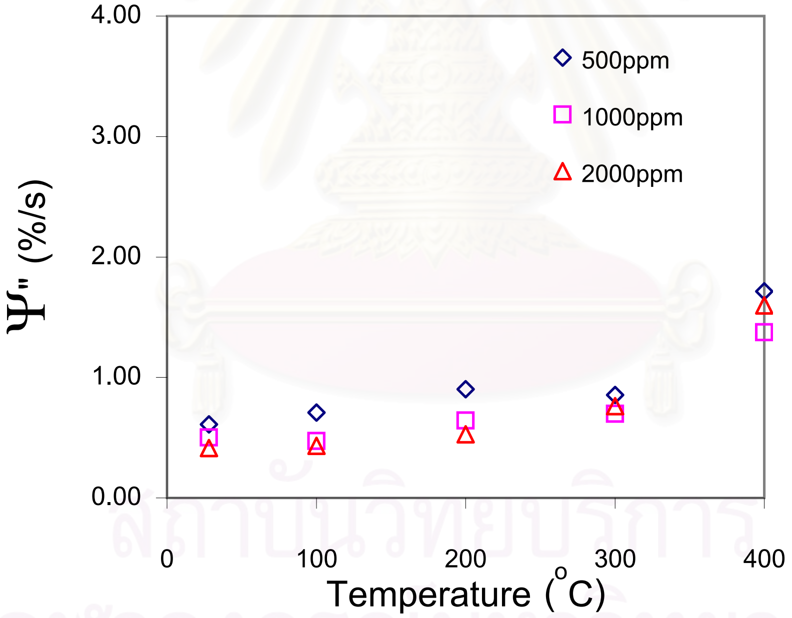

(b)

Figure 5.10 Effect of inlet concentration on the removal of toluene from N_2; I = 0.5 mA, cathode diameter 0.5mm. SV = 55.8 hr^{-1} at room temperature

Tamon et al.(1995) have reported that the removal efficiency tends to decrease when the inlet concentration is increased. In this thesis, the experimental result on the effect of inlet toluene concentration also exhibits the same tendency. The lower the inlet concentration of toluene, the higher the removal efficiency becomes**.** To explain the phenomenon, we consider the number ratio of electrons to toluene molecules. At a higher inlet toluene concentration, there are many more toluene molecules than at a lower inlet concentration of toluene. However, the number of electrons remains constant at the same current. This is the reason that the lower the inlet concentration of toluene, the higher the removal efficiency becomes regardless of the temperature of interest.

5.7.2 Effect of inlet concentration and temperature on the removal of toluene from N_2-O_2

Figure 5.**11** shows the removal efficiency of toluene from N_2-O_2. **Figure 5.11(a)** shows the removal efficiency versus temperature. The abscissa is the temperature, and the ordinate is the removal efficiency. As expected, when the temperature increases, the toluene removal efficiency becomes lower starting from room temperature to 300^{o}C and then the tendency reverses at 400^{o}C. **Figure 5.11(b)** shows the removal efficiency per residence time versus temperature The abscissa is the temperature and the ordinate is the removal efficiency per residence time. From this figure we find that the monotonically increasing tendency of the removal efficiency per residence time simply means that the overall reaction rate increases with the temperature.

5.8 Influence of water vapor and temperature on the removal of toluene

Figure 5.12 illustrates the removal efficiency of toluene from N_2. **Figure 5.12(a)** shows the removal efficiency versus temperature. The abscissa is the temperature and the ordinate is the removal efficiency. We see that as the temperature increases, the toluene removal efficiency becomes lower starting

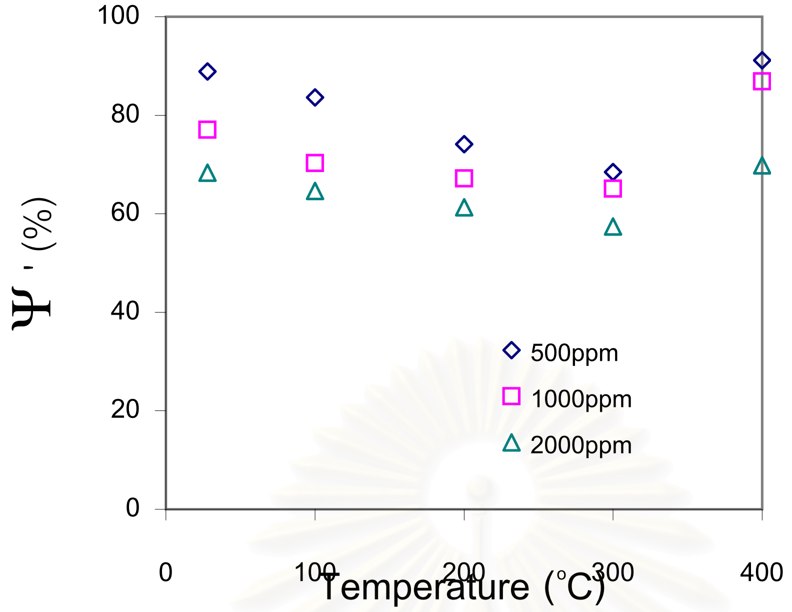

(a)

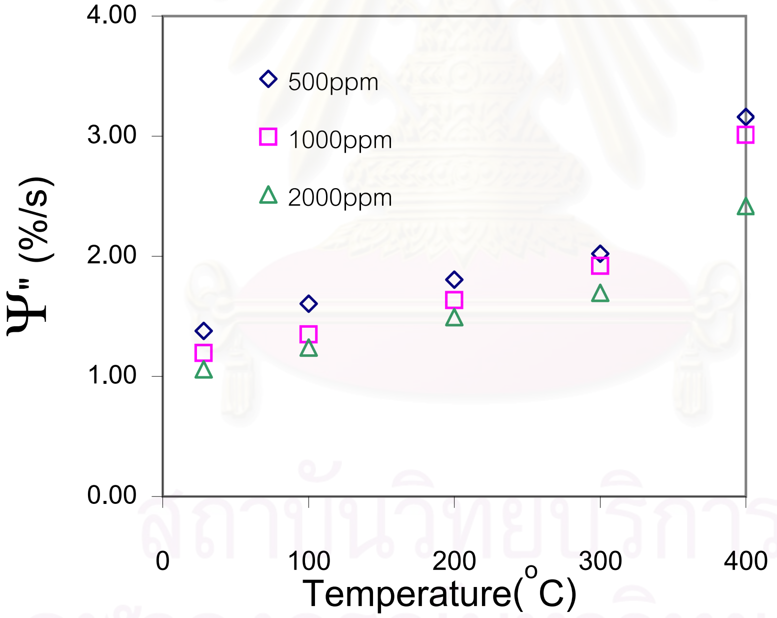

(b)

Figure 5.11 Effect of inlet concentration on the removal of toluene from N_2-O_2; I = 0.5 mA, cathode diameter 0.5mm. SV = 55.8 hr^{-1} at room temperature

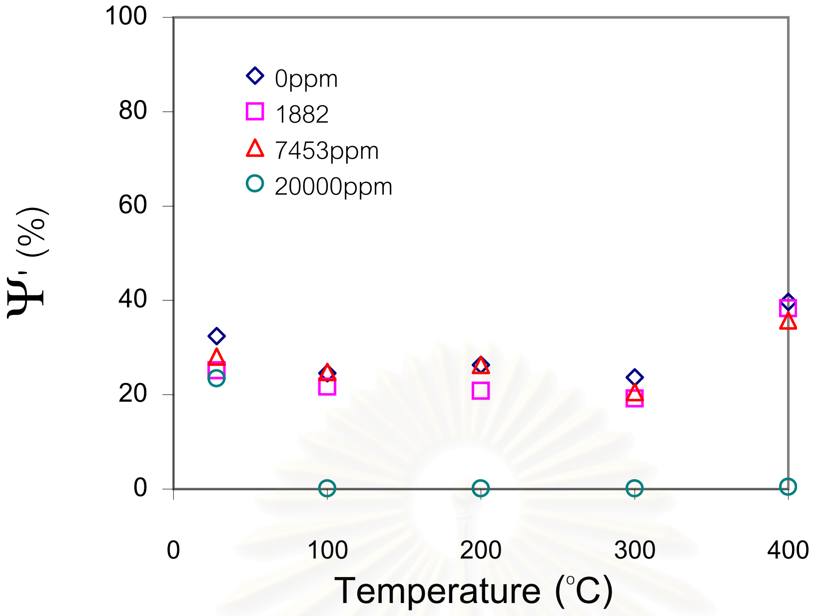

(a)

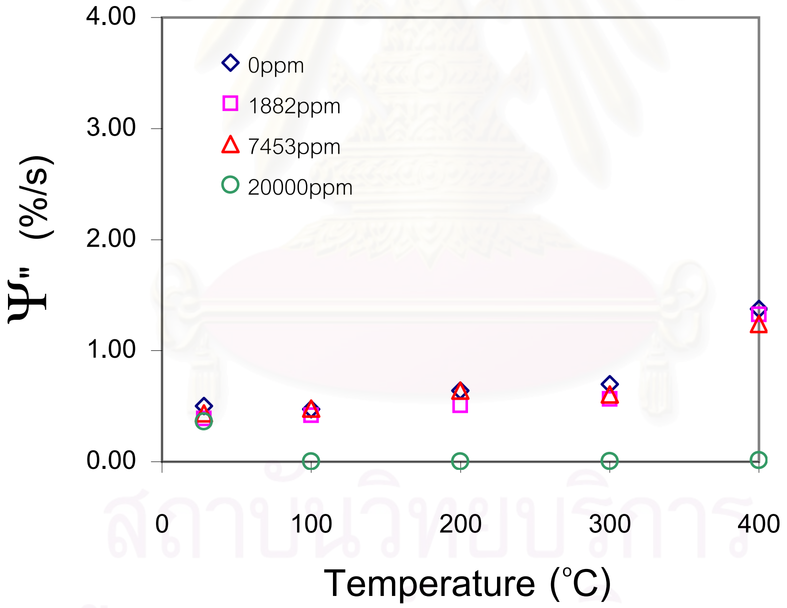

(b)

Figure 5.12 Effect of water vapor on the removal of toluene from N_2; I = 0.5 mA, cathode diameter 0.5mm. SV = 55.8 hr^{-1} at room temperature from room temperature to 300°C and then the tendency goes up again at 400°C. **Figure 5.12(b)** shows the removal efficiency per residence time versus temperature. The abscissa is the temperature and the ordinate is the removal efficiency per residence time. From this figure we see that the monotonically increasing tendency of the removal efficiency per residence time simply means that the overall reaction rate increases with the temperature.

In this Figure, the three different concentration (0 ppm, 1882 ppm and 7453 ppm) of H_2O have not led to significantly different removal efficiencies. In the extreme case of 20000 ppm of H_2O, some toluene can still be removed at room temperature but no toluene can be removed when the temperature rises above 100 till 400°C. It is postulated that toluene is slightly less electronegative than H_2O at room temperature. Since the rate of electron attachment to H_2O molecule is only slightly faster than that to toluene at room temperature, some toluene can be removed even when the H_2O concentration is 20000 ppm. Apparently when the reactor temperature rises above 100°C, the rate of electron attachment to H_2O molecule becomes much faster than that to toluene molecule. On the other hand, only a limited number of electrons with sufficient energy level is available when the discharge current is 0.5 mA. Thus all of these electrons are consumed by the excess H_2O molecules, thus resulting in zero toluene removal efficiency.

5.9 More explanation of the effect of temperature on the removal efficiency of toluene

We have found that the dependency of ψ' on T in all cases are essentially similar. In summary, as the temperature increases from room temperature to 300°C, the removal efficiency gradually decreases but increases again around 400°C. The increased removal efficiency at 400°C may be because a critical temperature of toluene decomposition has been reached and the thermal polymerization of toluene may be enhanced by electron impact.

When the removal efficiency per residence time, ψ'', is used to describe the intrinsic removal rate at various temperatures, we can see a clear trend that the removal efficiency does increase with the temperature. In other words, the higher the temperature, the higher the intrinsic removal efficiency.

5.10 The analysis of the solid deposit in the reactor

After some period of removal experiments, there is a gradual accumulation of solid deposit on the glass section at the top of the reactor. In room-temperature experiments, the color of the deposit is either colorless or white, but at the higher temperatures, the resulting deposit becomes a yellowish to brownish in color. Some sample of the deposit was taken for analysis using a Gas Chromatograph-Mass Spectrometer (GC-MS). There are six peaks detected. The result shows that some of the chemical species detected have heavier molecular weights than toluene. Though the individual peaks have not been identified yet, the evidence strongly suggests that the polymerization or the polycondensation of toluene should have occurred.

CHAPTER VI

CONCLUSIONS AND RECOMMENDATION

6.1 Conclusions

The main purpose of the present research is to study the effect of temperature on the gaseous removal efficiency based on electron attachment reaction. The additional parameters that are also investigated are the cathode diameter, discharge current, coexisting oxygen gas, inlet concentration, and water vapor. From the results, it can be concluded as follows:

6.1.1 Effect of cathode diameter on toluene removal

In the removal of toluene from nitrogen, the minimum removal efficiency ψ is 15.74% in the condition of the most slender cathode diameter of 0.3 mm. and the temperature of 200^{o}C. The maximum ψ is 48.28% in the condition of the thickest cathode diameter of 0.9 mm and the highest temperature of 400^{o}C. In the removal from nitrogen and oxygen (20% oxygen), the minimum ψ is 43.37% in the condition of the most slender cathode diameter of 0.3 mm and the temperature of 300^{o}C. The maximum ψ is 98.75% in the condition of the thickest cathode diameter of 0.9 mm and room temperature.

The removal efficiency of the thickest cathode is a maximum and the most slender cathode, the minimum. The removal efficiency of toluene from nitrogen and oxygen mixture is higher than from pure nitrogen because of the ozonation effect.

6.1.2 Effect of discharge current on the toluene removal

In the removal of toluene from nitrogen, the minimum removal efficiency ψ is 3.53% in the condition of the weakest discharge current of 0.1 mA and the temperature of 300°C. The maximum ψ is 37.77% in the condition of the strongest discharge current of 0.5 mA and the highest temperature of 400°C. In the removal from nitrogen and oxygen (20% oxygen), the minimum ψ is 33.8% in the condition of the weakest discharge current of 0.1 mA and the temperature of 300°C. The maximum ψ is 69.82% in the condition of the strongest discharge current of 0.5 mA and the highest temperature of 400°C.

Generally, the stronger the discharge current, the higher the removal efficiency. The removal efficiency of toluene from nitrogen and oxygen mixture is higher than from pure nitrogen because of the ozonation effect.

6.1.3 Effect of oxygen coexisting gas on toluene removal

In the absense of oxygen, the removal of toluene from nitrogen ψ is a minimum at 17.66% when the temperature is 300°C. The maximum ψ is 94.68% in the condition of the highest oxygen content of 30% and the highest temperature of 400°C.

Undoubtedly, the ozonation effect significantly enhances the removal efficiency.

6.1.4 Effect of inlet toluene concentration on toluene removal

In the removal of toluene from nitrogen, the minimum ψ is 21.66% in the condition of the highest inlet concentration of 2000 ppm and the temperature of 200°C. The maximum ψ is 49.47% in the condition of the lowest inlet concentration of 500 ppm and the highest temperature of 400°C. In the removal from nitrogen and oxygen (20% oxygen), the minimum ψ is 57.43% again in the condition of the highest inlet concentration of 2000 ppm and the temperature of 300°C. The maximum ψ is 91.15% in the condition of the lowest inlet concentration of 500 ppm and the highest temperature of 400°C.

Generally the lower the inlet concentration of toluene, the higher the removal efficiency. The removal efficiency of toluene from nitrogen and oxygen mixture is higher than from pure nitrogen because of the ozonation effect.

6.2 Effect of water vapor on removal of toluene

In the removal of toluene from nitrogen, the minimum ψ is 0.1% in the condition of the highest of water vapor concentration of 20000 ppm starting from 100 till 400°C. The maximum ψ is 39.71% in the absence of water vapor and at the highest temperature of 400°C.

6.3 Recommendation for future work

From the experimental results, NO_x is detected at high temperatures and its concentration increases with the temperature. NO_x is an unwanted and dangerous by-product that needs to be removed. Two corona-discharge reactors in series may be effective for removing NO_x and other by-products.

REFERENCES

Abouaf R., Paineau R. and Fiquet-Fayard F. Phys. B.: At Mol. Phys. 9 (1976): 303-314

Caledonia, G. E. A survey of the gas-phase negative ion kinetics of inorganic molecules - Electron Attachment Reactions. Chem. Rev. 75 (1975): 333-351.

Castle, G. S. P., Inculet, I. I., and Burgess, K. I. Ozone generation in positive corona electrostatic precipitators. IEEE Trans. Ind. and Gen. Appl. IGA-5 (1969): 489-496.

Castle, P. M., Kanter, I. E., Lee, P. K., and Kline, L. E. Corona glow detoxification study. Final Rep., Westinghouse Co., Contract No. DAAA 09-82-C-5396, 1984.

Chakarbarti, A., et al. Gas cleaning with semi-wet type plasma reactor. IEEE Trans. Ind. Appl. 31 (1995): 500-506.

Chang, J. S., and Masuda S. Mechanism of pulse corona induced plasma chemical processes for removal of NO_x and SO_x from combustion gases. Conf. Rec. IEEE/IAS 1988 Meeting (1988): 1599-1635.

Chang, J. S., and Maezono I. The electrode surface temperature profile in a corona discharge. J. Phys. D: Appl. Phys. 21 (1988): 1023-1024.

Chang, J. S., Lawless, P. A., and Yamamoto, T. Corona discharge processes. IEEE Trans. Plasma Sci. 19 (December 1991): 1152-1166.

Chang, M. B., Kushner, M. J., and Rood, M. J. Gas-phase removal of NO from gas streams via dielectric barrier discharges. Envir. Sci. and Tech. 26 (1992): 777-781.

Chang, M. B. Removal of SO_2 and NO from gas streams with combined plasma photolysis. J. Envir. Eng. ASCE, 119 (1993): 414-423.

Chang, M. B., and Tseng, T. D. Gas-phase removal of H_2S and NH_3 with dielectric barrier discharges. J. Envir. Eng. 122 (January 1996): 41-46.

Chantry, P.J. and G.J. Schulz, Phys. Rev., 156 (1967): 134

Clements, J. S., Mizuno, A., Finney, W. C., and Davis, R. H. Combined removal of SO_2, NO_x and fly ash from flue gas using pulsed streamer corona. IEEE Trans. Ind. Appl. 25 (1989): 62-69.

Davidson, J.H. and Mckinney, P.J. Chemical vapor deposition in the corona discharge of electrostatic air cleaners. Aerosol Science and Technology. 29(2) 1998.

Divers, E.; Ogawa, M. Ammonia amidosulphite. J. Chem. Society, Trans. 77 (1990): 327-335.

Dorsey, J. A., and Davidson, J. H. Ozone production in electrostatic air cleaners with contaminated electrodes. IEEE Trans. Ind. Appl. 30 (1994): 370-376.

Duecker, W. W., and J. R. West manufacture of sulfuric acid. ACS Monograph 144. Reinhold (1959)

Eliasson, B., Hirth, M., and Kogelschatz, U. Ozone synthesis from oxygen in dielectric barrier discharges. J. Phys. D: Applied Phys. 20 (1987): 1421-1437.

Hadj-Ziane, S., B. Held, P. Pignoleet, R. Peyrous and C. Coste, J. Phys. D: Appl. Phys. 25 (1992): 677.

Hattori, H., Ito, T., Ehara, Y., and Miyata, Y. Superposition effect on ozone synthesis by two types of discharges. Trans. IEE Japan 112A (1992): 41-46.

Helfritch, D. J., and Feldman, P. L. A pilot scale study of electron beam removal of SO_2 and NO_x from flue gas. Cottrel Envir. Sci. Somerville, N. J., Final Rep. to US DOE under Contract No. DE-FC22-81PC15079, 1985.

Helfritch, D. J. Pulsed corona discharge for hydrogen sulfide decomposition. IEEE Trans. Ind. Appl. 29, 1993.

Hickman, W. M., and R. E. Fox Electron Attachment in Sulfur Hexafluoride Usinf Monoenergetic Electron. J. Chem. Phys. 25 (1956): 642

Higashi, M., Sugaya, M., Ueki, K., and Fujii, K. Plasma processing of exhaust gas from a diesel engine vehicle. Proc. Int. Conf. on Plasma Chem. 2 (1985): 366-371.

Horvath, M. Ozone. Amsterdam, The Netherlands: Elsevier Sci., 1980.

Hsunling Bai, Fundamental Study of Ammonia-Sulfur Dioxide Reactions to Form Solid Particles. Doctoral Dissertation, Univ. of Cincinnati, USA, 1992.

Ito, T., Ehara, Y., Sakai, T., and Miyata, Y. Superposition effect on ozone synthesis by discharge. J. Jpn. Res. Group Elec. Discharges no. 127 (1990): 113-118.

Jordan, S., and Schikarski, W. Simultaneous $DeSO_x$ and $DeNO_x$ of flue gases by the EB-process in the agate pilot plant. Electron Beam Processing of Combustion Gases IAEA-TECDOC-428, (1987): 135-150.

Kamase, Y., Nagahama, T., and Mizuno, A. Removal of ethylene by streamer corona discharge. Rec. 1991 IEEE/IAS Ann. Meet. (1991): 747-751.

Kawamura, K., et al. Flue gas treatment of electron-beam irradiation. J. Atomic Energy Soc. Japan 20 (1978): 359-367.

Kohl, A. L., and Riesenfeld, F. C. Gas Purification. 3rd ed., Gulf Pub., Houston, 1979.

Khongphasarnkaln, P., Removal of Trimethylamine Acetaldehyde and Ammonia using electron attachment reaction. Master’s degree thesis. Chulalongkorn University 1998.

Lagarias, J. S. Discharge electrodes and electrostatic precipitors. JAPCA 10 (1960): 271-274.

Lakdawala V. K. and Moruzzi J. L. Attachment, detachment and ion-molecule reactions in SO_2 and SO_2- O_2 mixtures. J. Phys. D: Appl. Phys., 14 (1981): 2015-26.

Landreeth, R., de Pena, R.G., Heicklen, J. Thermodynamics of the Reactions $(NH_3)_nSO_{2(g)} = nNH_{3(g)} + SO_2$. J. Phys. Chem., 78 (1974): 1378-1380.

Larpsuriyakul, K., Sano, N., Tamon, H., Tanthapanichakoon, W., and Okazaki, M. Influence of structure of corona-discharge reactor on removal of dilute gases using electron attachment. Proc. Himeji Conf. Soc. Chem. Engrs. Japan (1996): 270-271.

Larpsuriyakul, K., Charinpanitkul, T., Tanthapanichakoon, W., Sano, N., Tamon, H., and Okazaki, M. Removal of dilute gaseous impurities by electron attachment reaction using corona-discharge reactors of different structures. 7th National Conf. Chem. Eng. and Appl. Chemistry 24-25 October 1997.

Lawless, P. A., McLean, K. J., Sparks, L. E., and Ramsey, G. H. Negative corona in wire-plate electrostatic precipitators. Part I: Characteristics of individual tuft-corona discharge. J. Electrostatics 18 (1986): 199-217.

Loiseau, J.F., F. Lacassie, C. Monge, R. Peyrous, B. Held and C. Coste, J., Phys, D, 29 (1994): 63

Massay, S. H. Negative Ions. Cambridge Univ. Press, Cambridge, England, 1976.

Massay, S. H. Atomic and Molecular Collisions. Taylor & Francis, London, 1979.

Masuda, S., Hirano, M., and Akutsu, K. Enhancement of electron beam denitrization process by means of electric field. Radiat. Phys. Chem. 17 (1981): 223-228.

Masuda, S., Sato, M., and Seki, T. High efficiency ozonizer using traveling wave pulse voltage. Conf. Rec. IEEE/IAS 1984 Ann. Meet. Chicago, IL, (1984): 978-985.

Masuda, S., and Nakao, H. Control of NO_x by positive and negative pulsed corona discharges. Conf. Rec. IEEE/IAS Ann. Meet. (1986): 1173-1182.

Masuda, S., Akutsu, K., Kuroda, M., Awatsu, Y., and Shibuya, Y. A ceramic-based ozonizer using high-frequency surface discharge. IEEE Trans. Ind. Appl. IA-24 (1988): 223-231.

Masuda, S., Pulse corona induced plasma chemical process. Pure Applied Chem. 60 (1988): 727-731.

Masuda, S., and Nakao, H. Control of NO_x by positive and negative pulsed corona discharges. IEEE Trans. Ind. Appl. 26 (1990): 374-383.

Masuda, S., et al. Destruction of gaseous pollutants by surface-induced plasma chemical process (SPCP). IEEE Trans. Ind. Appl. 29 (1993): 781-786.

Mizuno, A., Clements, J. S., and Davis, R. H. The use of energetic electrons in a particle precharger and in a sulfur dioxide reactor. Proc. 2nd Int. Conf. on Electrostatic Precipitation (1984): 498-512.

Mizuno, A. An electrostatic precipitator using a ferroelectric pellet layer for particle collection. Proc. IEEE/IES 1986 Ann. Conf. (Denver, Co.) (October 1986): 1106-1112.

Mizuno, A., Clements, J. S., and Davis, R. H. A method for the removal of sulfur dioxide from exhaust gas utilizing pulsed streamer corona for electron energization. IEEE Trans. Ind. Appl. IA-22 (1986): 516-522.

Mizuno, A., and Ito, H. An electrostatic precipitator using a ferroelectric pellet layer for particle collection. Proc. 3rd Int. Conf. on Electrostatic Precipitation (1988): 617-624.

Mizuno, A., Chakrabarti, A., and Okazaki, K. Application of corona technology in the reduction of greenhouse gases and other gaseous pollutants. Nonthermal Plasma Tech. Pollution Contr. B. M. Penetrante and S. E. Schultheis, Ed., Berlin: Springer-Verlag, NATO ASI Series, 34 (1993): 165-185.

Mizuno, A., et al. NO_x removal process using pulsed discharge plasma. IEEE Trans. Ind. Appl. 3 (1995): 957-963.

Moruzzi, J. L., and Phelps, A. V. Survey of negative-ion-molecule reactions in O_2, CO_2, H_2O, CO, and mixtures of these gases at high pressures. J. Chem. Phys. 45 (December 1966): 4617-4627.

Nashimoto, K. The effect of electrode materials on O_3 and NO_x emissions by corona discharging. J. Imaging Sci. 32 (1988): 205-210.

Oda, T., et al. Decomposition of gaseous organic contaminants by surface discharge induced plasma chemical process-SPCP. IEEE Trans. Ind. Appl. 32 (1996): 118-124.

Oda, T., Yamashita, R., Takahashi, T., and Masuda, S. Atmospheric pressure discharge plasma decomposition for gaseous air contaminants-Trichlorotrifluoroethane and Trichloroethylene. IEEE Trans. Ind. Appl. 32 (1996): 227-232.

Oglesby, S., and Nichols, G. B. Electrostatic Precipitation. Marcel Dekker, New York, 1978.

Palumbo, F. J., and Fraas, F. The removal of sulfur from stack gases by an electric discharge. J. Air Pollution Contr. Assoc. 21 (1971): 143-144.

Penny, G. W., and Craig, S. E. Sparkover as influenced by surface conditions in dc corona. AIEE (1960): 112-118.

Perry, R.H., and Green, D. W. Perry’s Chemical Engineers’ handbook. 7th ed. New York: McGraw-Hill, 1997.

Rapp, D. And D. D. Brriglia, J. Chem. Phys., 43 (1965): 1480

Sano, N., Nagamoto, T., Tamon, H., and Okazaki, M. Removal of iodine and methyl iodide in gas by wetted-wall reactor based on selective electron attachment. J. Chem. Eng. Japan 29 (1996): 59-64.

Sano, N. Development of Gas Purification Technology by Selective Electron Attachment. Doctoral Dissertation, Kyoto Univ., Japan, 1997.

Tamaki, K., et al. Oxidation of nitrogen monoxide by corona discharge - Effect of discharge conditions. Proc. Chem. Soc. Japan 11 (1979): 1582.

Tamon, H., Yano, H., and Okazaki, M. A new method of gas mixture separation based on selective electron attachment. Kagaku Kogaku Ronbunshu 15 (1989): 663-668.

Tamon, H., et al. New concept of gas purification by electron attachment. AIChE J. 41 (1995): 1701-1711.

Tanthapanichakoon, W., Larpsuriyakul, K., Sano, N., Tamon, H., and Okazaki, M. Effect of reactor structure on removal of methyl iodide and chlorofluorocarbon in gas using selective electron attachment. Proc. Regional Sym. Chem. Eng. 1996 Jakarta, Indonesia, (October 1996): 3.2.1-3.2.14.

Tanthapanichakoon, W., Larpsuriyakul, K., Charinpanitkul, T., Sano, N., Tamon, H., and Okazaki, M. Effect of structure of corona-discharge reactor on removal of dilute gaseous pollutants using selective electron attachment. J. Chem. Eng. Japan (in press).

Uhm, H.S., Influence of chamber temperature on properties of the corona discharge system. Physics of Plasmas 6(2) 1999: 623-626.

Urabe, T., et al. Removal of Hg vapor by the pulse energization. Proc. Chem. Eng. Conf. Japan (in Japanese) July 1986.

Viner, A. S., Lawless, P. A., and Ensor, D. S. Ozone generation in dc-energized electrostatic precipitators. Proc. 1989 IEEE/IAS (1989): 2167-2174.

Waddams, A. L., Acetylene derivatives Chemicals from Petroleum (1980): 58.

Weiss, H. R. Plasma induced dissociation of carbon dioxide. Proc. Int. Conf. on Plasma Chem. 2 (1985): 383-388.

White, H. J., and Cole, W. H. Design and performance of high-velocity, high-efficiency air cleaning precipitators. JAPCA 10 (1960): 239-245.

Yamamoto, T., Lawless, P. A., and Sparks, L. E. Narrow-gap point-to-plane corona with high velocity flows. IEEE Trans. Ind. Appl. 24 (1988): 934-939.

Yamamoto, T., et al. Control of volatile organic compounds by an ac energized ferroelectric pellet reactor and a pulsed corona reactor. IEEE Trans. Ind. Appl. 28 (1992): 528-534.

Yamamoto, T., Shioji, S., and Masuda, S. Synthesis of ultra-fine particles by surface discharge induced plasma chemical process (SPCP) and its application. IEEE Trans. Ind. Appl. 28 (1992): 1189-1193.

Yamamoto, T., et al. Catalysis-assisted plasma technology for carbon tetrachloride destruction. IEEE Trans. Ind. Appl. 32 (1996): 100-105.

Zhang, R., Yamamoto, T., and Bundy, D. S. Control of ammonia and odors in animal house by a ferroelectric plasma reactor. IEEE Trans. Ind. Appl. 32 (1996): 113-117.

APPENDICES

APPENDIX A

CALIBRATION CURVE

Calibration Curve between GC Peak Area and Concentration of Toluene

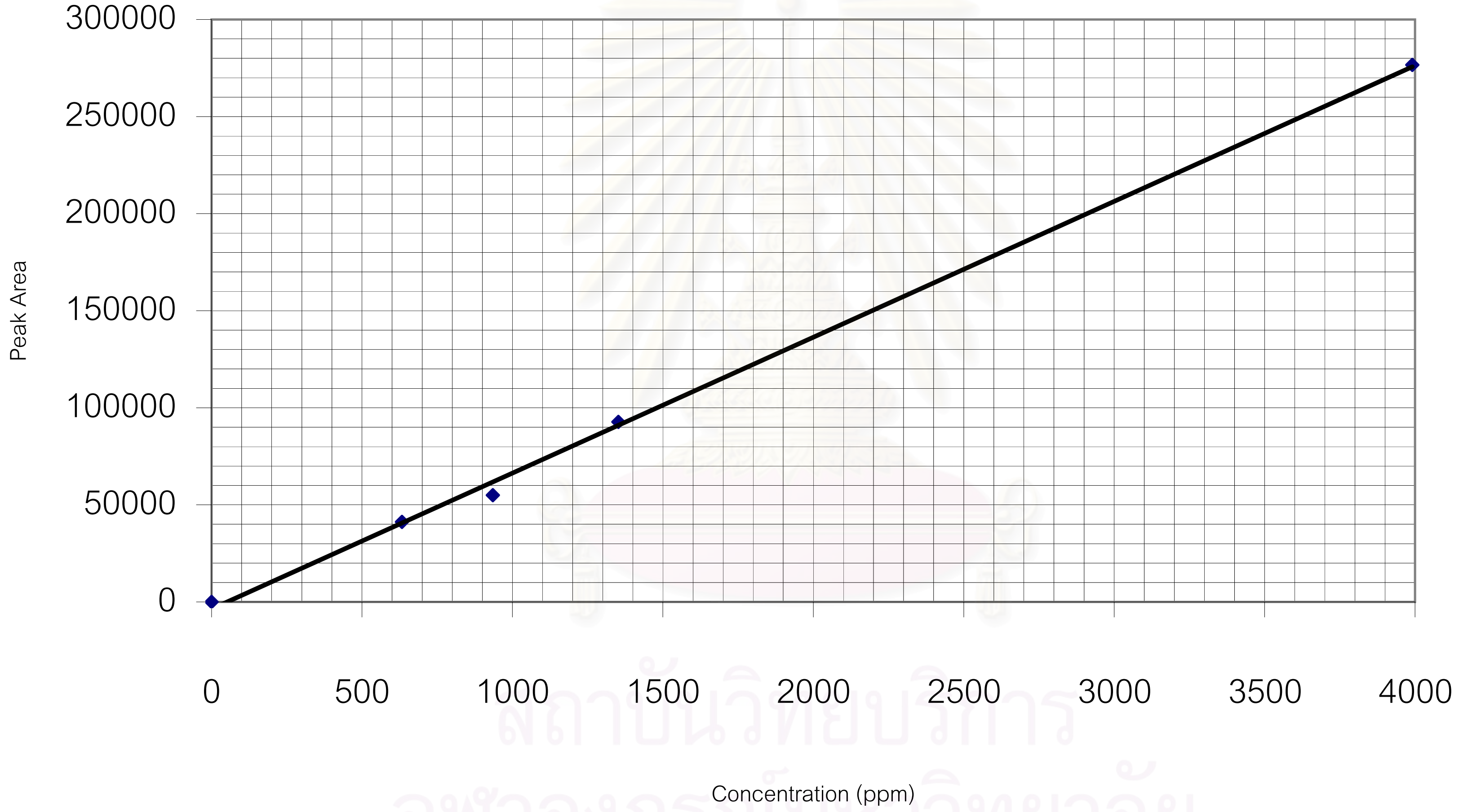

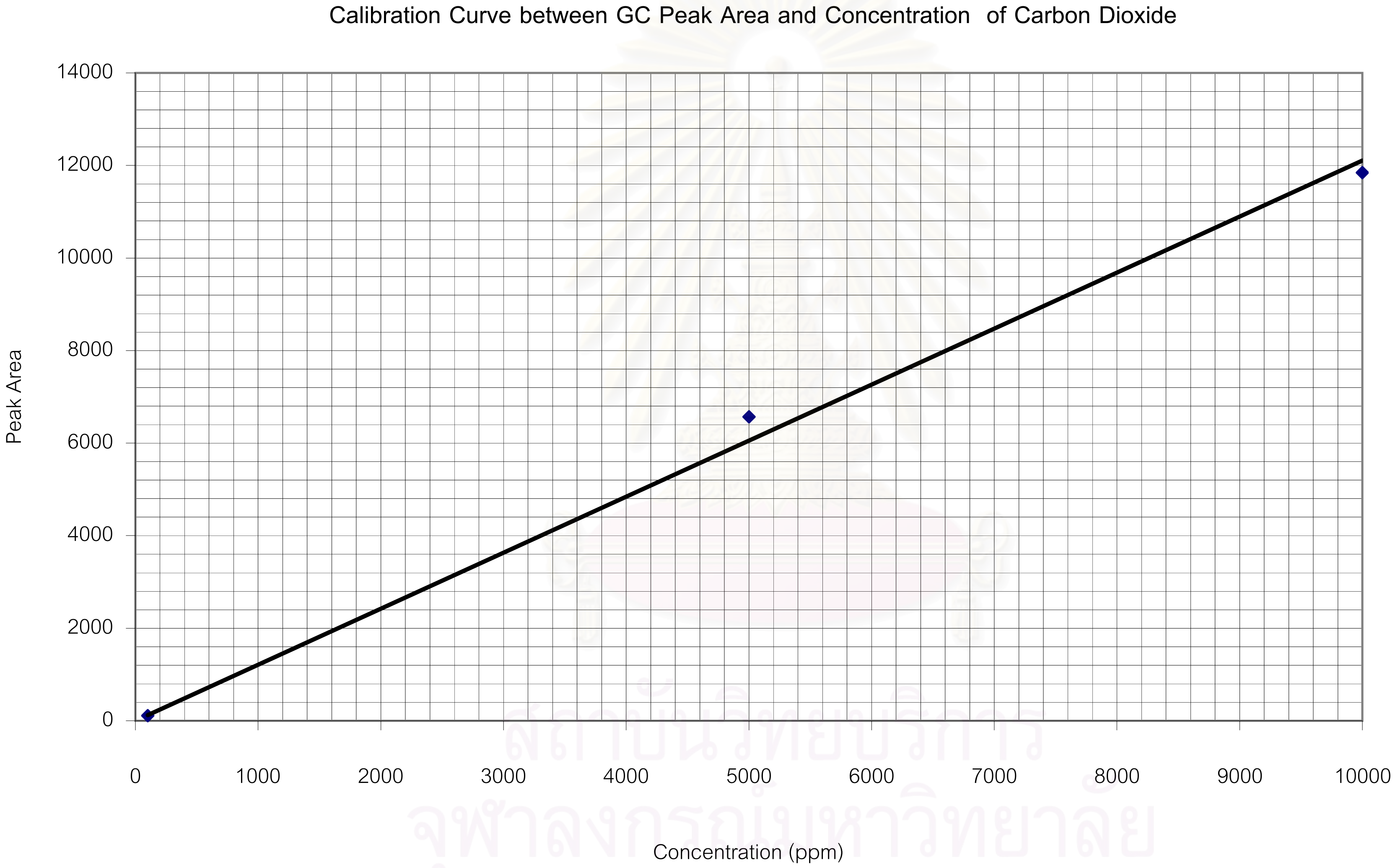
Calibration Curve between GC Peak Area and Concentration of Carbon Dioxide
Peak Area
14000
12000
10000
8000
6000
4000
2000
0
0
1000
2000
3000
4000
5000
6000
7000
8000
9000
10000
Concentration (ppm)

Calibration Curve between GC Peak Area and Concentration of Water Vapor

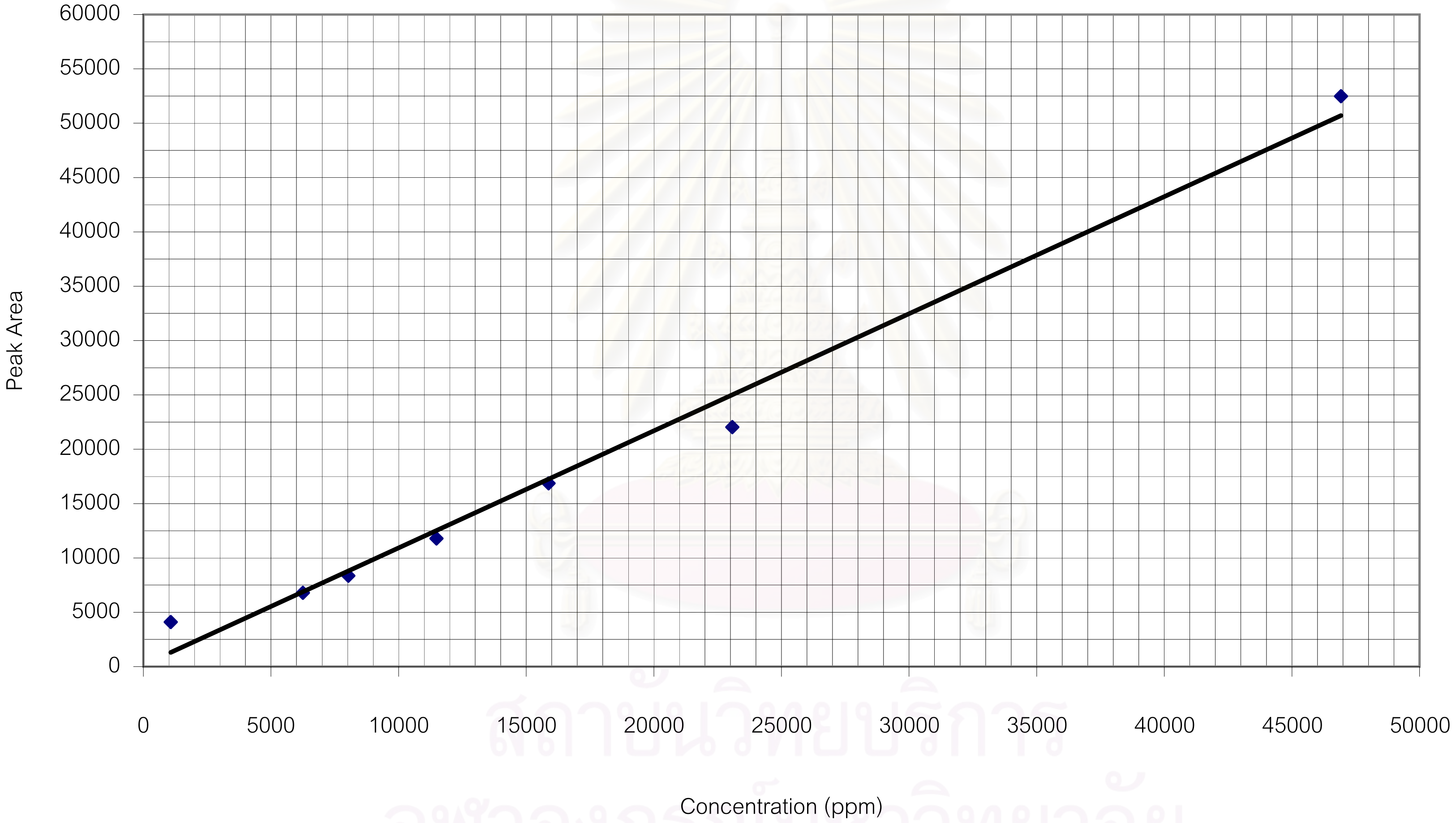

APPENDIX B

ALL OF EXPERIMENTAL DATA

Removal of toluene from nitrogen

Inlet concentration	2000	ppm
Current	0.5	mA
Oxygen	0	%
Cathode diameter	0.3	mm

Temp(C)	I (mA)	V (kV)	P (W)	Cin	Cout (0mA)	Cout (0.5 mA)	ψ (%)	ψ' (%)	ψ''(%/s)	E/N (Volt mol^{-1} m^{2})
28	0.5	12.1	6.05	1982	1685	1420	28.38	15.74	0.24	6267
100	0.5	11.3	5.65	2014	1813	1510	25.02	16.69	0.32	6131
200	0.5	9.2	4.60	1972	1913	1611	18.32	15.79	0.38	5615
300	0.5	6.3	3.15	1956	1917	1606	17.91	16.23	0.48	4186
400	0.5	4.4	2.20	2098	2056	1448	30.98	29.57	1.02	4056

Removal of toluene from nitrogen

Inlet concentration	2000	ppm
Current	0.5	mA
Oxygen	0	%
Cathode diameter	0.5	mm

Temp(C)	I (mA)	V (kV)	P (W)	Cin	Cout (0mA)	Cout (0.5 mA)	ψ (%)	ψ' (%)	ψ''(%/s)	E/N (Volt mol^{-1} m^{2})
28	0.5	12.1	6.05	2020	1717	1292	36.04	24.75	0.38	7817
100	0.5	9.8	4.90	1944	1750	1441	25.87	17.66	0.34	7061
200	0.5	7.1	3.55	1901	1844	1458	23.30	20.93	0.51	5176
300	0.5	5.4	2.70	1899	1861	1494	21.33	19.72	0.58	4034
400	0.5	4.1	2.05	1927	1888	1176	38.97	37.71	1.31	2411

Removal of toluene from nitrogen

Inlet concentration of Toluene	2000	ppm
Current	0.5	mA
Oxygen	0	%
Cathode diameter	0.9	mm

Temp(C)	I (mA)	V (kV)	P (W)	Cin	Cout (0mA)	Cout (0.5 mA)	ψ (%)	ψ' (%)	ψ''(%/s)	E/N (Volt mol^{-1} m^{2})
28	0.5	14.9	7.45	1945	1653	1130	41.90	31.64	0.49	10444
100	0.5	11.8	5.90	1982	1784	1336	32.59	25.11	0.48	10250
200	0.5	8.5	4.25	1907	1850	1412	25.96	23.68	0.58	9363
300	0.5	6.5	3.25	1964	1925	1477	24.80	23.27	0.69	8673
400	0.5	5	2.50	1930	1891	978	49.33	48.28	1.67	7836

Removal of toluene from nitrogen-oxygen

Inlet concentration of Toluene	2000	ppm
Current	0.5	mA
Oxygen	20	%
Cathode diameter	0.3	mm

Temp(C)	I (mA)	V (kV)	P (W)	Cin	Cout (0mA)	Cout (0.5 mA)	ψ (%)	ψ' (%)	ψ''(%/s)	E/N (Volt mol^{-1} m^2)
28	0.5	14.8	7.40	1972	1676	813	58.77	51.49	0.80	8136
100	0.5	9.7	4.85	1991	1792	962	51.68	46.32	0.89	6608
200	0.5	7.5	3.75	1987	1927	974	50.98	49.46	1.20	6479
300	0.5	6	3.00	1993	1953	1106	44.51	43.37	1.28	6279
400	0.5	4.9	2.45	1977	1937	788	60.14	59.32	2.06	6023

Removal of toluene from nitrogen-oxygen

Inlet concentration of Toluene	2000	ppm
Current	0.5	mA
Oxygen	20	%
Cathode diameter	0.5	mm

Temp(C)	I (mA)	V (kV)	P (W)	Cin	Cout (0mA)	Cout (0.5 mA)	ψ (%)	ψ' (%)	ψ''(%/s)	E/N (Volt mol^{-1} m^2)
28	0.5	15.3	7.65	1961	1667	528	73.07	68.33	1.06	9359
100	0.5	11.5	5.75	1912	1721	609	68.15	64.61	1.24	8717
200	0.5	8.7	4.35	1903	1846	714	62.48	61.32	1.49	8363
300	0.5	7	3.50	1997	1957	833	58.29	57.43	1.69	8151
400	0.5	5.1	2.55	2008	1968	594	70.42	69.82	2.42	6975

Removal of toluene from nitrogen-oxygen

Inlet concentration of Toluene	2000	ppm
Current	0.5	mA
Oxygen	20	%
Cathode diameter	0.9	mm

Temp(C)	I (mA)	V (kV)	P (W)	Cin	Cout (0mA)	Cout (0.5 mA)	ψ (%)	ψ' (%)	ψ''(%/s)	E/N (Volt mol^{-1} m^{2})
28	0.5	17	8.50	1980	1683	21	98.94	98.75	1.53	11916
100	0.5	13.6	6.80	1958	1762	389	80.13	77.92	1.50	11813
200	0.5	10.5	5.25	1990	1930	566	71.56	70.67	1.72	11566
300	0.5	8.5	4.25	1974	1935	623	68.44	67.80	2.00	11342
400	0.5	6.4	3.20	1988	1948	190	90.44	90.25	3.13	10030

Removal of toluene from nitrogen-oxygen

Inlet concentration of Toluene	2000 ppm
Current	0.1 mA
Oxygen	20 %
Cathode diameter	0.5 mm

Temp(C)	I (mA)	V (kV)	P (W)	Cin	Cout (0mA)	Cout (0.1 mA)	ψ (%)	ψ' (%)	ψ''(%/s)
28	0.1	11.7	1.17	1980	1683	1026	48.18	39.04	0.61
100	0.1	9.2	0.92	1958	1762	1113	43.16	36.83	0.71
200	0.1	8	0.80	1990	1930	1203	39.55	37.67	0.92
300	0.1	7.2	0.72	1974	1935	1281	35.11	33.80	1.00
400	0.1	6	0.60	1988	1948	988	50.30	49.28	1.71

Removal of toluene from nitrogen-oxygen

Inlet concentration of Toluene	2000	ppm
Current	0.3	mA
Oxygen	20	%
Cathode diameter	0.5	mm

Temp(C)	I (mA)	V (kV)	P (W)	Cin	Cout (0mA)	Cout (0.3 mA)	ψ (%)	ψ' (%)	ψ''(%/s)
28	0.3	13.4	4.02	1951	1658	907	53.51	45.30	0.70
100	0.3	11.7	3.51	1944	1750	939	51.70	46.34	0.89
200	0.3	10.2	3.06	1892	1835	927	51.00	49.48	1.21
300	0.3	8.9	2.67	1977	1937	1097	44.51	43.37	1.28
400	0.3	6.9	2.07	2088	2046	832	60.15	59.34	2.06

Removal of toluene from nitrogen-oxygen

Inlet concentration of Toluene	2000	ppm
Current	0.5	mA
Oxygen	20	%
Cathode diameter	0.5	mm

Temp(C)	I (mA)	V (kV)	P (W)	Cin	Cout (0mA)	Cout (0.5 mA)	ψ (%)	ψ' (%)	ψ''(%/s)
28	0.5	15.7	7.85	1976	1680	532	73.08	68.33	1.06
100	0.5	13.4	6.70	2011	1810	641	68.13	64.59	1.24
200	0.5	12	6.00	1999	1939	750	62.48	61.32	1.49
300	0.5	10	5.00	1912	1874	798	58.26	57.42	1.69
400	0.5	7.3	3.65	1944	1905	575	70.42	69.82	2.42

Removal of toluene from nitrogen

Inlet concentration of Toluene	2000	ppm
Current	0.1	mA
Oxygen	0	%
Cathode diameter	0.5	mm

Temp(C)	I (mA)	V (kV)	P (W)	Cin	Cout (0mA)	Cout (0.1 mA)	ψ (%)	ψ' (%)	ψ"(%/s)
28	0.1	8.2	0.82	1952	1659	1498	23.26	9.70	0.15
100	0.1	7	0.70	1931	1738	1574	18.49	9.44	0.18
200	0.1	6	0.60	1907	1850	1707	10.49	7.73	0.19
300	0.1	3.8	0.38	2079	2037	1965	5.48	3.53	0.10
400	0.1	3.1	0.31	1955	1916	1561	20.15	18.53	0.64

Removal of toluene from nitrogen

Inlet concentration of Toluene	2000	ppm
Current	0.3	mA
Oxygen	0	%
Cathode diameter	0.5	mm

Temp(C)	I (mA)	V (kV)	P (W)	Cin	Cout (0mA)	Cout (0.3 mA)	ψ (%)	ψ' (%)	ψ"(%/s)
28	0.3	13.5	4.05	1996	1697	1483	25.70	12.61	0.20
100	0.3	10.3	3.09	1894	1705	1490	21.33	12.61	0.24
200	0.3	9.1	2.73	1842	1787	1467	20.36	17.91	0.44
300	0.3	7.4	2.22	1899	1861	1645	13.38	11.61	0.34
400	0.3	4.6	1.38	2034	1993	1406	30.88	29.45	1.02

Removal of toluene from nitrogen

Inlet concentration of Toluene	2000	ppm
Current	0.5	mA
Oxygen	0	%
Cathode diameter	0.5	mm

Temp(C)	I (mA)	V (kV)	P (W)	Cin	Cout (0mA)	Cout (0.5 mA)	ψ (%)	ψ' (%)	ψ''(%/s)
28	0.5	14.7	7.35	1968	1673	1259	36.03	24.75	0.38
100	0.5	13	6.50	1893	1704	1403	25.88	17.66	0.34
200	0.5	10.6	5.30	1927	1869	1478	23.30	20.92	0.51
300	0.5	8.3	4.15	1916	1878	1507	21.35	19.76	0.58
400	0.5	5.2	2.60	1964	1925	1198	39.00	37.77	1.31

Removal of toluene from nitrogen-oxygen

Inlet concentration of Toluene	2000	ppm
Current	0.5	mA
Oxygen	0	%
Cathode diameter	0.5	mm

Temp(C)	I (mA)	V (kV)	P (W)	Cin	Cout (0mA)	Cout (0.1 mA)	ψ (%)	ψ' (%)	ψ''(%/s)
28	0.5	14.7	7.35	1968	1673	1259	36.03	24.75	0.38
100	0.5	13	6.50	1893	1704	1403	25.88	17.66	0.34
200	0.5	10.6	5.30	1927	1869	1478	23.30	20.92	0.51
300	0.5	8.3	4.15	1916	1878	1507	21.35	19.76	0.58
400	0.5	5.2	2.60	1964	1925	1198	39.00	37.77	1.31

Removal of toluene from nitrogen-oxygen

Inlet concentration of Toluene	2000	ppm
Current	0.5	mA
Oxygen	5	%
Cathode diameter	0.5	mm

Temp(C)	I (mA)	V (kV)	P (W)	Cin	Cout (0mA)	Cout (0.1 mA)	ψ (%)	ψ' (%)	ψ''(%/s)
28	0.5	15	7.50	1939	1648	941	51.47	42.90	0.67
100	0.5	13.2	6.60	1946	1751	1007	48.25	42.49	0.82
200	0.5	11.1	5.55	1973	1914	1091	44.70	43.00	1.05
300	0.5	8.9	4.45	1991	1951	1148	42.34	41.16	1.21
400	0.5	6.4	3.20	1952	1913	905	53.64	52.69	1.83

Removal of toluene from nitrogen-oxygen

Inlet concentration of Toluene	2000	ppm
Current	0.5	mA
Oxygen	20	%
Cathode diameter	0.5	mm

Temp(C)	I (mA)	V (kV)	P (W)	Cin	Cout (0mA)	Cout (0.5 mA)	ψ (%)	ψ' (%)	ψ''(%/s)
28	0.5	15.7	7.85	1961	1667	528	73.07	68.33	1.06
100	0.5	13.4	6.70	1912	1721	609	68.15	64.61	1.24
200	0.5	12	6.00	1903	1846	714	62.48	61.32	1.49
300	0.5	10	5.00	1997	1957	833	58.29	57.43	1.69
400	0.5	7.3	3.65	2008	1968	594	70.42	69.82	2.42

Removal of toluene from nitrogen-oxygen

Inlet concentration of Toluene 2000 ppm

Current 0.5 mA

Oxygen 30 %

Cathode diameter 0.5 mm

Temp(C)	I (mA)	V (kV)	P (W)	Cin	Cout (0mA)	Cout (0.5 mA)	ψ (%)	ψ' (%)	ψ''(%/s)	CO_2 (ppm)	H_2O (ppm)
28	0.5	16.7	8.35	1927	1638	355	81.58	78.33	1.21	670	154
100	0.5	15.8	7.90	1986	1787	229	88.47	87.19	1.67	716	249
200	0.5	13.6	6.80	1942	1884	179	90.78	90.50	2.20	1206	608
300	0.5	11.3	5.65	1919	1881	155	91.92	91.76	2.71	1536	1554
400	0.5	8.3	4.15	1976	1936	103	94.79	94.68	3.28	5034	2399

Removal of toluene from nitrogen

Inlet concentration of Toluene	500	ppm
Current	0.5	mA
Oxygen	0	%
Cathode diameter	0.5	mm

Temp(C)	I (mA)	V (kV)	P (W)	Cin	Cout (0mA)	Cout (0.5 mA)	ψ (%)	ψ' (%)	ψ"(%/s)
28	0.5	15	7.50	1934	1644	996	48.50	39.42	0.61
100	0.5	13.4	6.70	1978	1780	1124	43.17	36.85	0.71
200	0.5	10.9	5.45	1964	1905	1200	38.90	37.01	0.90
300	0.5	8.8	4.40	2076	2034	1444	30.44	29.01	0.86
400	0.5	5.8	2.90	2011	1971	996	50.47	49.47	1.71

Removal of toluene from nitrogen

Inlet concentration of Toluene	1000	ppm
Current	0.5	mA
Oxygen	0	%
Cathode diameter	0.5	mm

Temp(C)	I (mA)	V (kV)	P (W)	Cin	Cout (0mA)	Cout (0.5 mA)	ψ (%)	ψ' (%)	ψ"(%/s)
28	0.5	14.9	7.45	1946	1654	1118	42.55	32.41	0.50
100	0.5	13.2	6.60	1958	1762	1329	32.12	24.57	0.47
200	0.5	10.8	5.40	1925	1861	1371	28.78	26.33	0.64
300	0.5	8.6	4.30	2001	1961	1497	25.19	23.66	0.70
400	0.5	5.5	2.75	2077	2035	1227	40.92	39.71	1.38

Removal of toluene from nitrogen

Inlet concentration of Toluene	2000	ppm
Current	0.5	mA
Oxygen	0	%
Cathode diameter	0.5	mm

Temp(C)	I (mA)	V (kV)	P (W)	Cin	Cout (0mA)	Cout (0.5 mA)	ψ (%)	ψ' (%)	ψ''(%/s)
28	0.5	14.7	7.35	1893	1654	1211	36.03	26.78	0.42
100	0.5	13	6.50	1844	1762	1366	25.92	22.47	0.43
200	0.5	10.6	5.30	1902	1861	1458	23.34	21.66	0.53
300	0.5	8.3	4.15	1946	1961	1455	25.23	25.80	0.76
400	0.5	5.2	2.60	1857	2035	1097	40.93	46.09	1.60

Removal of toluene from nitrogen-oxygen

Inlet concentration of Toluene	500	ppm
Current	0.5	mA
Oxygen	20	%
Cathode diameter	0.5	mm

Temp(C)	I (mA)	V (kV)	P (W)	Cin	Cout (0mA)	Cout (0.5 mA)	ψ (%)	ψ' (%)	ψ"(%/s)
28	0.5	16	8.00	1999	1699	189	90.55	88.88	1.38
100	0.5	13.8	6.90	1916	1724	283	85.23	83.58	1.61
200	0.5	12.5	6.25	1973	1914	495	74.91	74.14	1.81
300	0.5	10.4	5.20	1946	1907	601	69.12	68.48	2.02
400	0.5	7.7	3.85	1857	1820	161	91.33	91.15	3.16

Removal of toluene from nitrogen-oxygen

Inlet concentration of Toluene	1000	ppm
Current	0.5	mA
Oxygen	20	%
Cathode diameter	0.5	mm

Temp(C)	I (mA)	V (kV)	P (W)	Cin	Cout (0mA)	Cout (0.5 mA)	ψ (%)	ψ' (%)	ψ''(%/s)
28	0.5	15.9	7.95	1893	1609	369	80.51	77.07	1.19
100	0.5	13.6	6.80	1844	1660	493	73.26	70.30	1.35
200	0.5	12.3	6.15	1902	1845	606	68.14	67.15	1.64
300	0.5	10.2	5.10	1946	1907	666	65.78	65.08	1.92
400	0.5	7.5	3.75	1857	1820	239	87.13	86.87	3.01

Removal of toluene from nitrogen-oxygen

Inlet concentration of Toluene	2000	ppm
Current	0.5	mA
Oxygen	20	%
Cathode diameter	0.5	mm

Temp(C)	I (mA)	V (kV)	P (W)	Cin	Cout (0mA)	Cout (0.5 mA)	ψ (%)	ψ' (%)	ψ''(%/s)
28	0.5	15.7	7.85	1961	1667	528	73.07	68.33	1.06
100	0.5	13.4	6.70	1912	1721	609	68.15	64.61	1.24
200	0.5	12	6.00	1903	1846	714	62.48	61.32	1.49
300	0.5	10	5.00	1997	1957	833	58.29	57.43	1.69
400	0.5	7.3	3.65	2008	1968	594	70.42	69.82	2.42

Removal of toluene from nitrogen-water vapor

Inlet concentration of Toluene	2000	ppm
Current	0.5	mA
Oxygen	0	%
Cathode diameter	0.5	mm
Water vapor	0	ppm

Temp(C)	I (mA)	V (kV)	P (W)	Cin	Cout (0mA)	Cout (0.5 mA)	ψ (%)	ψ' (%)	ψ''(%/s)
28	0.5	14.7	7.35	1893	1654	1118	40.94	32.41	0.50
100	0.5	13	6.50	1844	1762	1329	27.93	24.57	0.47
200	0.5	10.6	5.30	1902	1861	1371	27.92	26.33	0.64
300	0.5	8.3	4.15	1946	1961	1497	23.07	23.66	0.70
400	0.5	5.2	2.60	1857	2035	1227	33.93	39.71	1.38

Removal of toluene from nitrogen-water vapor

Inlet concentration of Toluene	2000	ppm
Current	0.5	mA
Oxygen	0	%
Cathode diameter	0.5	mm
Water vapor	1882	ppm

Temp(C)	I (mA)	V (kV)	P (W)	Cin	Cout (0mA)	Cout (0.5 mA)	ψ (%)	ψ' (%)	ψ"(%/s)
28	0.5	9.7	4.85	1923	1635	1223	36.40	25.20	0.39
100	0.5	8.7	4.35	1918	1726	1351	29.56	21.73	0.42
200	0.5	8.5	4.25	1960	1901	1505	23.21	20.83	0.51
300	0.5	6.4	3.20	1946	1907	1541	20.81	19.19	0.57
400	0.5	5.5	2.75	1937	1898	1171	39.55	38.30	1.33

Removal of toluene from nitrogen-water vapor

Inlet concentration of Toluene	2000	ppm
Current	0.5	mA
Oxygen	0	%
Cathode diameter	0.5	mm
Water vapor	7453	ppm

Temp(C)	I (mA)	V (kV)	P (W)	Cin	Cout (0mA)	Cout (0.5 mA)	ψ (%)	ψ' (%)	ψ"(%/s)
28	0.5	11.7	5.85	1971	1675	1205	38.86	28.06	0.44
100	0.5	10.9	5.45	1981	1783	1340	32.36	24.85	0.48
200	0.5	9.7	4.85	1976	1917	1413	28.49	26.29	0.64
300	0.5	8.8	4.40	1974	1935	1537	22.14	20.57	0.61
400	0.5	5.8	2.90	1989	1949	1252	37.05	35.76	1.24

Removal of toluene from nitrogen-water vapor

Inlet concentration of Toluene	2000	ppm
Current	0.5	mA
Oxygen	0	%
Cathode diameter	0.5	mm
Water vapor	20000	ppm

Temp(C)	I (mA)	V (kV)	P (W)	Cin	Cout (0mA)	Cout (0.5 mA)	ψ (%)	ψ' (%)	ψ''(%/s)
28	0.5	11.8	5.90	1927	1638	1253	34.98	23.50	0.36
100	0.5	11	5.50	1955	1950	1948	0.36	0.10	0.0020
200	0.5	10.2	5.10	1988	1980	1977	0.55	0.15	0.0037
300	0.5	8.9	4.45	1973	1968	1965	0.41	0.15	0.0045
400	0.5	5.9	2.95	1994	1989	1980	0.70	0.45	0.0157

Blank Test for the investigating of temperature to Toluene

Inlet concentration of Toluene	2000	ppm
Current	0	mA
Oxygen	0	%
Cathode diameter	0.5	mm

Temperature (C)	Peak Area		Concentration	
	Inlet	Outlet	Inlet	Outlet
28	142541	100824	2089	1880
100	147847	123840	2120	2000
200	149007	134923	2160	2120
300	148802	125910	2130	2090
400	143483	121744	2102	1791

Blank Test for the investigating of temperature to Toluene

Inlet concentration of Toluene	2000	ppm
Current	0	mA
Oxygen	20	%
Cathode diameter	0.5	mm

Temperature (C)	Peak Area		Concentration	
	Inlet	Outlet	Inlet	Outlet
28	138981	117053	2038	1724
100	132300	124566	1942	1832
200	140144	132998	2054	1952
300	133284	125440	1956	1844
400	141463	103475	2073	1530

APPENDIX C

ADDITIONAL FIGURES

APP. C1 EFFECT OF CATHODE SIZE DIAMETER

Removal of toluene from nitrogen

Inlet concentration of Toluene	2000 ppm
Current	0.5 mA
Oxygen	0 %

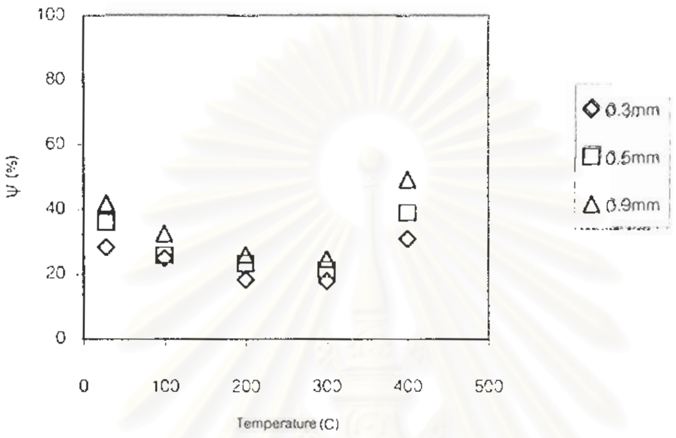

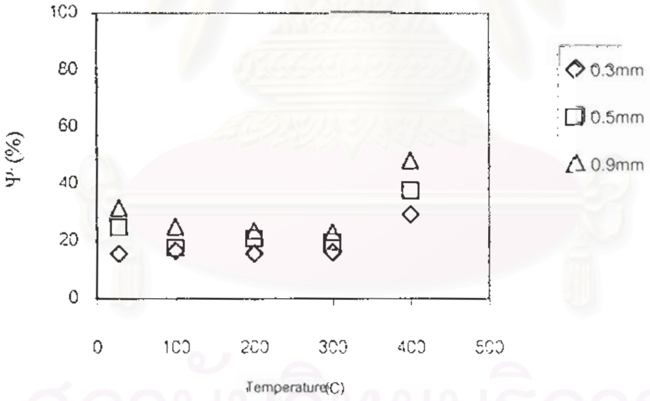

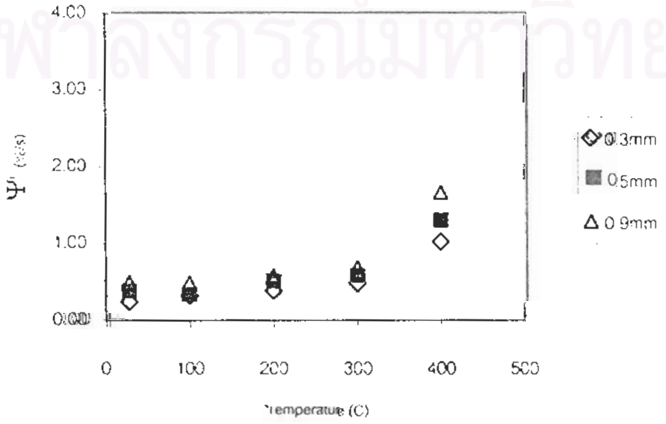

EFFECT OF CATHODE SIZE DIAMETER

Removal of toluene from nitrogen-oxygen

Inlet concentration of Toluene	2000 ppm
Current	0.5 mA
Oxygen	20 %

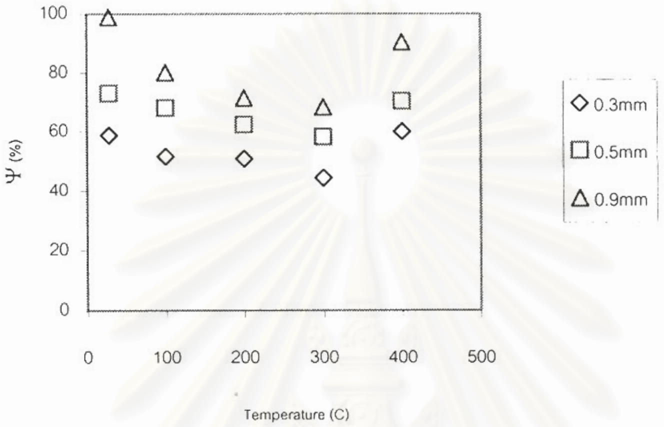

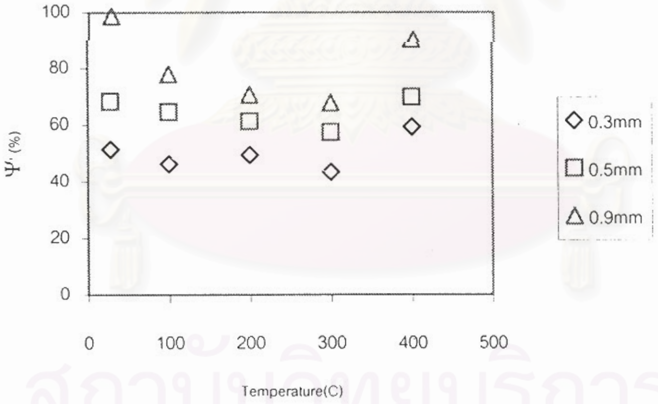

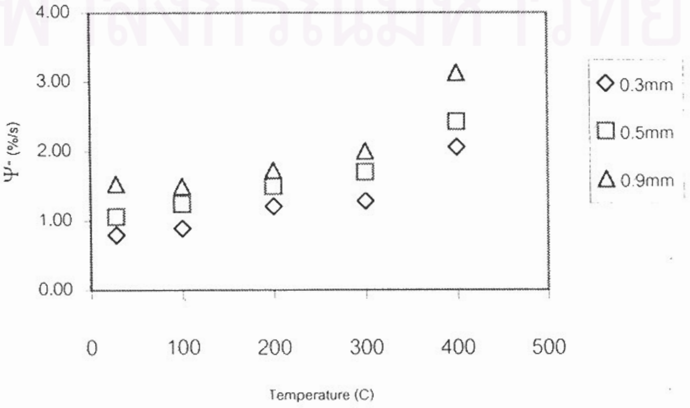

APP.C2 EFFECT OF DISCHARGE CURRENT

Removal of toluene from nitrogen

Inlet concentration of Toluene	2000 ppm
Cathode	0.5 mm
Oxygen	0 %

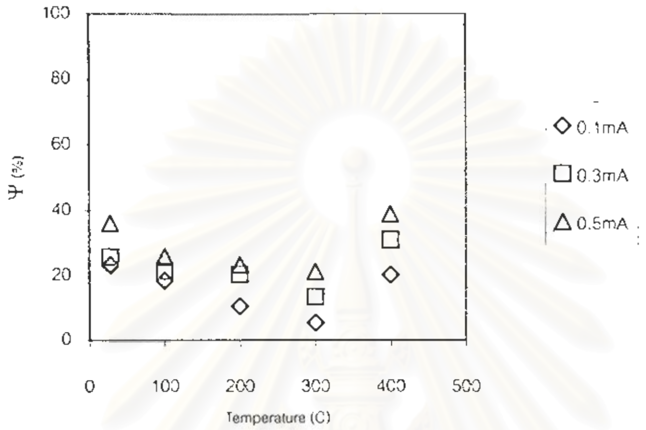

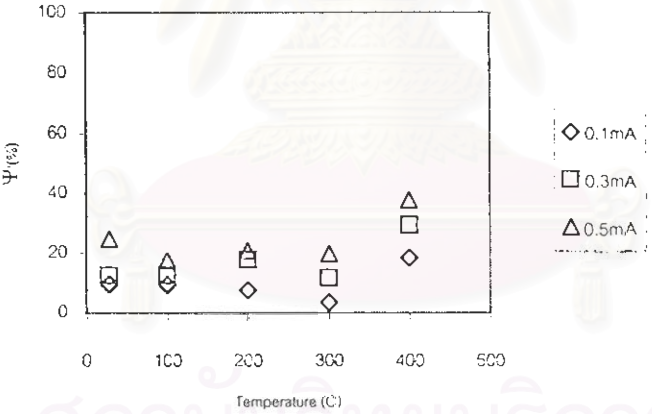

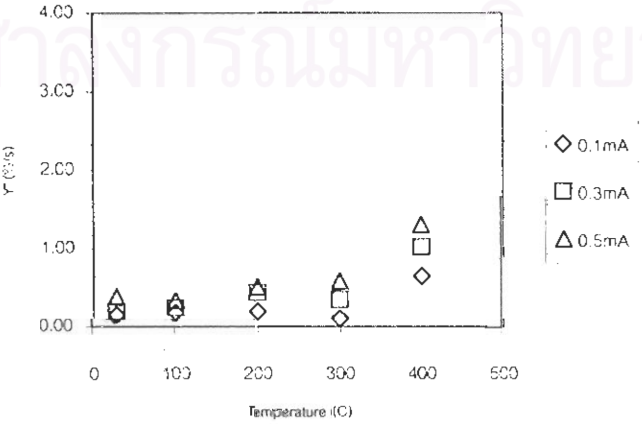

EFFECT OF DISCHARGE CURRENT

Removal of toluene from nitrogen-oxygen

Inlet concentration of Toluene	2000 ppm
Cathode	0.5 mm
Oxygen	20 %

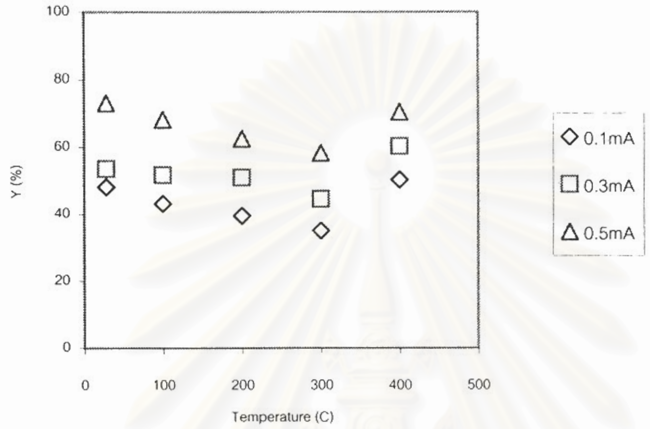

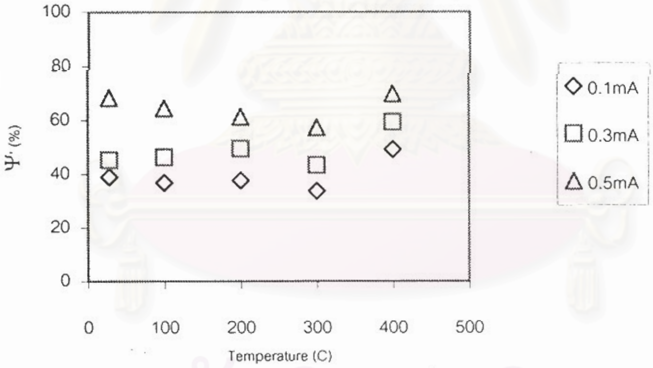

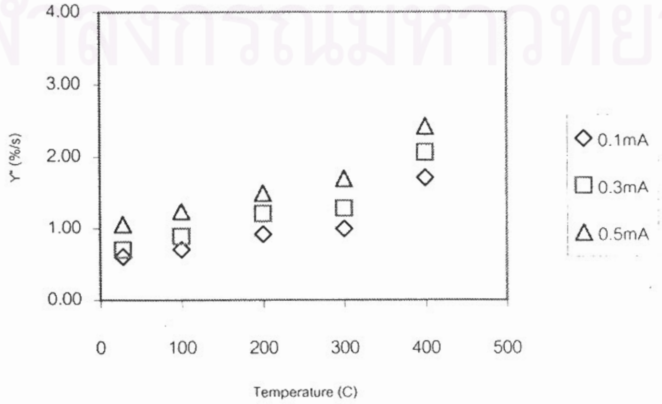

APP.C3 EFFECT OF OXYGEN COEXISTING GAS

Removal of toluene from nitrogen

Inlet concentration of Toluene 2000 ppm

Cathode 0.5 mm

Current 0.5 mA

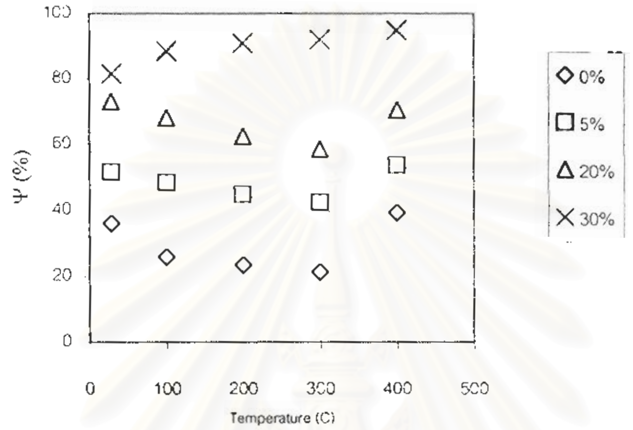

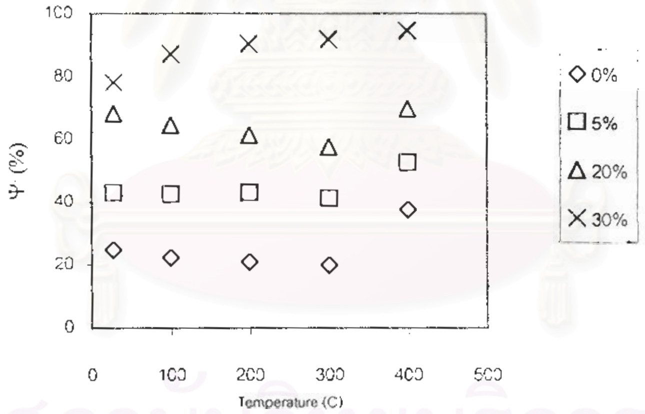

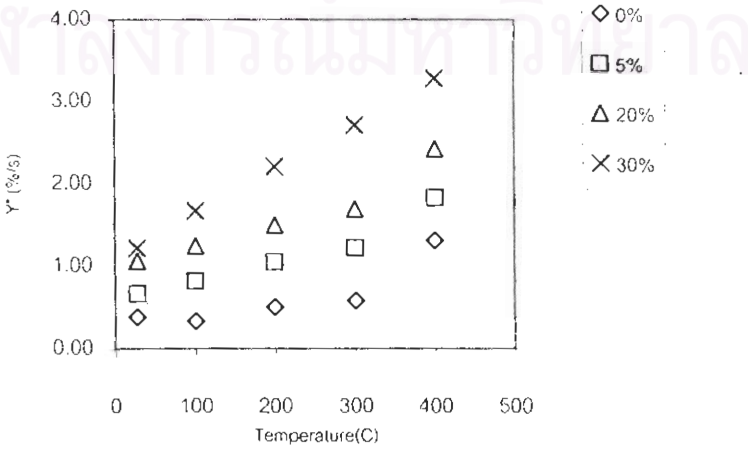

APP. C4 EFFECT OF INLET CONCENTRATION

Removal of toluene from nitrogen

Current	0.5 mA
Cathode	0.5 mm
Oxygen	0 %

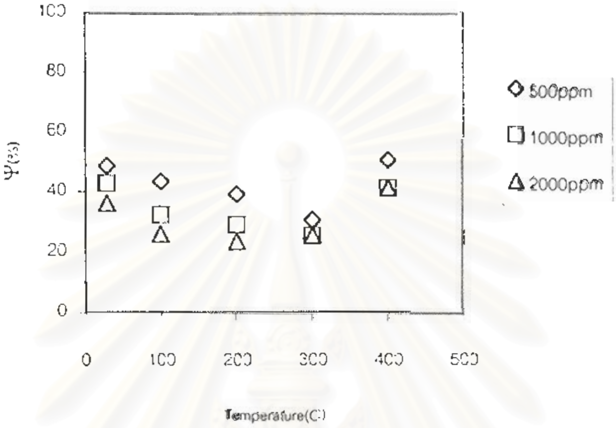

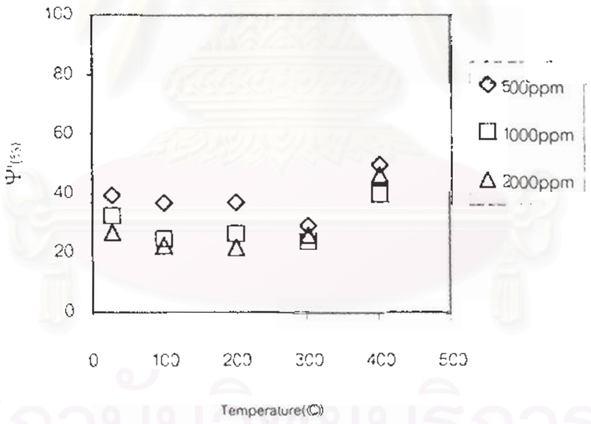

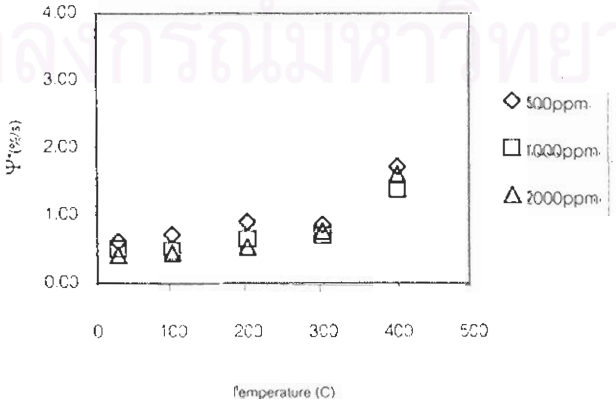

EFFECT OF INLET CONCENTRATION

Removal of toluene from nitrogen-oxygen

Current 0.5 mA

Cathode 0.5 mm

Oxygen 20 %

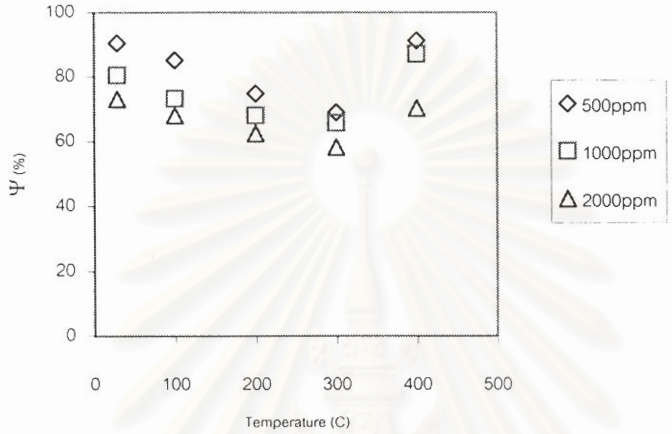

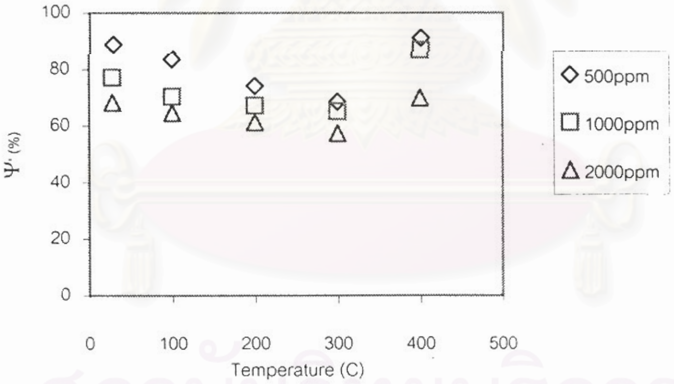

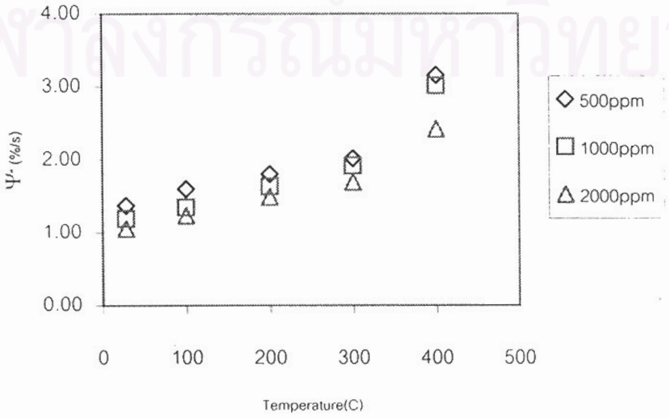

APPENDIX D

ANALYSIS FOR THE SOLID DEPOSIT FROM GC-MS

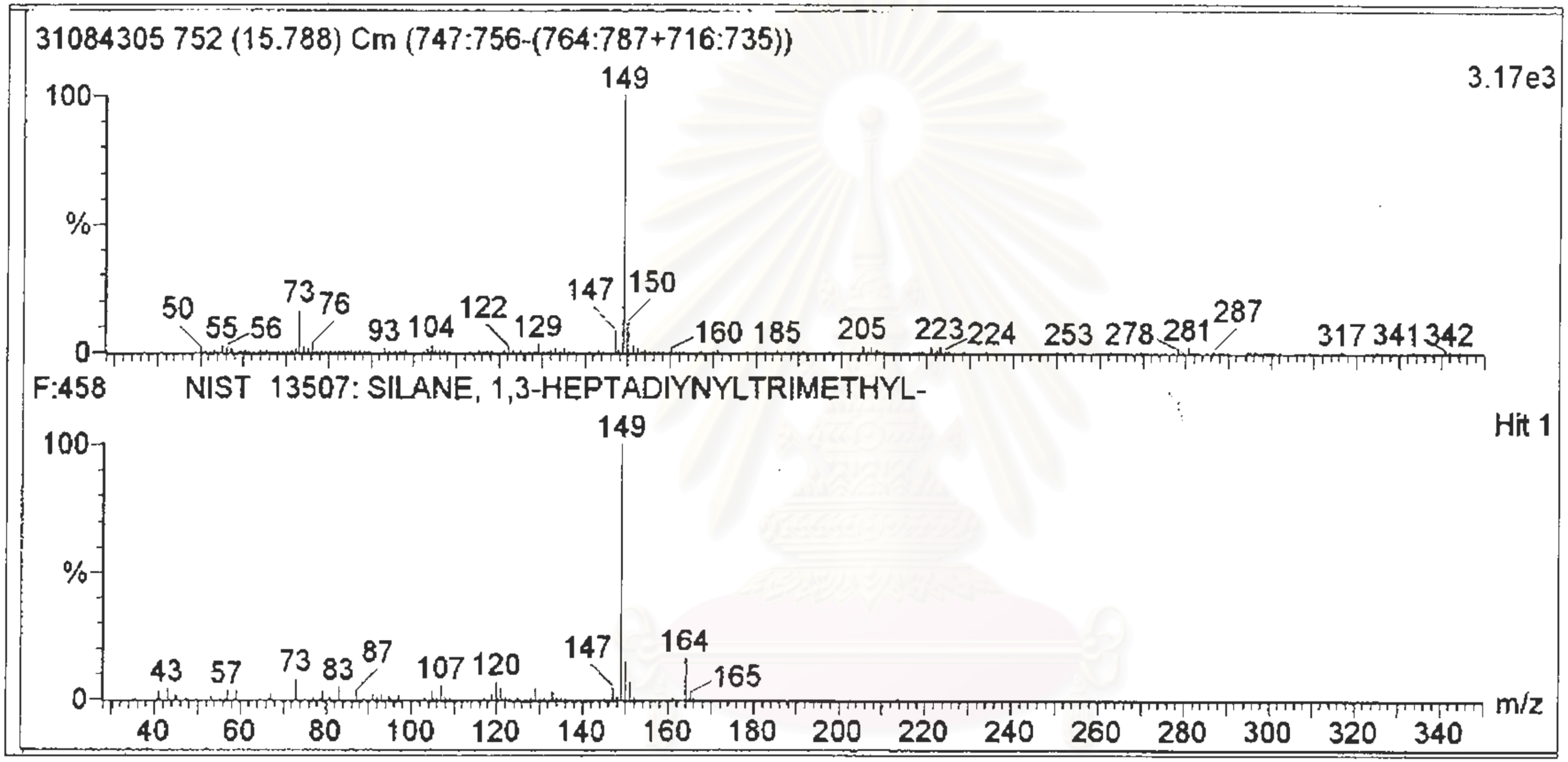
31084305 752 (15.788) Cm (747:756-(764:787+716:735))
3.17e3
100
%
0
149
50
55
56
73
76
93
104
122
129
147
150
160
185
205
223
224
253
278
281
287
317
341
342
F:458
NIST 13507: SILANE, 1,3-HEPTADIYNYLTRIMETHYL-
Hit 1
100
%
0
149
43
57
73
83
87
107
120
147
164
165
40
60
80
100
120
140
160
180
200
220
240
260
280
300
320
340
m/z

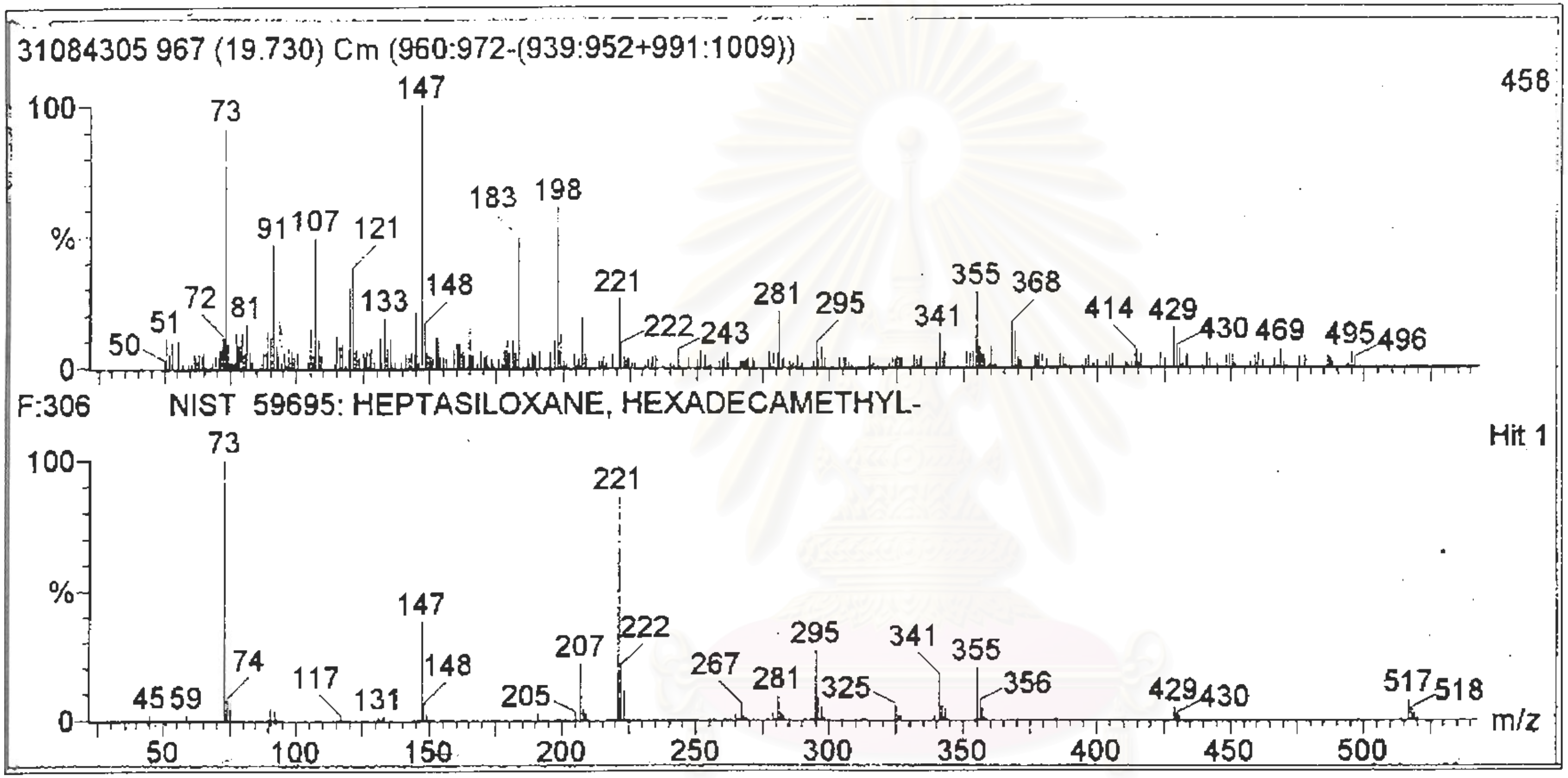
31084305 967 (19.730) Cm (960:972-(939:952+991:1009))
458
100
%
0
73
147
183
198
91
107
121
133
148
50
51
72
81
221
222
243
281
295
341
355
368
414
429
430
469
495
496
F:306
NIST 59695: HEPTASILOXANE, HEXADECAMETHYL-
Hit 1
100
%
0
73
221
147
207
222
295
341
355
267
281
325
356
74
45
59
117
131
148
205
429
430
517
518
m/z
50
100
150
200
250
300
350
400
450
500

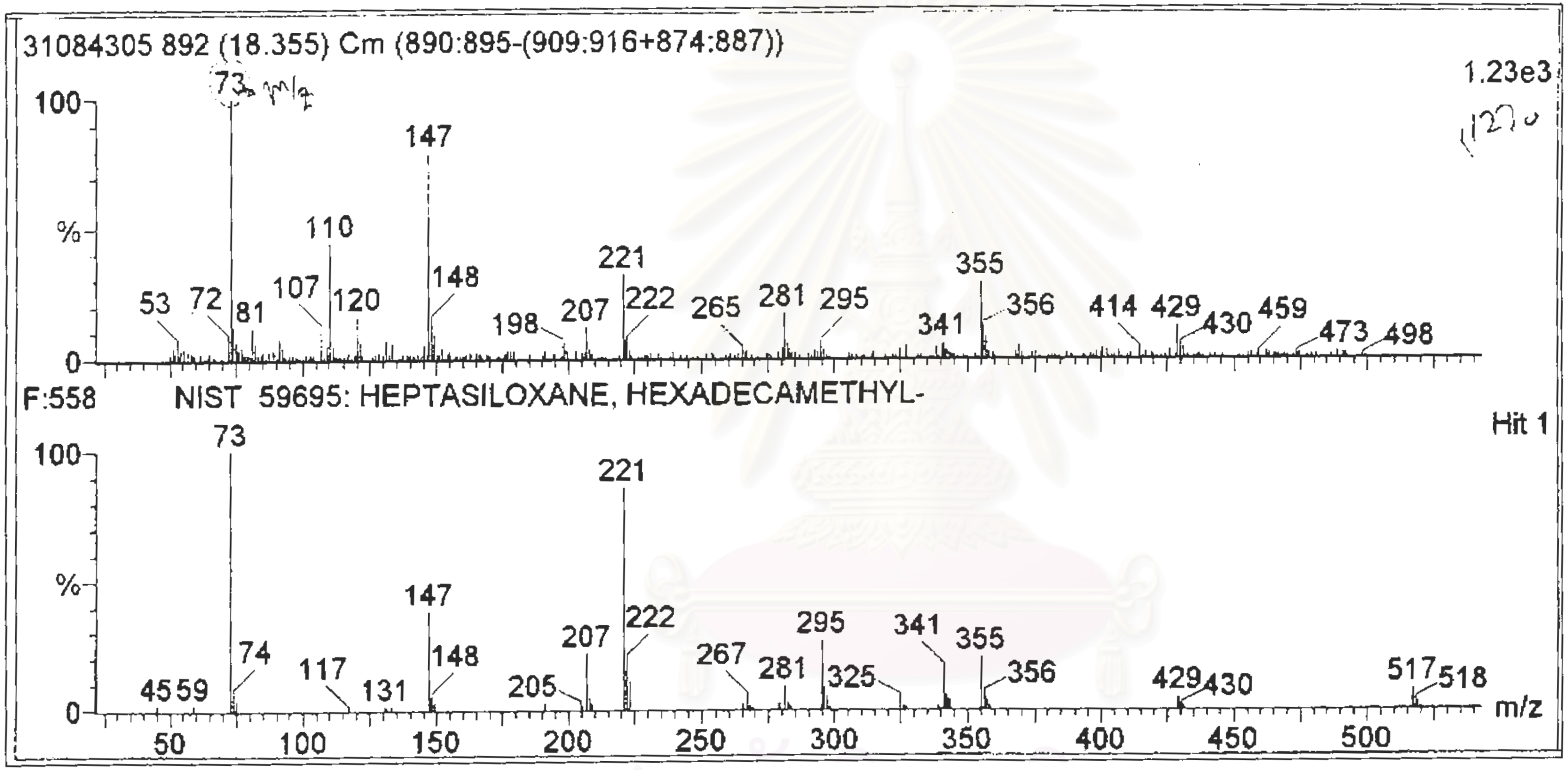
31084305 892 (18.355) Cm (890:895-(909:916+874:887))
1.23e3
1270
73 m/z
100
%
0
53
72
81
107
110
120
147
148
198
207
221
222
265
281
295
341
355
356
414
429
430
459
473
498
F:558
NIST 59695: HEPTASILOXANE, HEXADECAMETHYL-
Hit 1
73
100
%
0
45
59
74
117
131
147
148
205
207
221
222
267
281
295
325
341
355
356
429
430
517
518
m/z
50
100
150
200
250
300
350
400
450
500

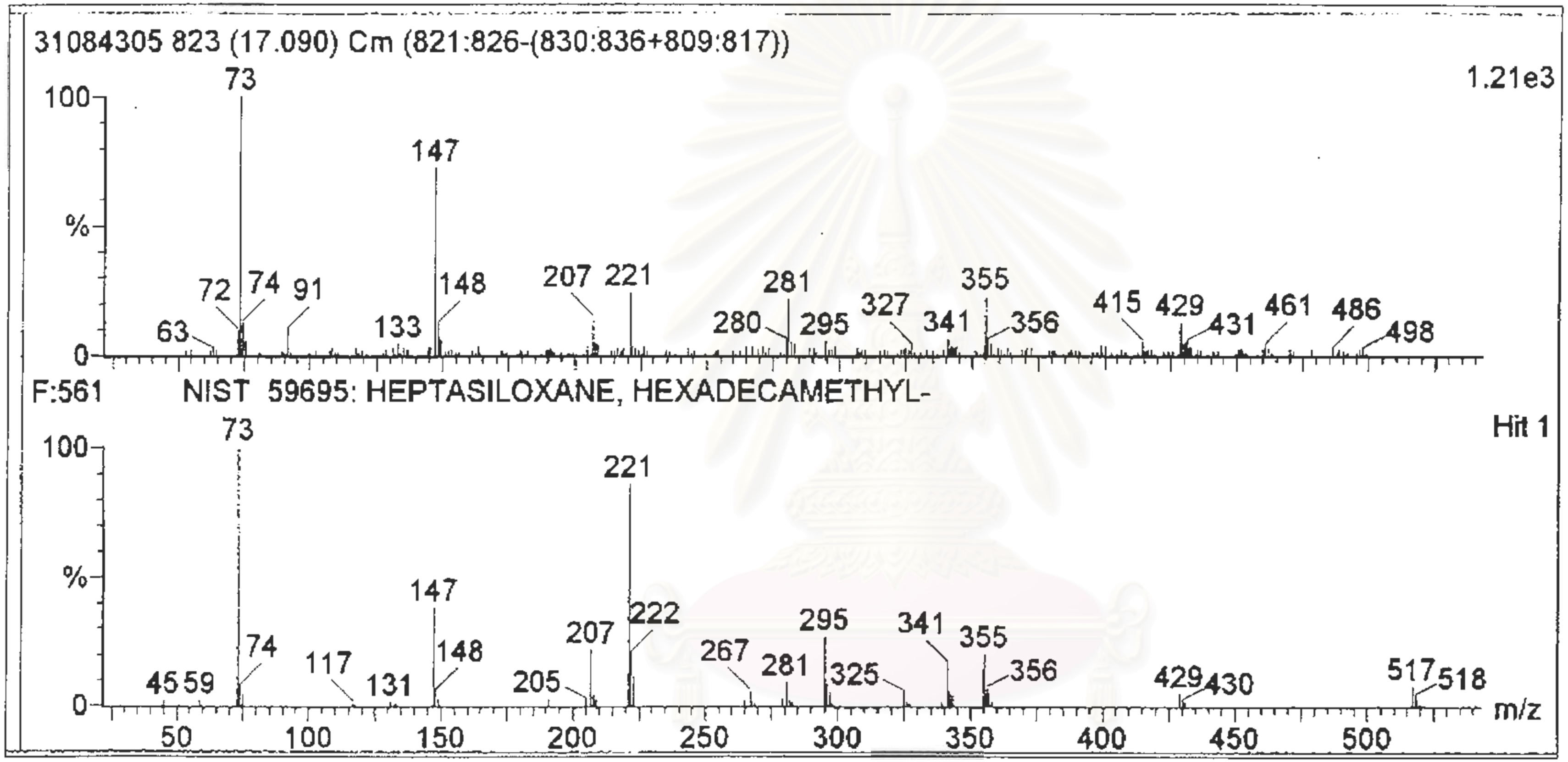
31084305 823 (17.090) Cm (821:826-(830:836+809:817))
1.21e3
100
%
0
73
147
63
72
74
91
133
148
207
221
280
281
295
327
341
355
356
415
429
431
461
486
498
F:561 NIST 59695: HEPTASILOXANE, HEXADECAMETHYL-
Hit 1
100
%
0
73
221
147
222
74
45
59
117
131
148
205
207
267
281
295
325
341
355
356
429
430
517
518
m/z
50
100
150
200
250
300
350
400
450
500

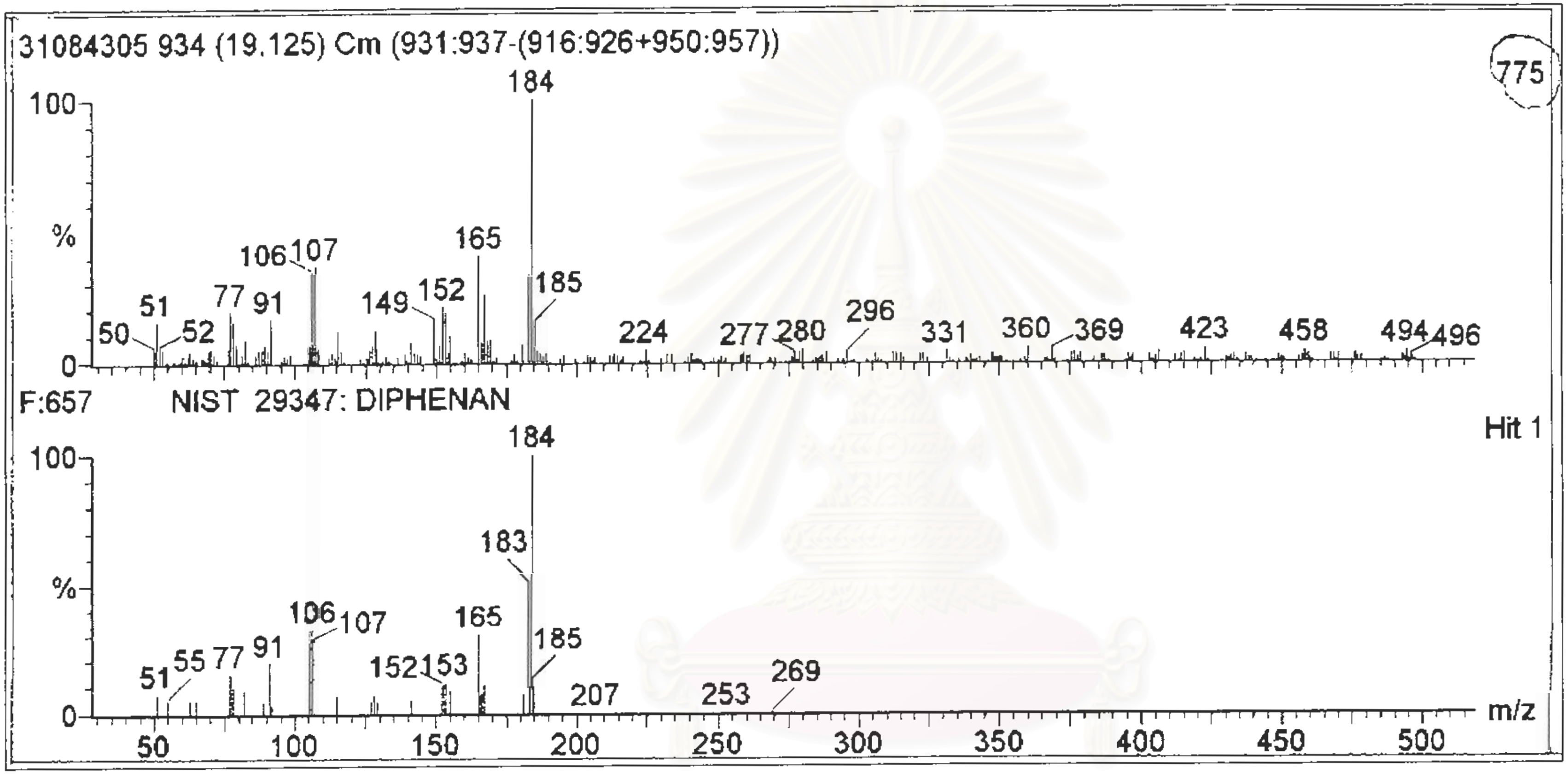
31084305 934 (19.125) Cm (931:937-(916:926+950:957))
100
%
0
184
165
106
107
185
149
152
51
77
91
50
52
224
277
280
296
331
360
369
423
458
494
496
F:657
NIST 29347: DIPHENAN
Hit 1
184
183
106
107
165
185
91
77
55
51
152
153
207
253
269
m/z
50
100
150
200
250
300
350
400
450
500

775

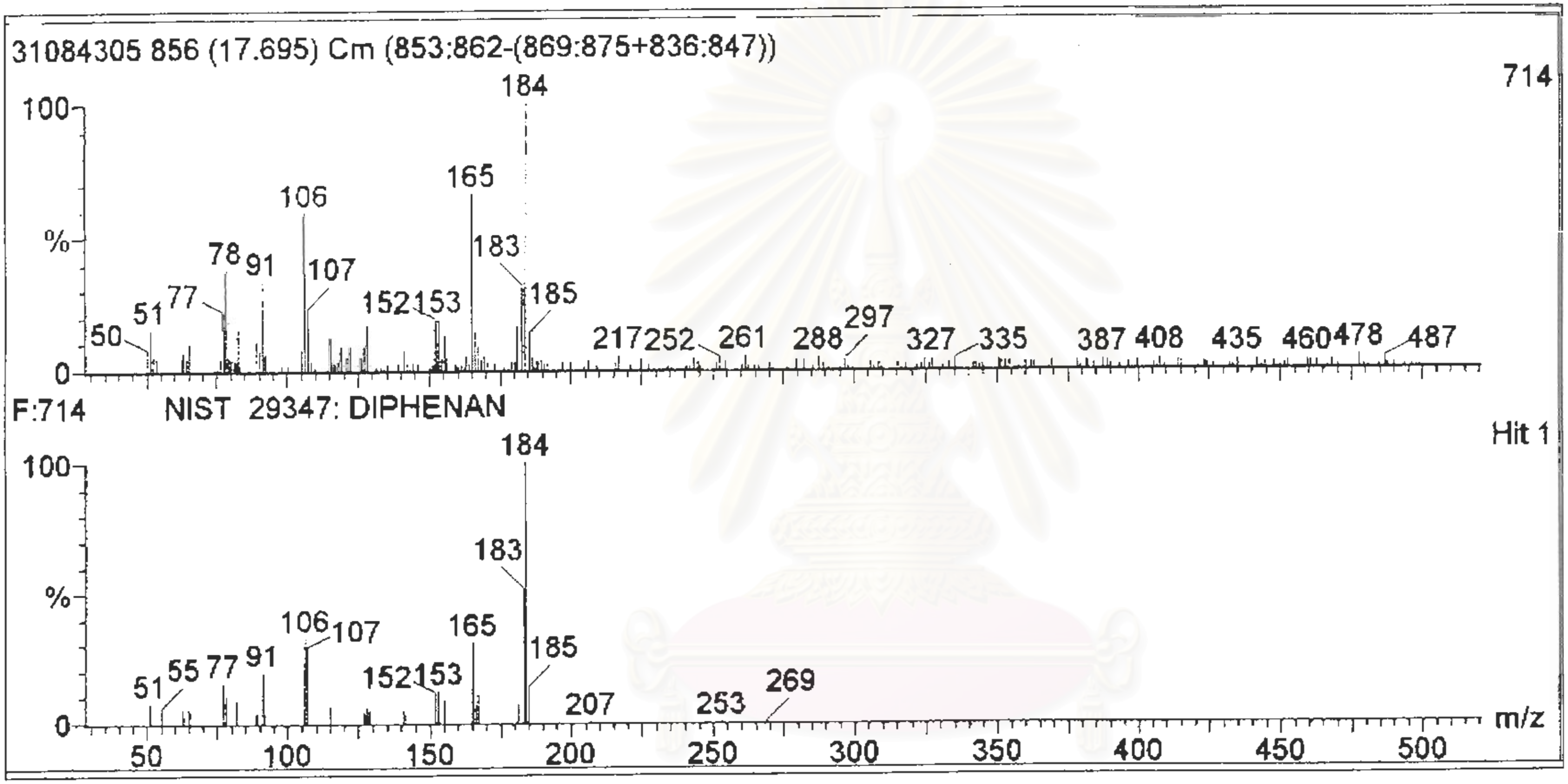
31084305 856 (17.695) Cm (853:862-(869:875+836:847))
714
100
%
0
184
165
106
183
78
91
107
51
77
152153
185
50
217252
261
288
297
327
335
387
408
435
460478
487
F:714
NIST 29347: DIPHENAN
Hit 1
184
183
106107
165
91
77
55
51
152153
185
207
253
269
m/z
50
100
150
200
250
300
350
400
450
500

VITA

Miss Nantamas Dhattavorn was born in Saraburi province, Thailand, on October 25, 1975. She finished her secondary school from Horwang School in Bangkok, in March 1993. After that, She studied in the major of Chemical Technology in Faculty of Science at Chulalongkorn University. She continued her further study for Master's degree in Chemical Engineering at Chulalongkorn University. In April 2001, she was graduated the degree of Master of Engineering in Chemical Engineering.